A brief introduction to synchrotron radiation

Esen Ercan Alp

Argonne National Laboratory

&

Chair of SESAME Scientific Advisory Committee

SESAME SUNSTONE training programme – First Edition, April 8, 2025, Amman, Jordan (on-line)

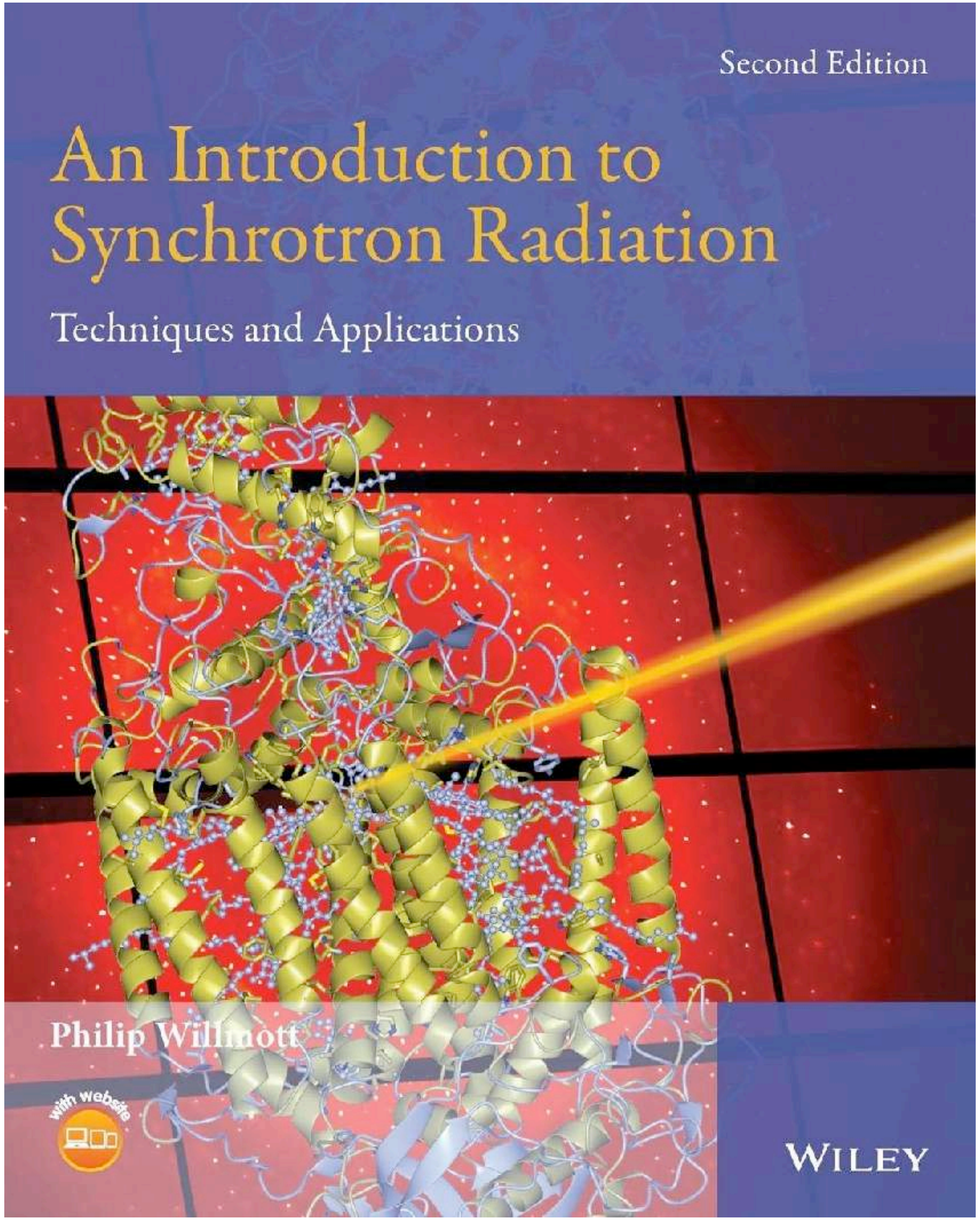
Second Edition
An Introduction to Synchrotron Radiation
Techniques and Applications
Philip Willmott
with website
WILEY

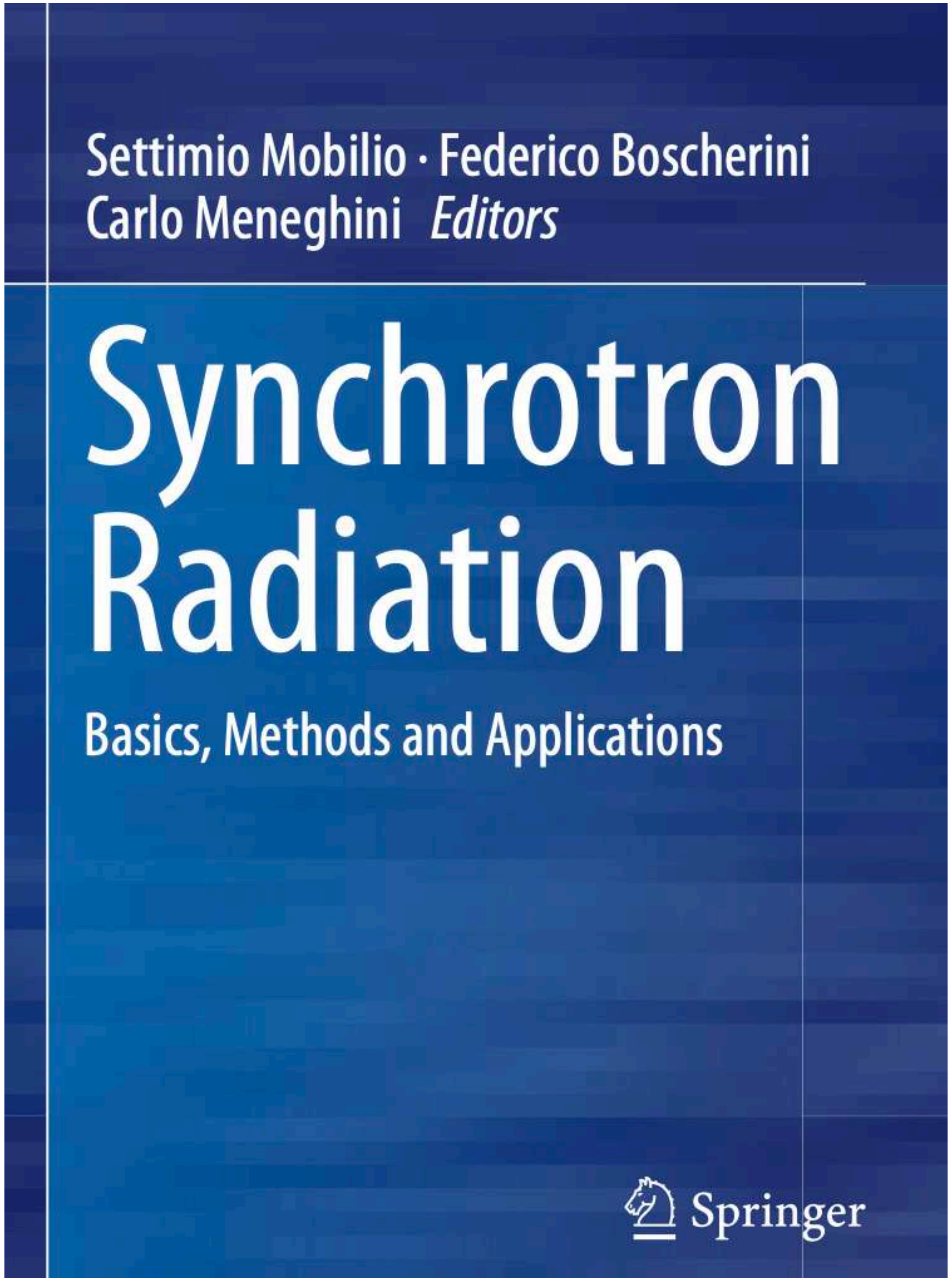
Settimio Mobilio · Federico Boscherini
Carlo Meneghini Editors
Synchrotron Radiation
Basics, Methods and Applications
Springer

Final words at the beginning

Synchrotron radiation (SR) is one of the many tools scientists have in their tool chest.

Yet, it is very versatile and powerful, such that many unsolvable problems can be addressed using SR.

Also, it is quite different in many ways, as you are about to discover. It requires strong team work, mastery of few technically difficult skills, patience and perseverance, and strong communication skills.

Synchrotron floor is where you can shine, even if you are a beginner.

Why do we need science and large scientific facilities ?

Some of the material challenges we are facing today are related to

- alternative sources of **energy** (production, storage, & distribution)
- improving **health** care, and **environment**
- better **communication**,
- access to **transportation**,
- access to **education,** and
- better **housing** & **nutrition**

These challenges can be best addressed by **making advances that improves our understanding and control of matter.** Particularly, matter that consists of **natural** or **artificial** nanoscale building blocks defined either by atomic structural arrangements or by electron or spin formations.

Proteomics, **electronics**, **spintronics,** **nanoscience** are all late 20th-early 21th century concepts that support trillion dollar industries and they shape the world political and economical order.

Thus, **visualization, exploration, and controlled manipulation of macroscopic matter** have long been important technological goals.

Scientific developments in the last century have focused our attention on understanding matter at the atomic scale through the underlying framework of quantum mechanics and correlations.

Accelerators are part and parcel of this desire to understand and control of the natural as well as the synthetic domain.

- **Linear or Circular Particle Accelerators**
  - **Electron**
  - **Proton**
  - **Muon**
  - **Ion**
  - **Radioactive isotopes**

- **Basic acceleration mechanisms**
  - **Static DC acceleration: Cockroft & Walton, 1928**
  - **Resonant acceleration: Ising, 1924**
  - **Linear accelerator: Wideröe, 1928**
  - **Wakefield accelerator : Dawson, 1979**

First observation of Synchrotron Radiation, 1947

If electrons moving at relativistic speeds are forced by magnetic fields to follow curved trajectories they emit electromagnetic radiation.

Synchrotron radiation is produced in an 100 MeV electron accelerator in General Electric Laboratories in Schenectady, New York in 1947.

Theoretical foundation was prepared by Maxwell, Lorentz, Pomeranchuk, and Schwinger.

Synchrotron radiation is extremely intense and extends over a broad energy range from the infrared through the visible and ultraviolet, into the soft and hard x-ray regions of the electromagnetic spectrum.

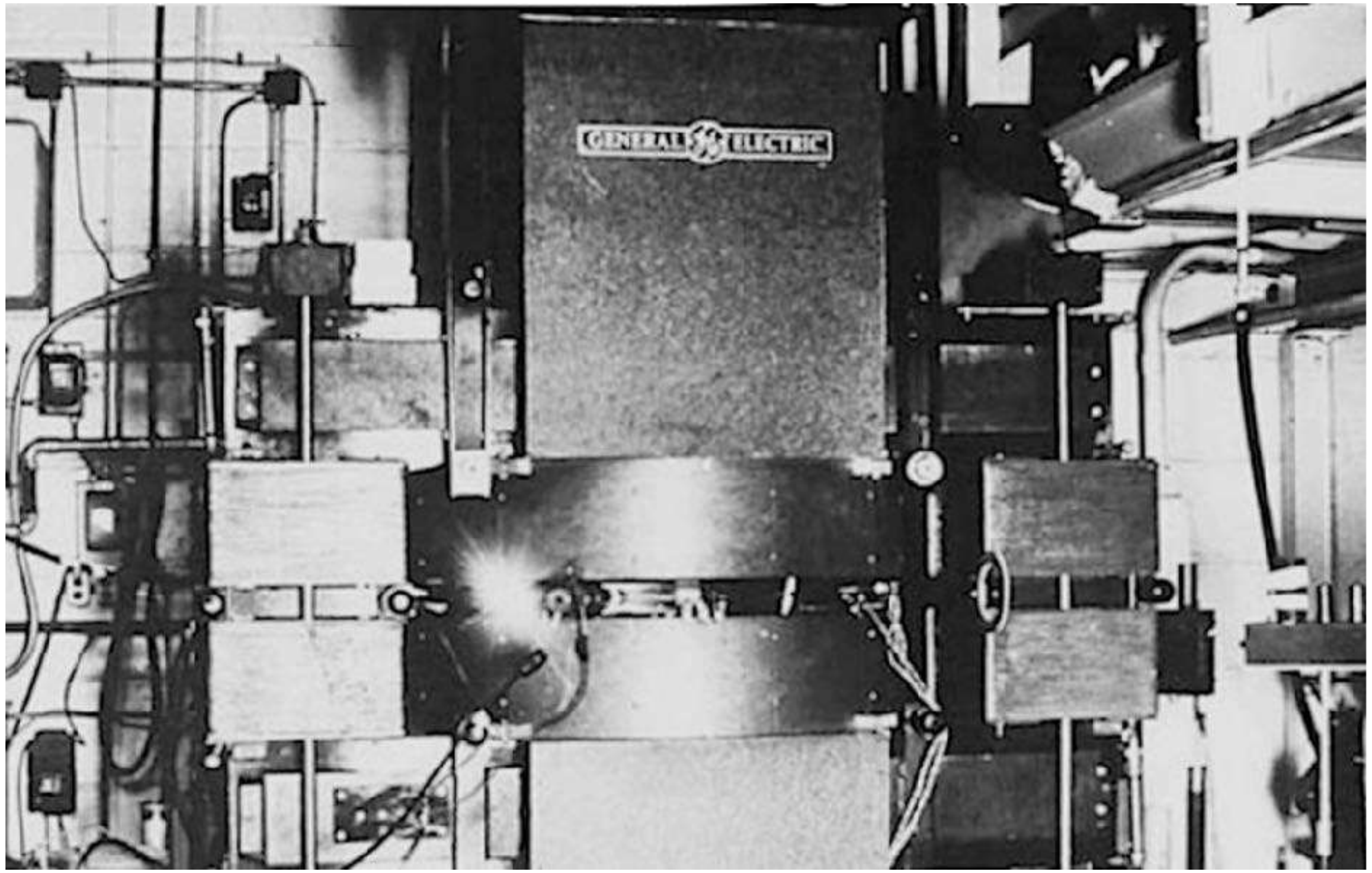

J. Vac. Sci. Technol. A. 2022;40(3). doi:10.1116/6.0001686

Very brief and incomplete history of accelerators

1857 Geissler tubes
1869 Crookes tube
1895 discovery of x-rays with Crookes tube, Roentgen
1897 identification of cathode rays as electrons, J. J. Thomson
1897 Braun: cold cathode ray tube
1913 Coolidge tube
1931 van de Graaf generator (1.5 MV)
1931 E. Lawrence, 11” diameter CYCLOTRON
1932 Cockroft-Walton generator (voltage multiplier)
 800 keV, disintegration of Li by protons
1947 First observation of synchrotron radiation
1959 DESY, Hamburg
1988 Wake field accelerators, Argonne
1999 LEUTL-First SASE at 530 nm, Argonne
2004 FLASH-DESY, now operating at 5 nm
2009 LCLS, Stanford, 0.1 nm
2010 Large Hadron Collider, 7 TeV
2014 EuropeanXFEL

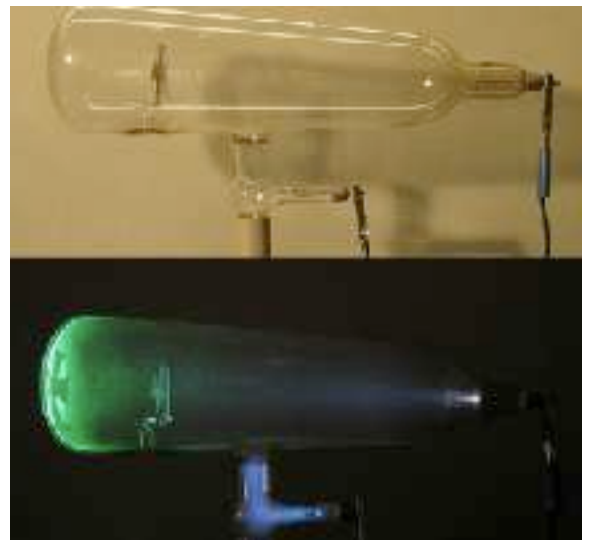

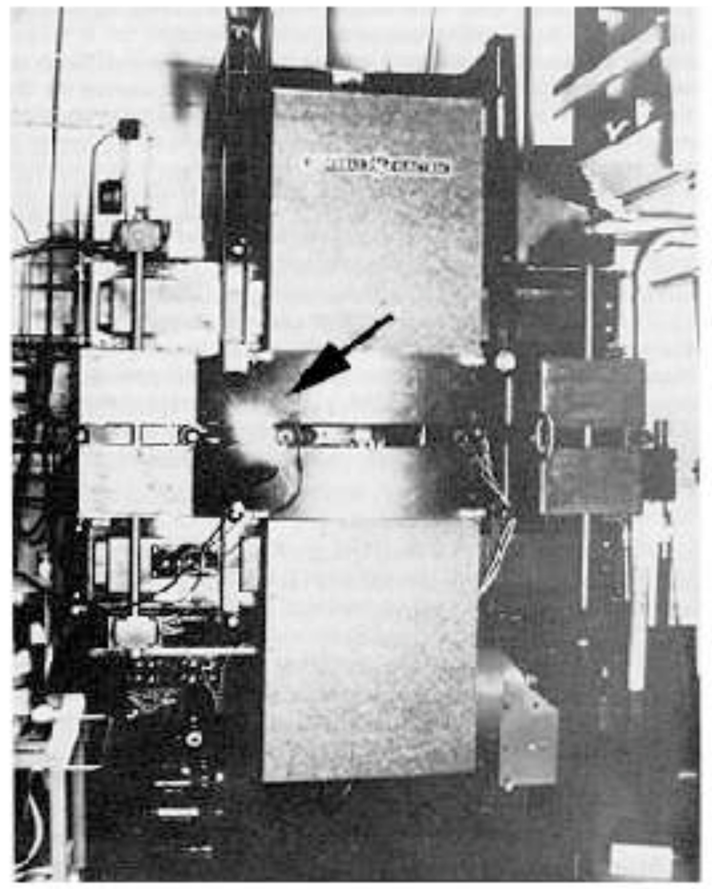

Synchrotron light from the 70-MeV electron synchrotron at GE.

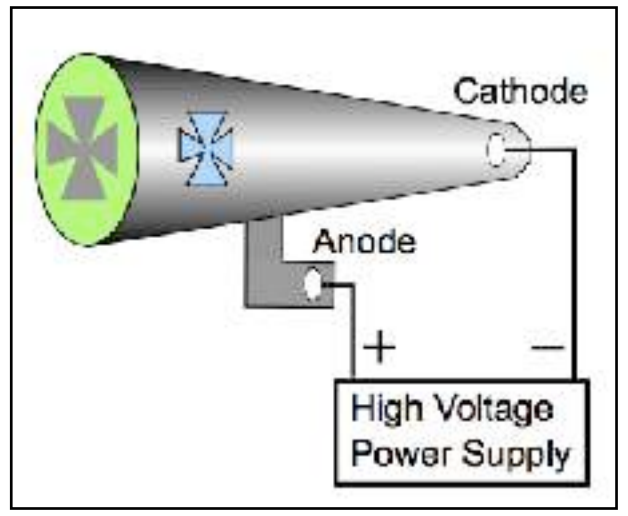

"Dr Livingston has asked me to advise you that he has obtained 1,100,000 volt protons. He also suggested that I add ‘Whoopee'!"

—Telegram to Lawrence, 3 August 1931

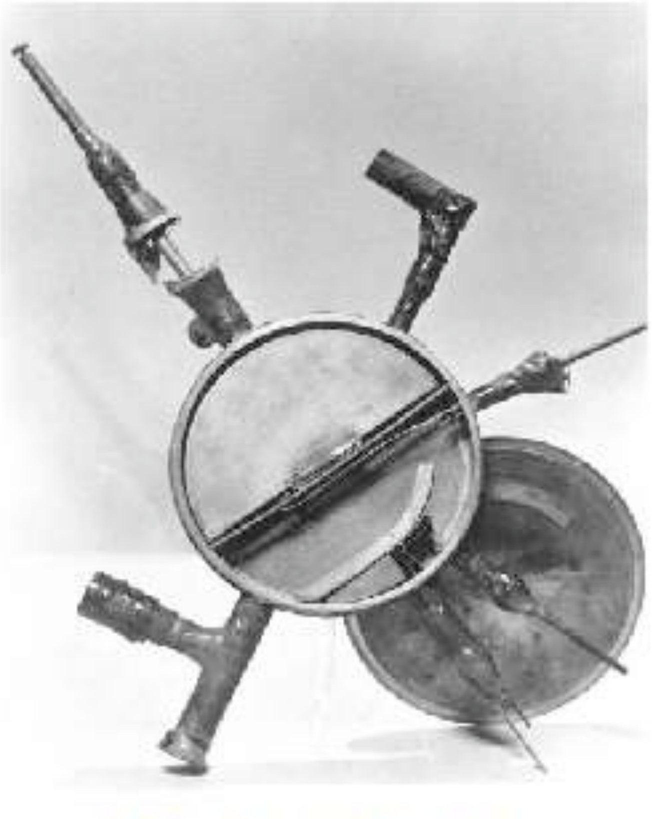

Photo courtesy Lawrence Berkeley National Laboratory
The first particle accelerator (cyclotron) developed by Ernest O. Lawrence in 1929

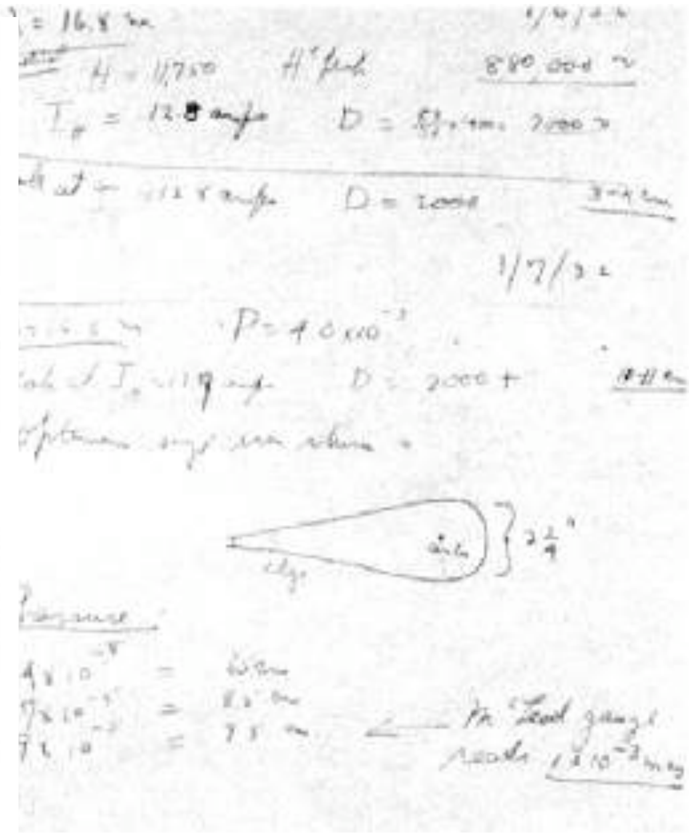

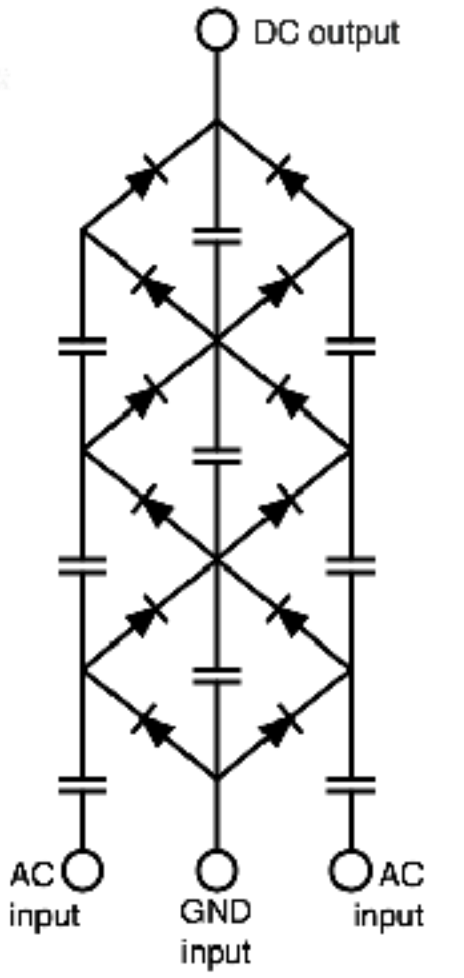

Accelerators for photons:
Infrared, ultraviolet, x-ray --> γ

1895: Roentgen's discovery of x-rays
1904: Barkla demonstrates the true nature of x-rays as electromagnetic radiation
1909: Barkla and Sadler discover characteristic x-ray radiation (1917 Nobel to Barkla)
1912: von Laue, Friedrich, and Knipping observe x-ray diffraction (1914 Nobel to von Laue)
1913: **Bragg**, father and son, build an x-ray spectrometer (1915 Nobel)
1913: Moseley develops quantitative x-ray spectroscopy and Moseley's Law
1916: Siegbahn and Stenstrom observe emission satellites (1924 Nobel to Siegbahn)
1921: Wentzel observes two-electron excitations
1922: Meitner discovers Auger electrons
1924: Lindh and Lundquist resolve chemical shifts
1927: Coster and Druyvesteyn observe valence-core multiplets
1931: **Johann** develops bent-crystal spectroscopy
1947: First observation of light from a synchrotron, GE-Schenectady, Blewett, Pollack
1956: Tomboulian-Hartmann measures the spectrum at Cornell --> CHESS
1961: NBS (SURF),
Frascati,
Tokyo (IN-SOR) ---> Photon Factory --> AR
1965- Electron storage rings:
Tantalus-I --> Aladdin (Wisconsin) ,
DESY --> DORIS --> PETRA-II-III --> FLASH --> EuroXFEL
1971: Orsay, LURE : ACO--> Super-ACO --> SOLEIL
1974: SLAC- SSRF --> SSRL-III --> LCLS --> PEP-X
1984: Brookhaven: NSLS --> NSLS-II
1993: ESRF-Grenoble --> ESRF-II
1995: Argonne: APS --> APS-U
1998: SPring-8 --> SACLA

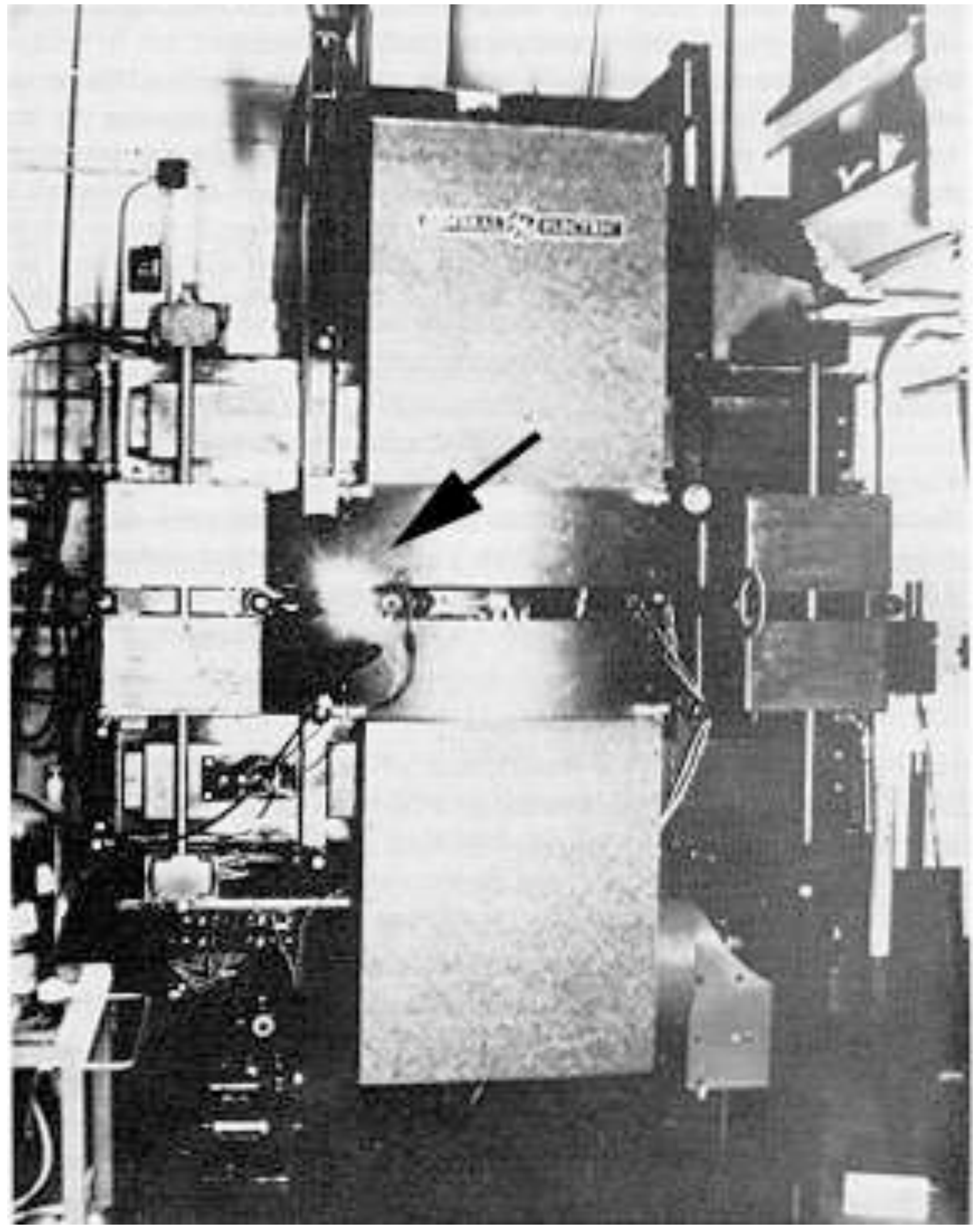

2000's: ALBA-DIAMOND-SOLEIL-ELETTRA-SLS-SIRIUS-SESAME-Pohang-Max IV-PETRA-III
2010: LCLS : Linear Coherent Light Source
2011: SACLA
2014: EuroXFEL
2015: SwissFEL

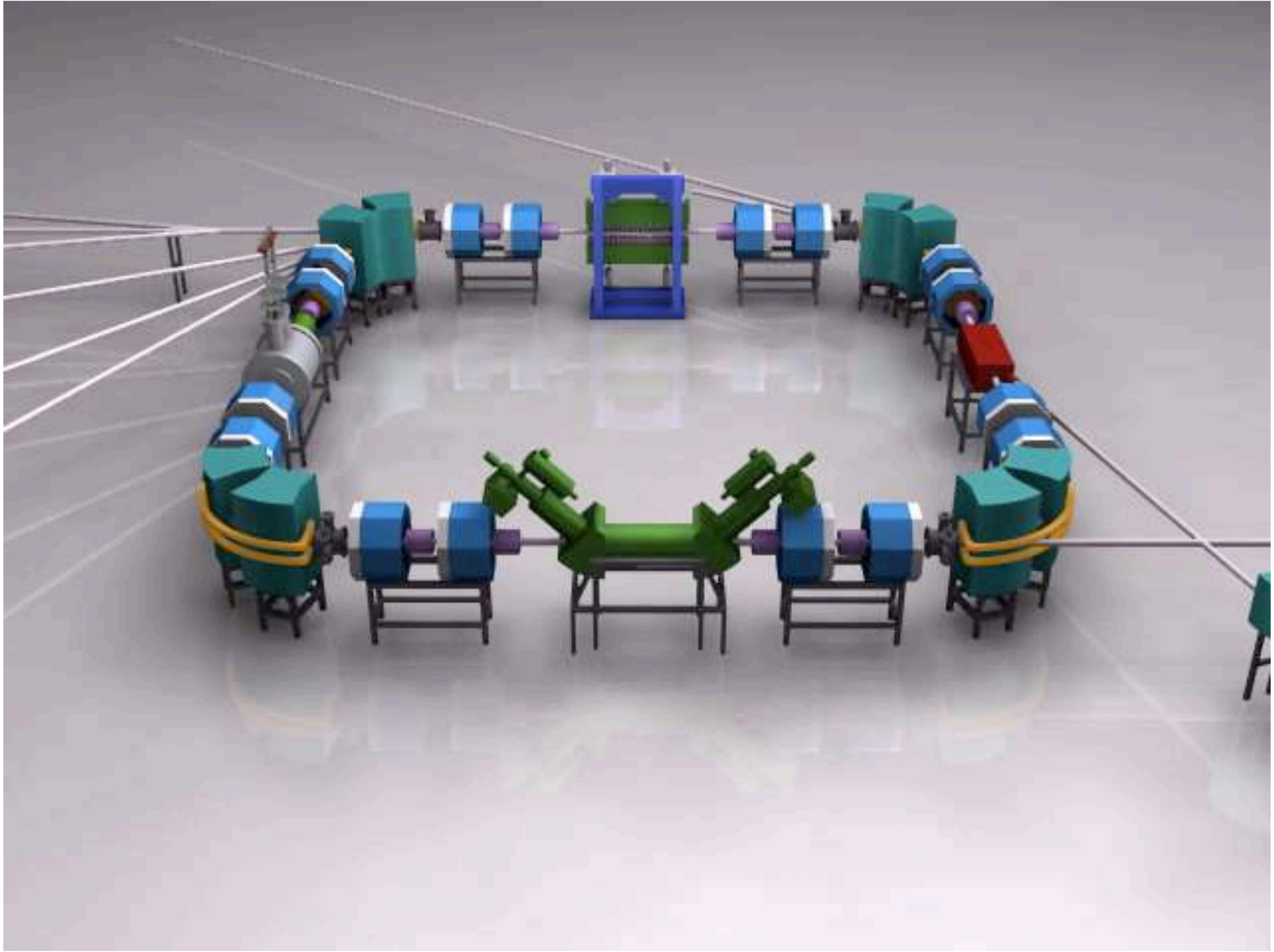

Some of the early synchrotron radiation sources

FRASCATI: 1959-1975 (Italy)

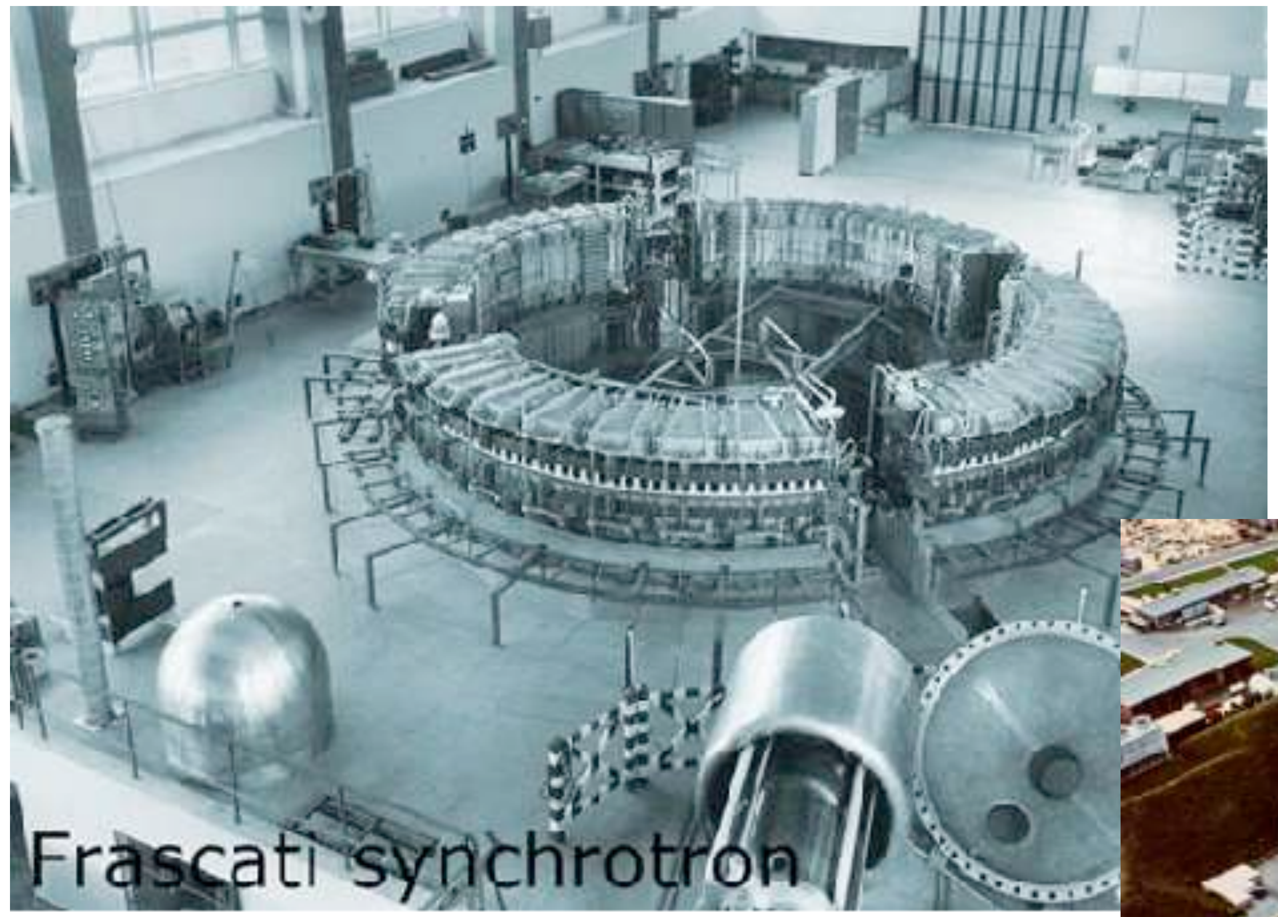

DESY :1964-1978 (Germany)

Stanford: 1972-2004 (USA)

INS-SF: 1974-1997 (Japan)

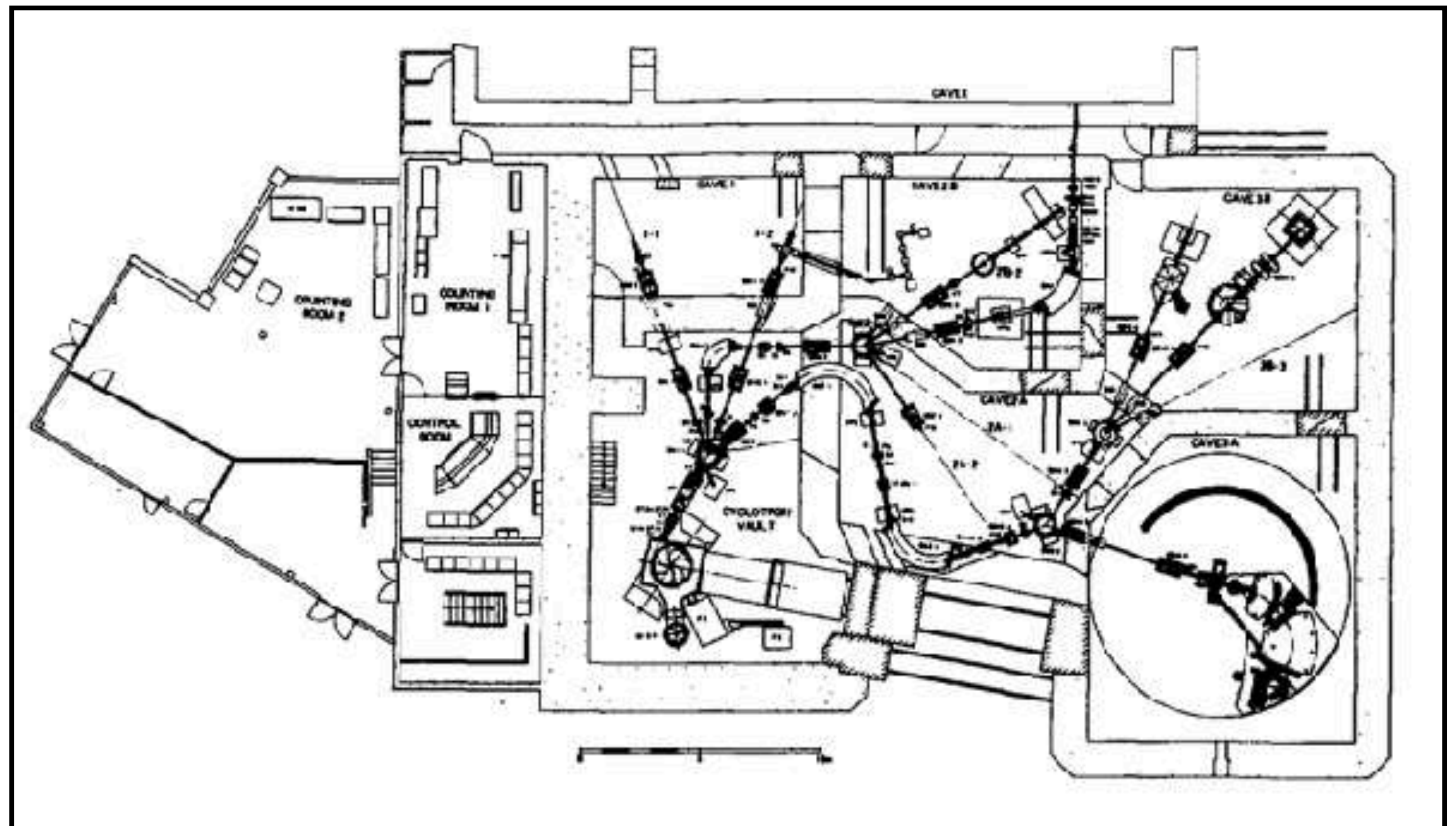

Fig.3 Plan view of the INS SF-cycloton laboratory.

Where are the current synchrotrons in the World ?

Some of the synchrotron radiation centers around the world

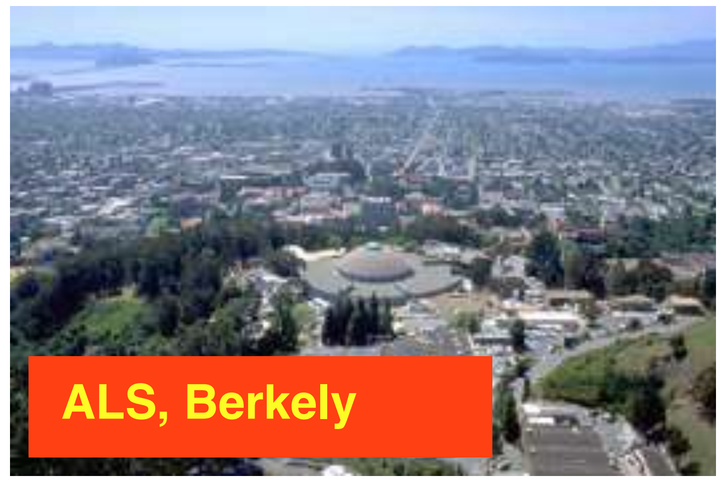

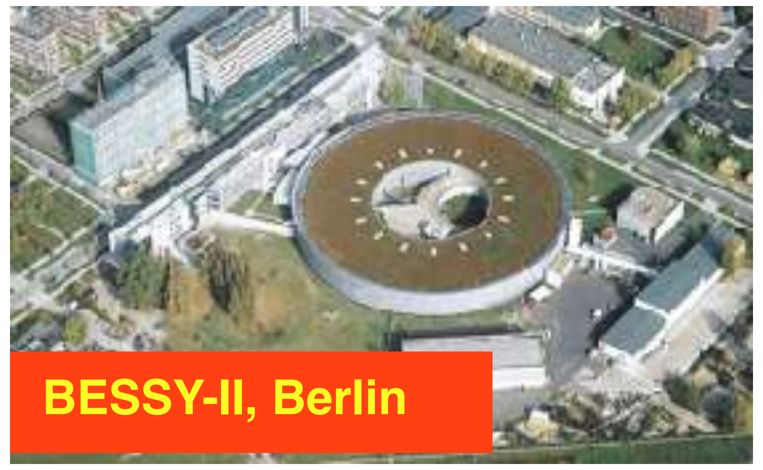

Early Italian-French experiments @ FRASCATI (~1962)

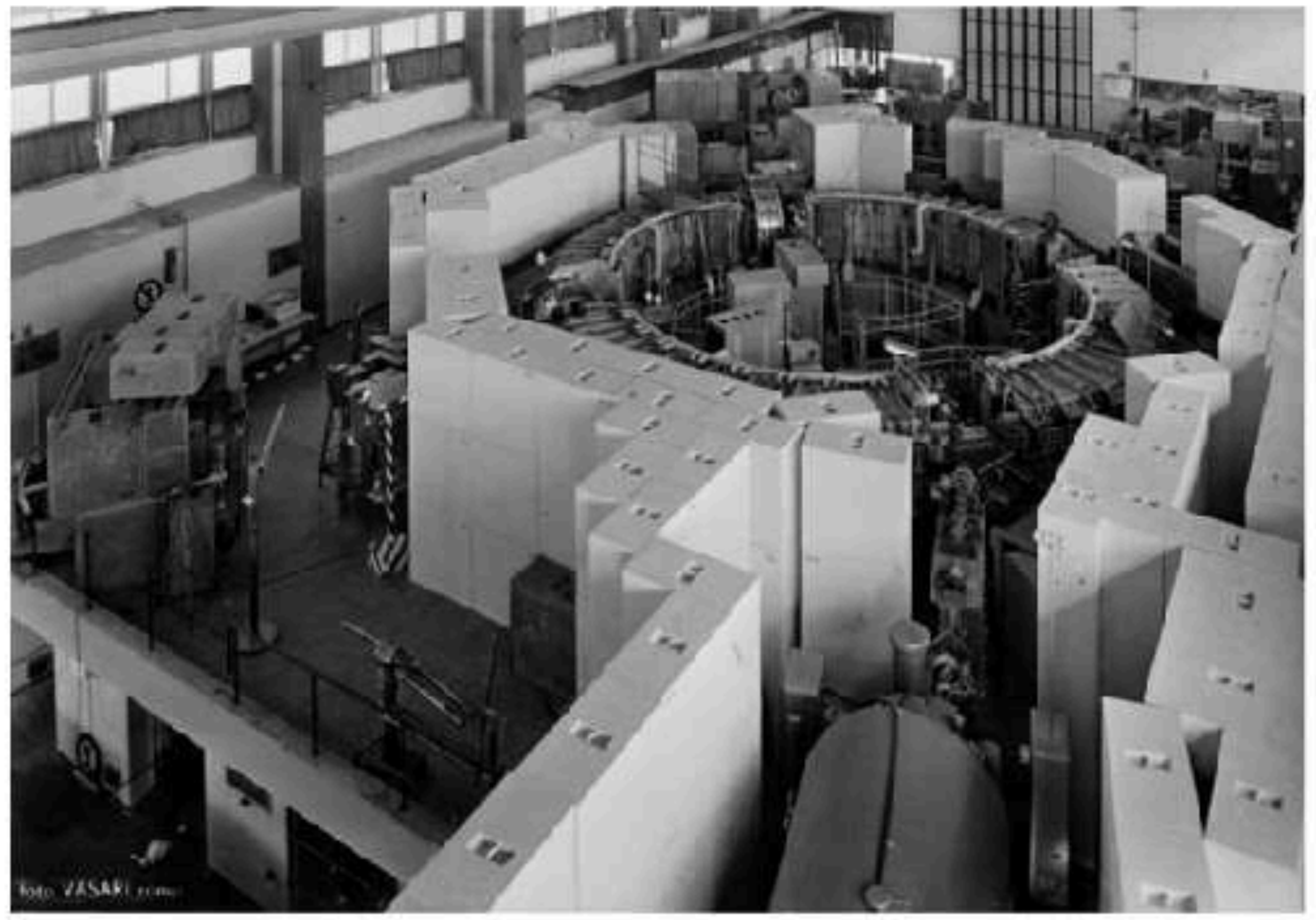

Figure 1
View of the Frascati electron synchrotron, in operation from 1959 to 1975, with all the beamlines derived from it. The Italian–French cooperative experimental set-up was located in the front left-hand side sector.

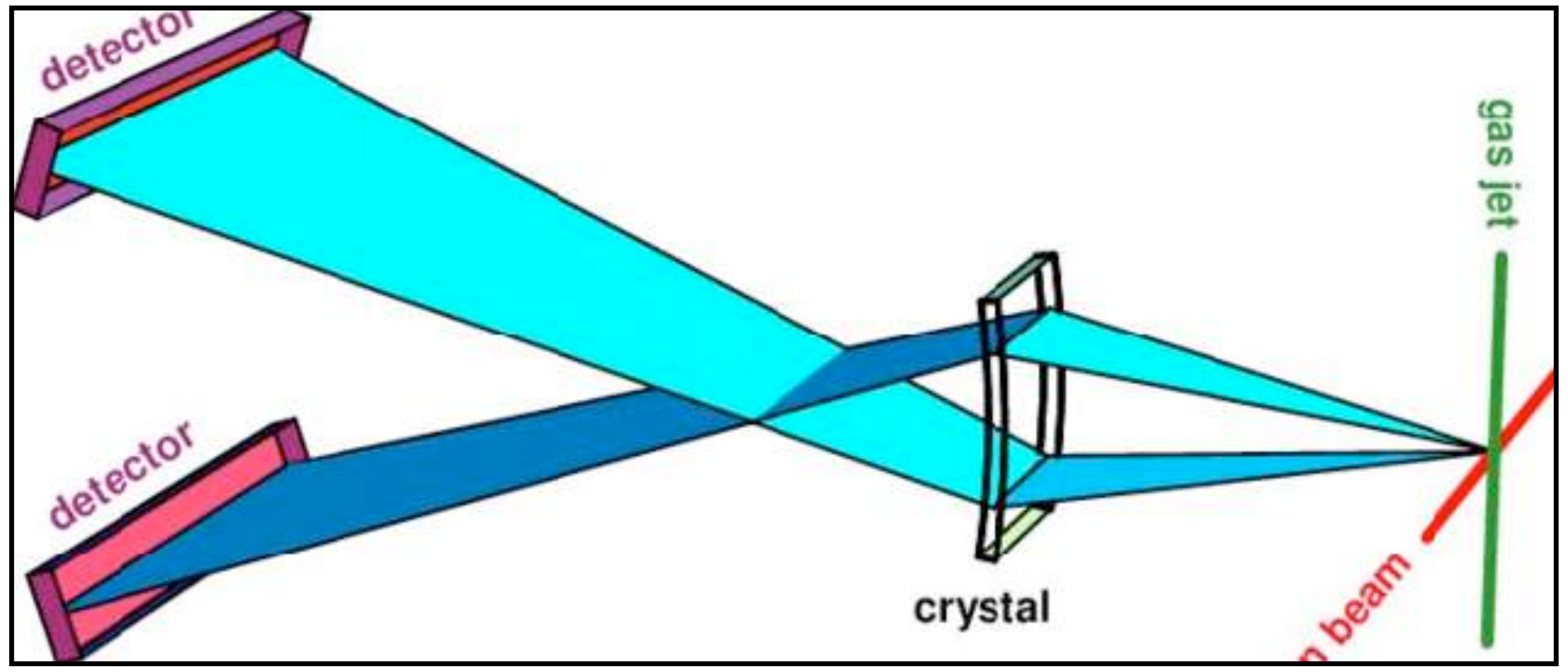

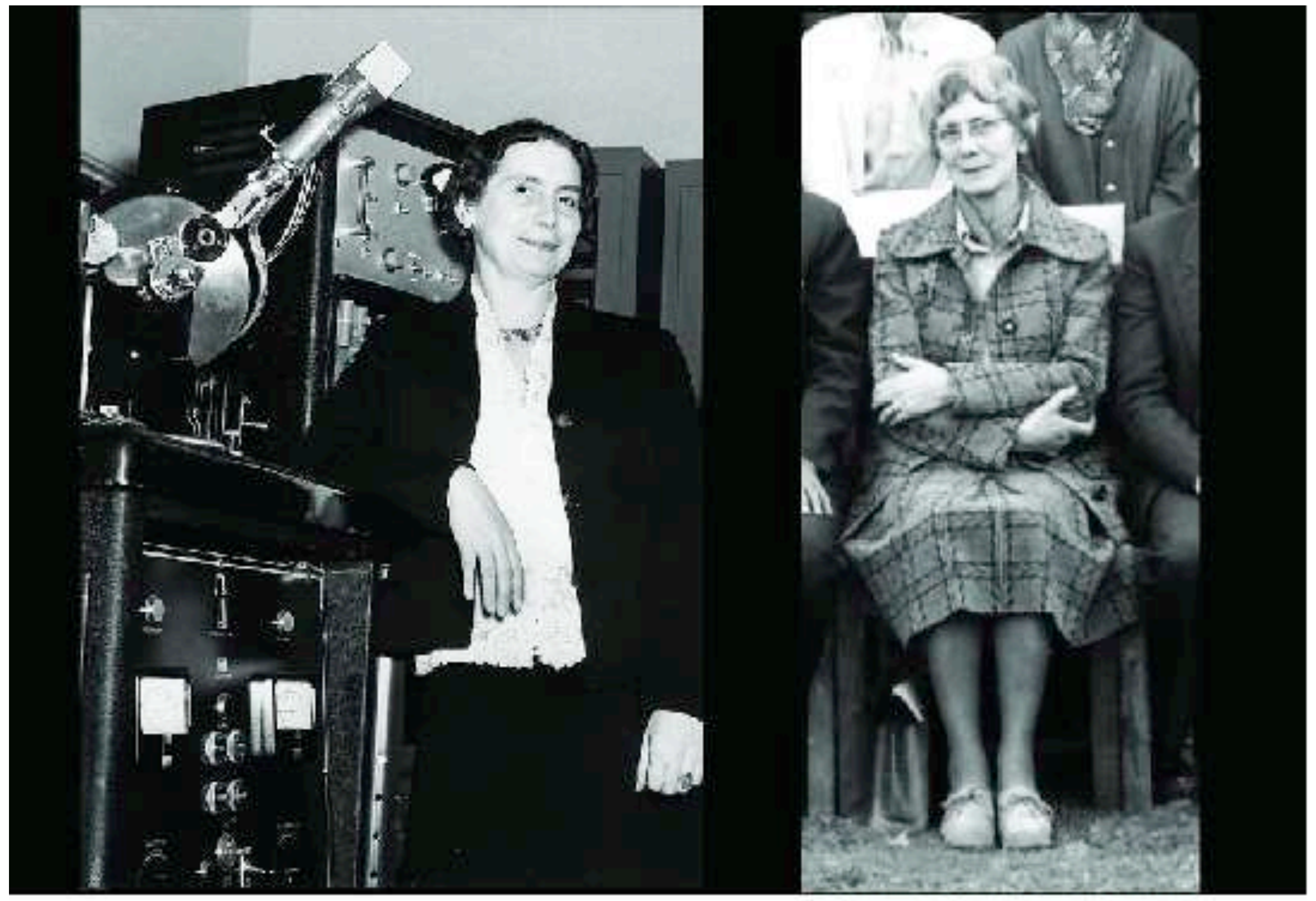

SÉANCE DU 8 JUILLET 1963. 409

RAYONNEMENT ÉLECTROMAGNÉTIQUE. — *Premiers spectres X du rayonnement d'orbite du synchrotron de Frascati.* Note (*) de Mlle **Yvette Cauchois**, Mme **Christiane Bonnelle** et M. **Guido Missoni**, présentée par M. Francis Perrin.

Avec un spectrographe à vide et différents cristaux courbés, des spectres dus au rayonnement X émis par les électrons du synchrotron de Frascati fonctionnant jusqu'à 1,1 GeV ont été obtenus entre 5 et 14 Å. L'absorption K de l'aluminium, entre autres, est observée pour la première fois avec ce type de source, après des expositions très brèves par rapport aux sources usuelles.

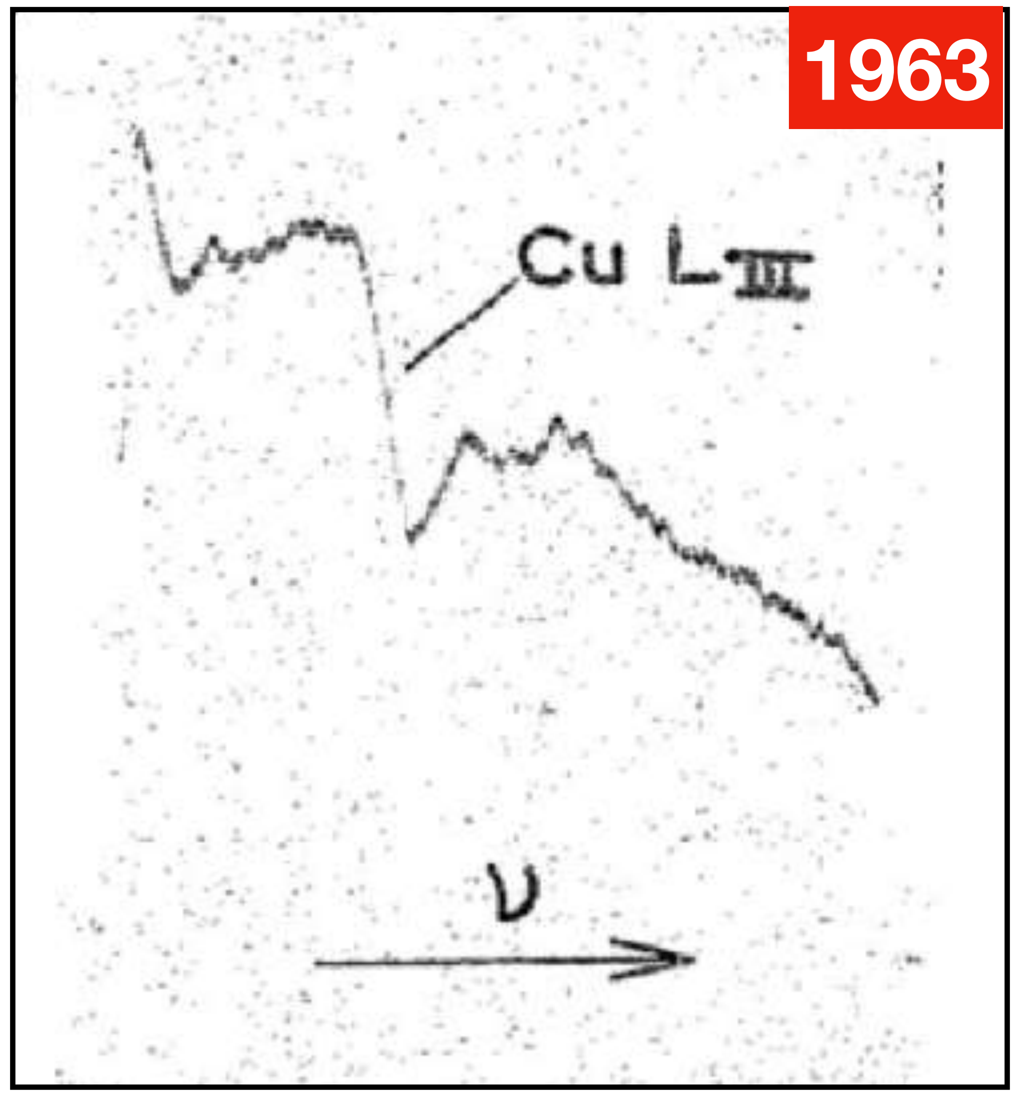

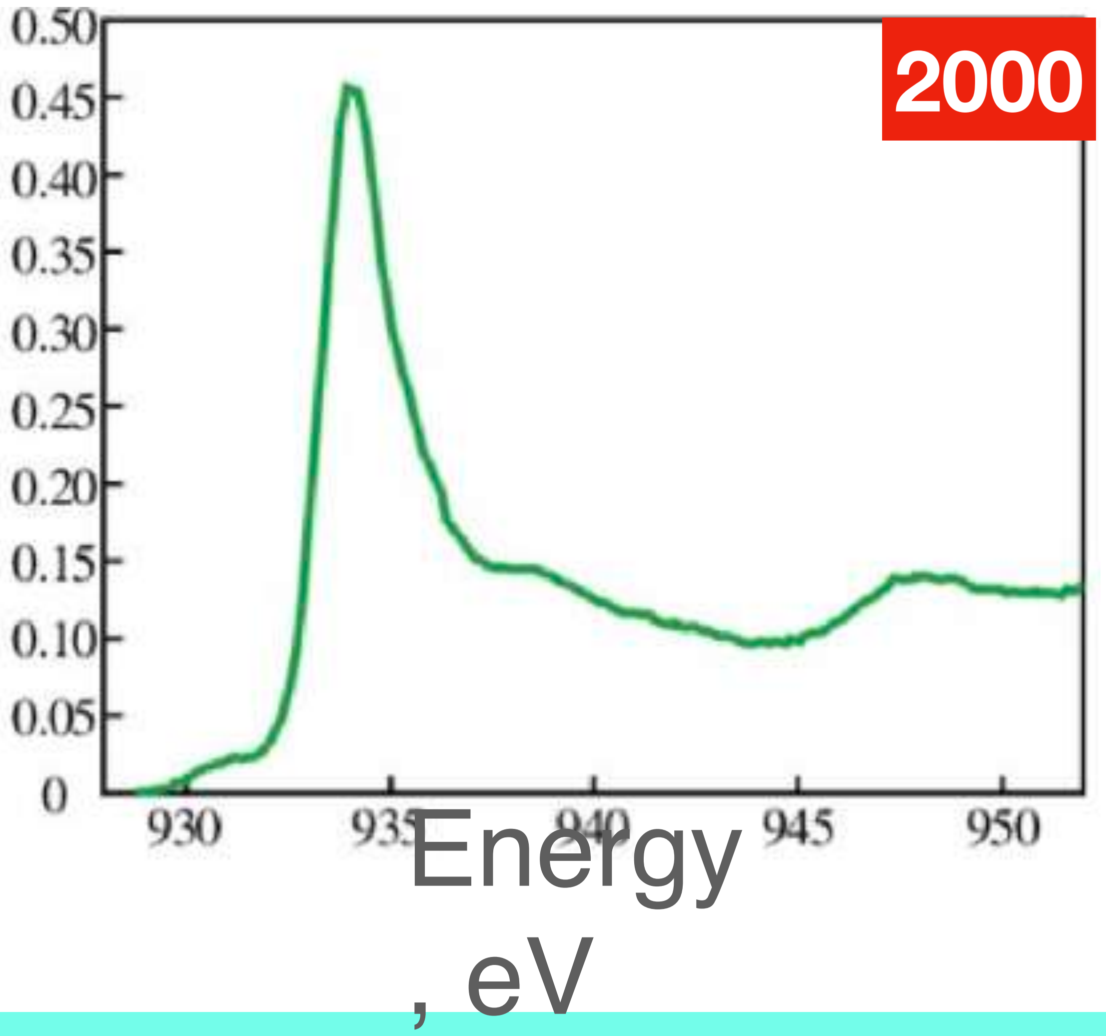

Cauchois, Y., Bonnelle, C. & Missoni, G. (1963a). C. R. Acad. Sci. Paris, 257, 409–412.
Cauchois, Y., Bonnelle, C. & Missoni, G. (1963b). C. R. Acad. Sci. Paris, 257, 1242–1244.

TANTALUS @ Madison, Wisconsin, USA
First dedicated synchrotron source (1968)

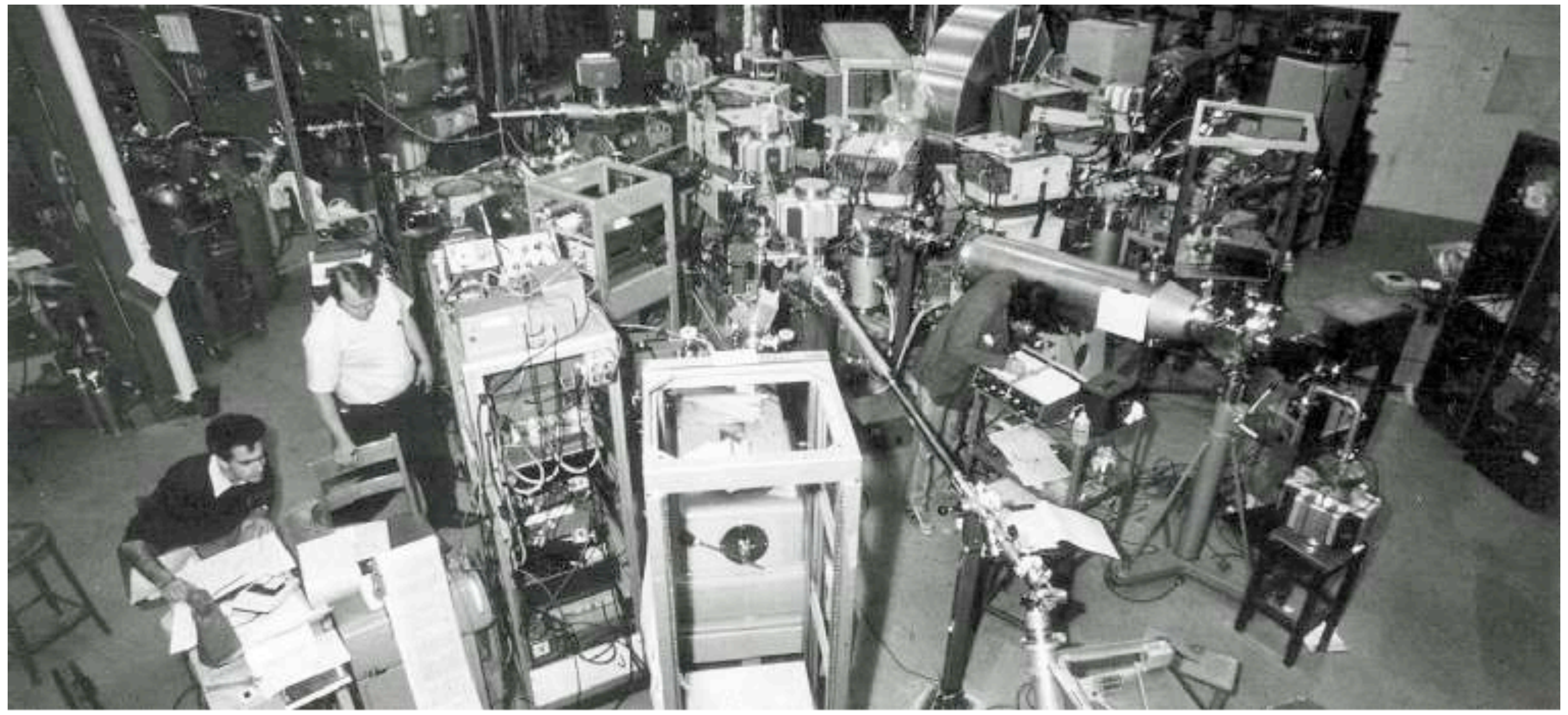

Figure 2: Tantalus and Ed Rowe, its primary builder and director of SRC.

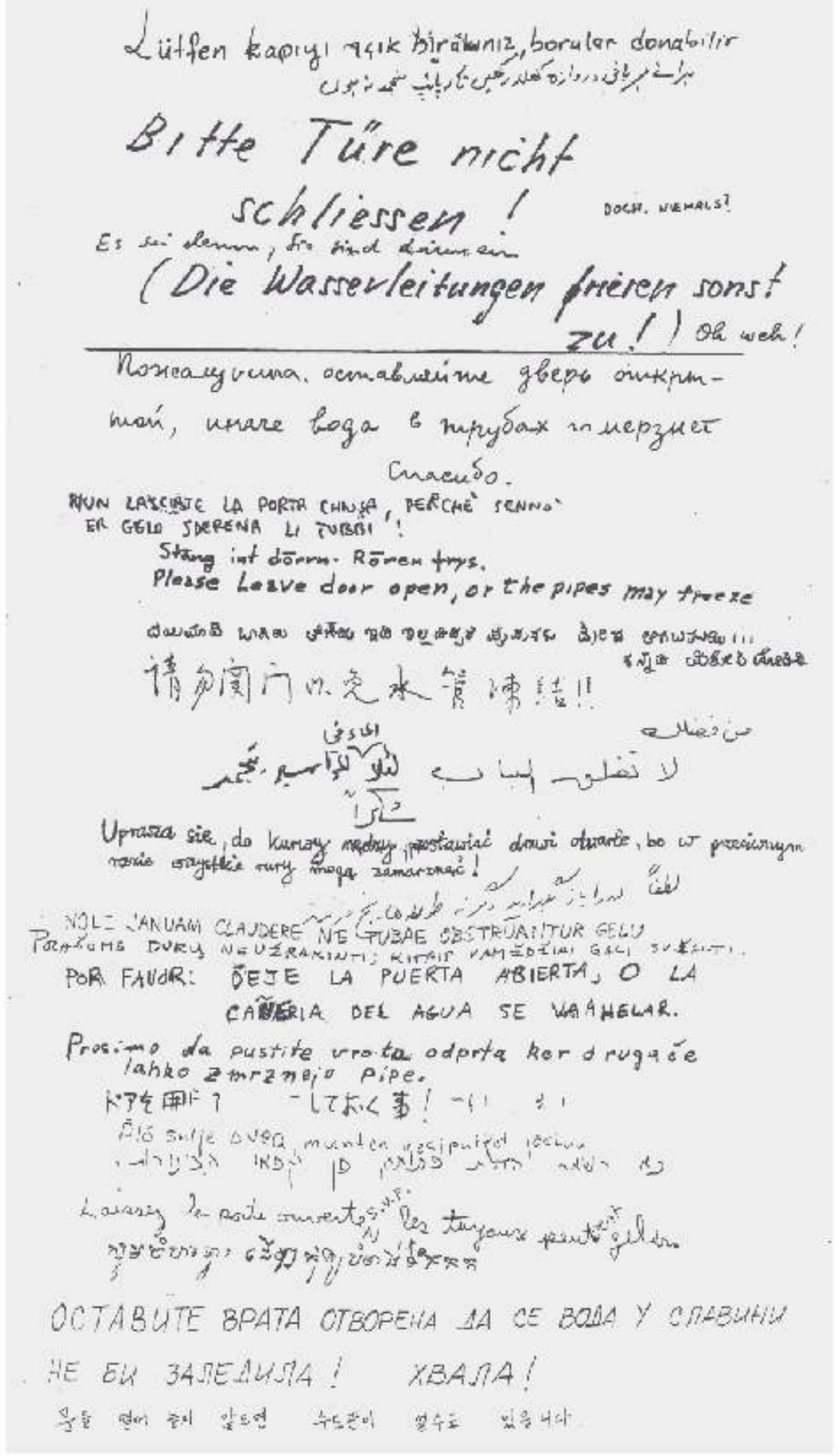

Figure 3: Restroom door in the Tantalus vault requesting users, no matter what language they spoke, to leave the door open when they leave.

A very brief history

1960-1970's in parasitic operations

X-ray diffraction,
Protein crystallography
X-Ray spectroscopy (XAFS-XANES-UV-IR
Absorption Contrast Imaging

1970-1980 First generation dedicated sources

Mostly bending magnet radiation beam lines

1980-1990 Second generation, some wigglers and undulators

1990-2010 Third generation, undulator/wiggler dominant sources

2010-2020 X-Ray Free electron laser development

2020-2030 4th. Generation high brightness multi bend achromat lattices

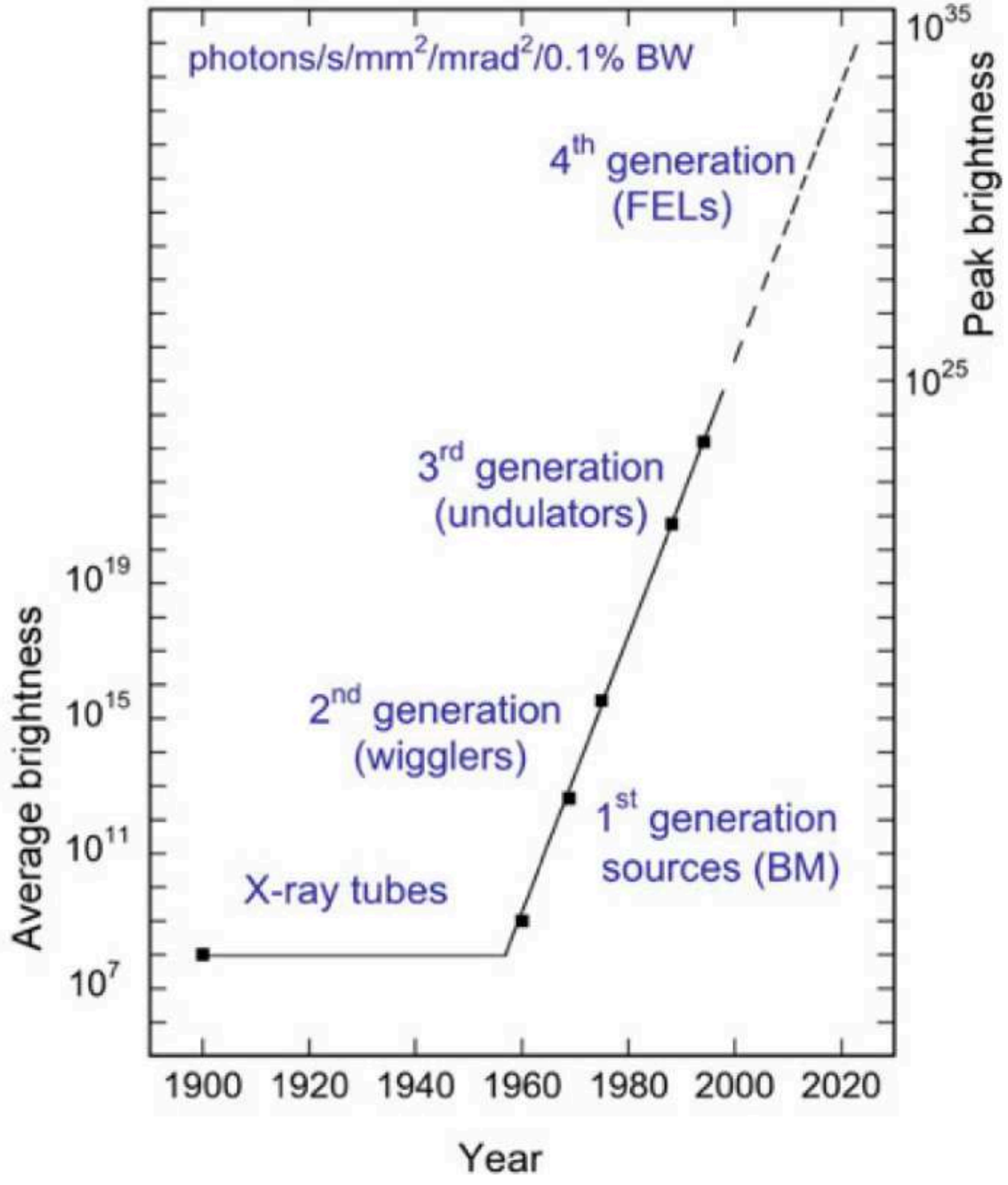

What are the unique characteristics of synchrotron radiation?

1. Bright
2. Collimated
3. Polarized
4. Pulsed
5. Tunable
6. Coherent

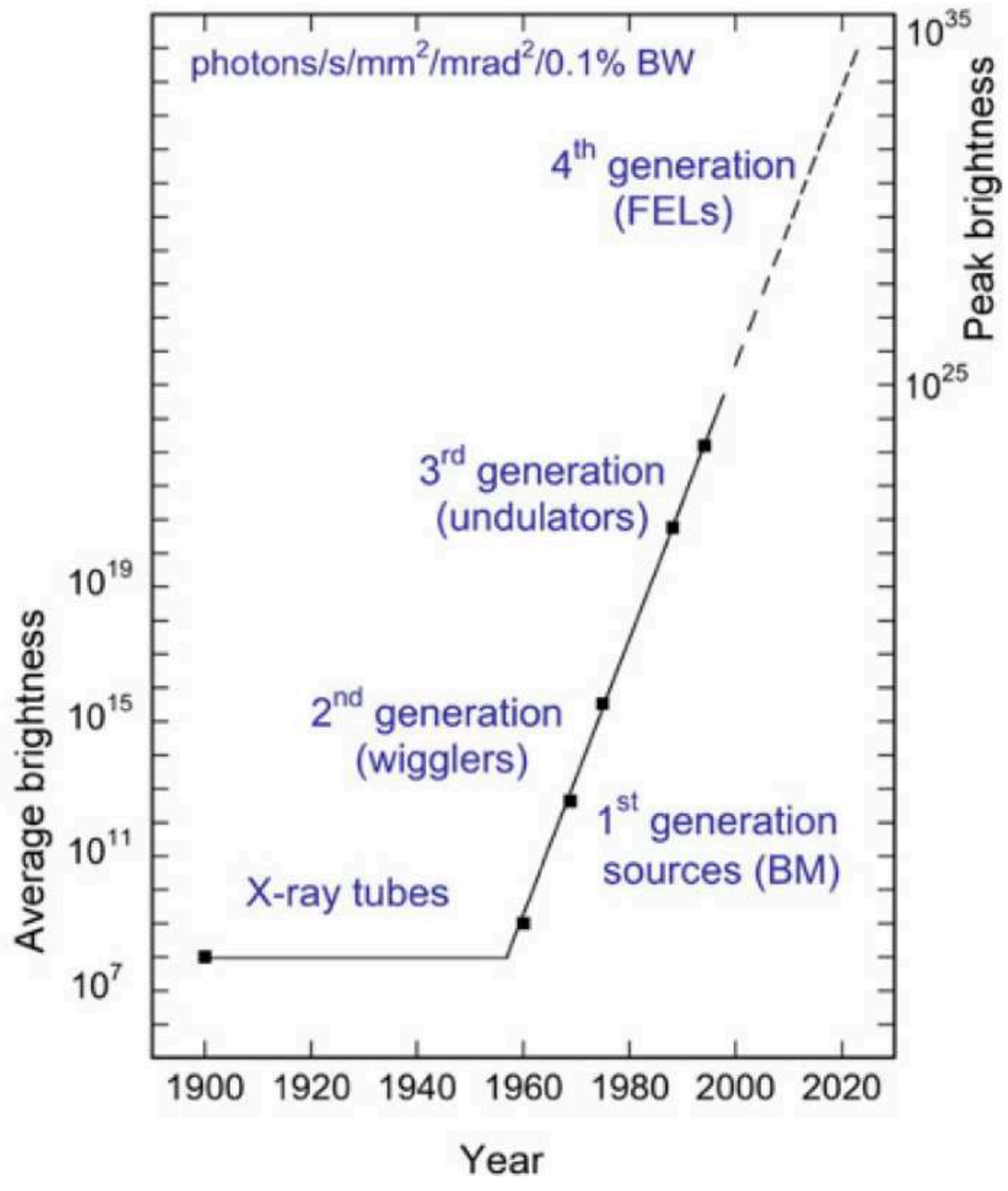

SESAME parameters

Flux on the sample is a function of
i) current in the ring
ii) Area of the electron beam
iii) Source and photon divergence
iv) Energy bandwidth selected by the optics

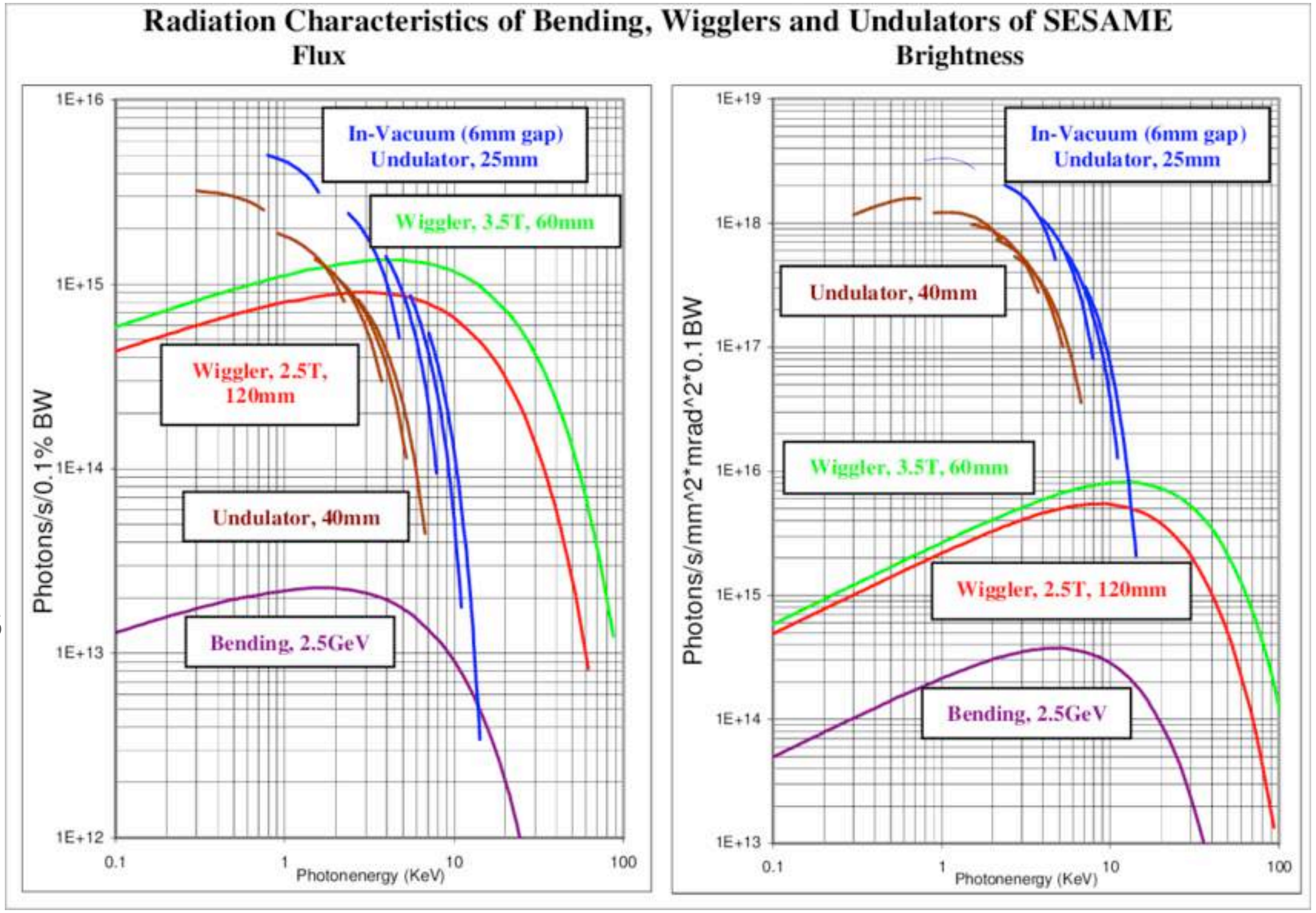

Brightness: photons / sec. mm^2. mrad^2 .(0.1% BandWidth)
Flux : photons/sec. (0.1 % BW)

What are the different sources of radiation at a

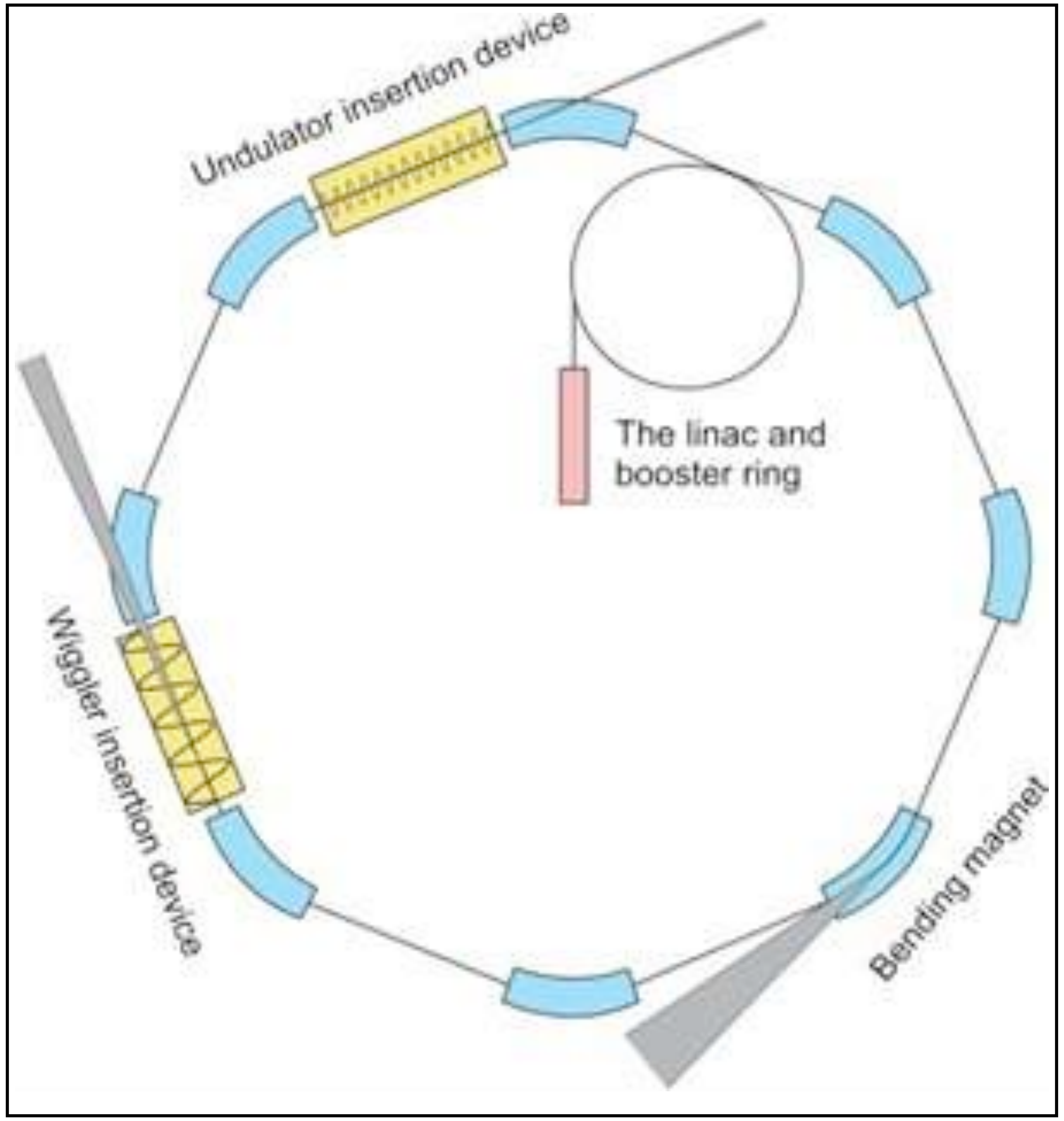

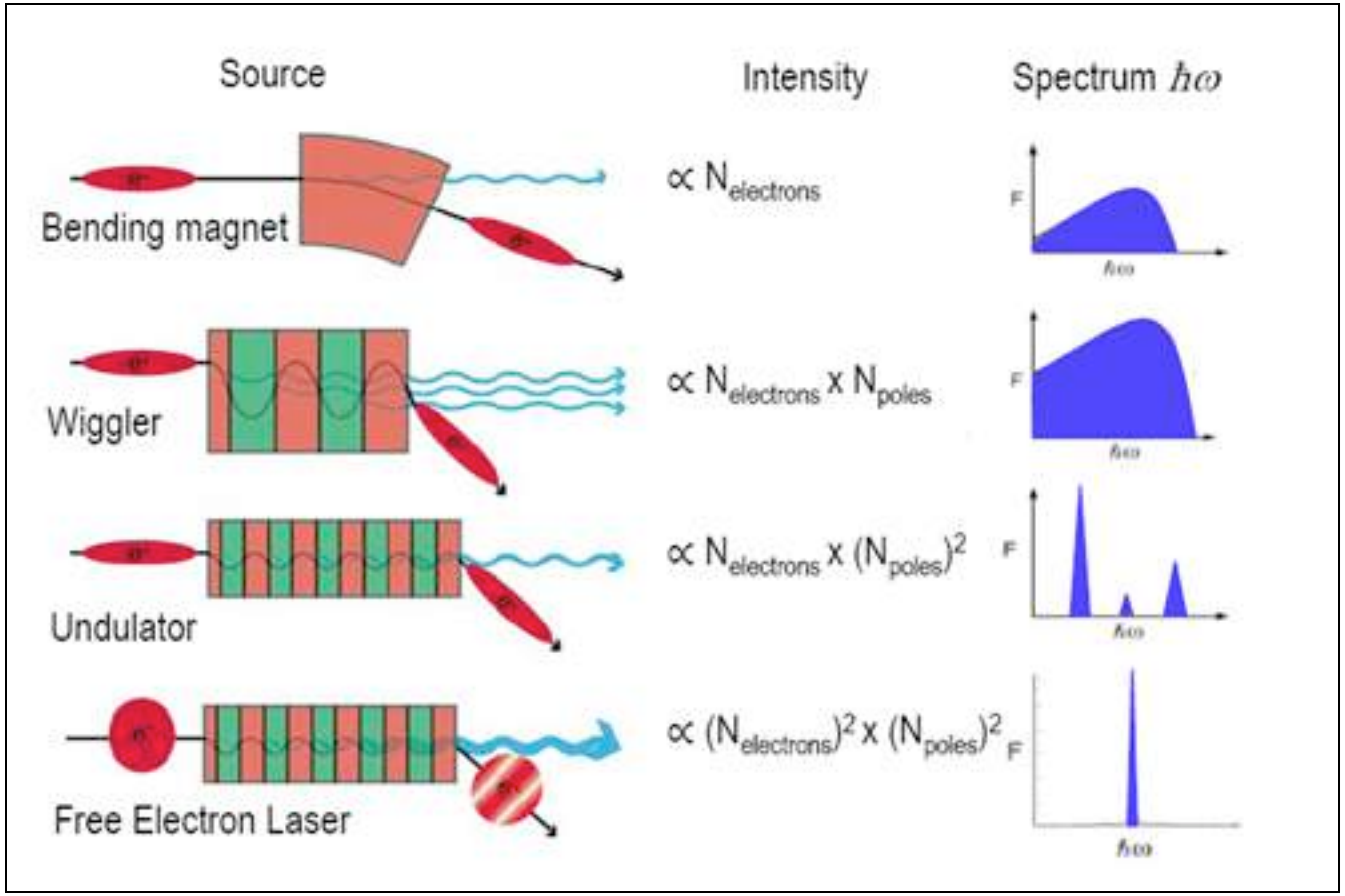

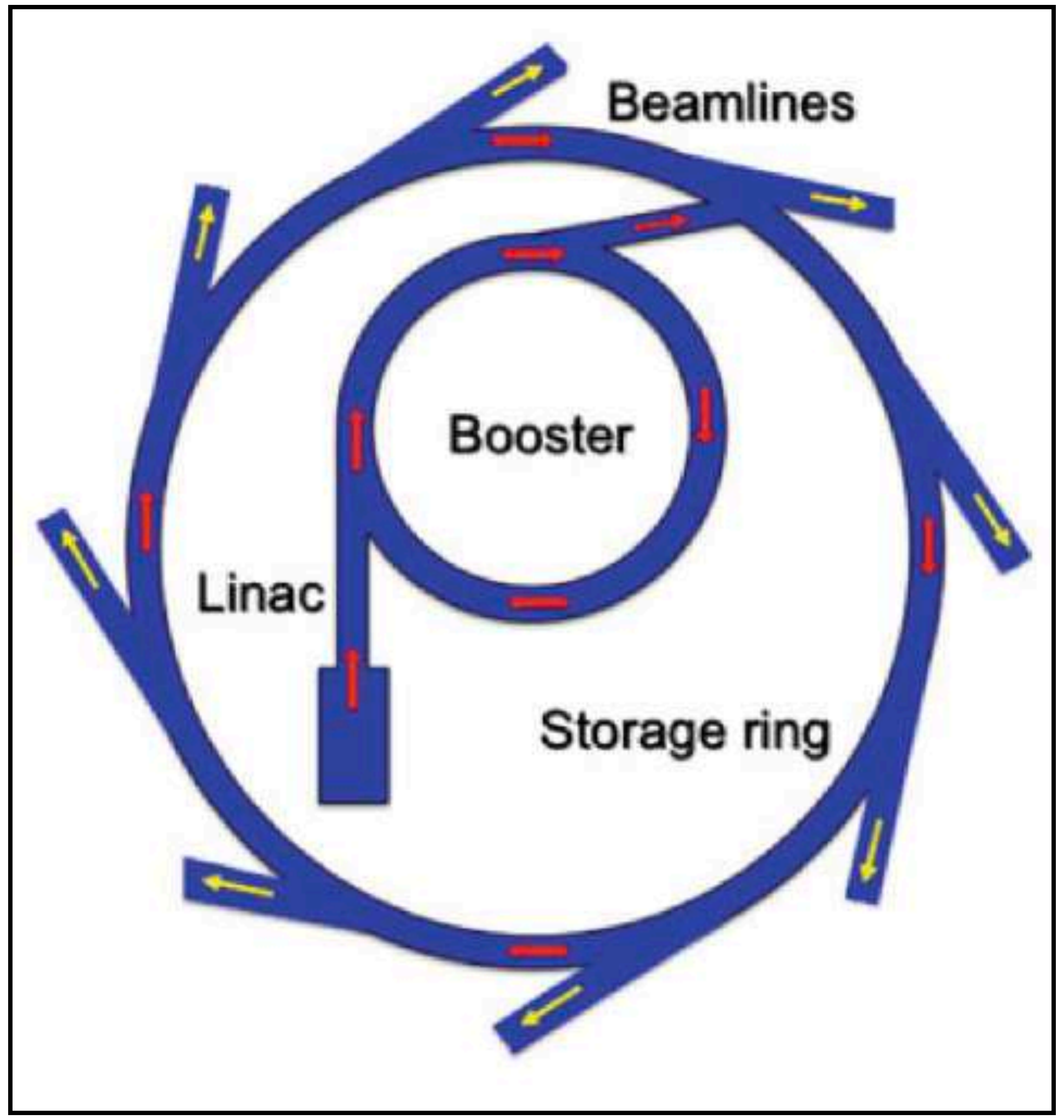
Beamlines
Booster
Linac
Storage ring

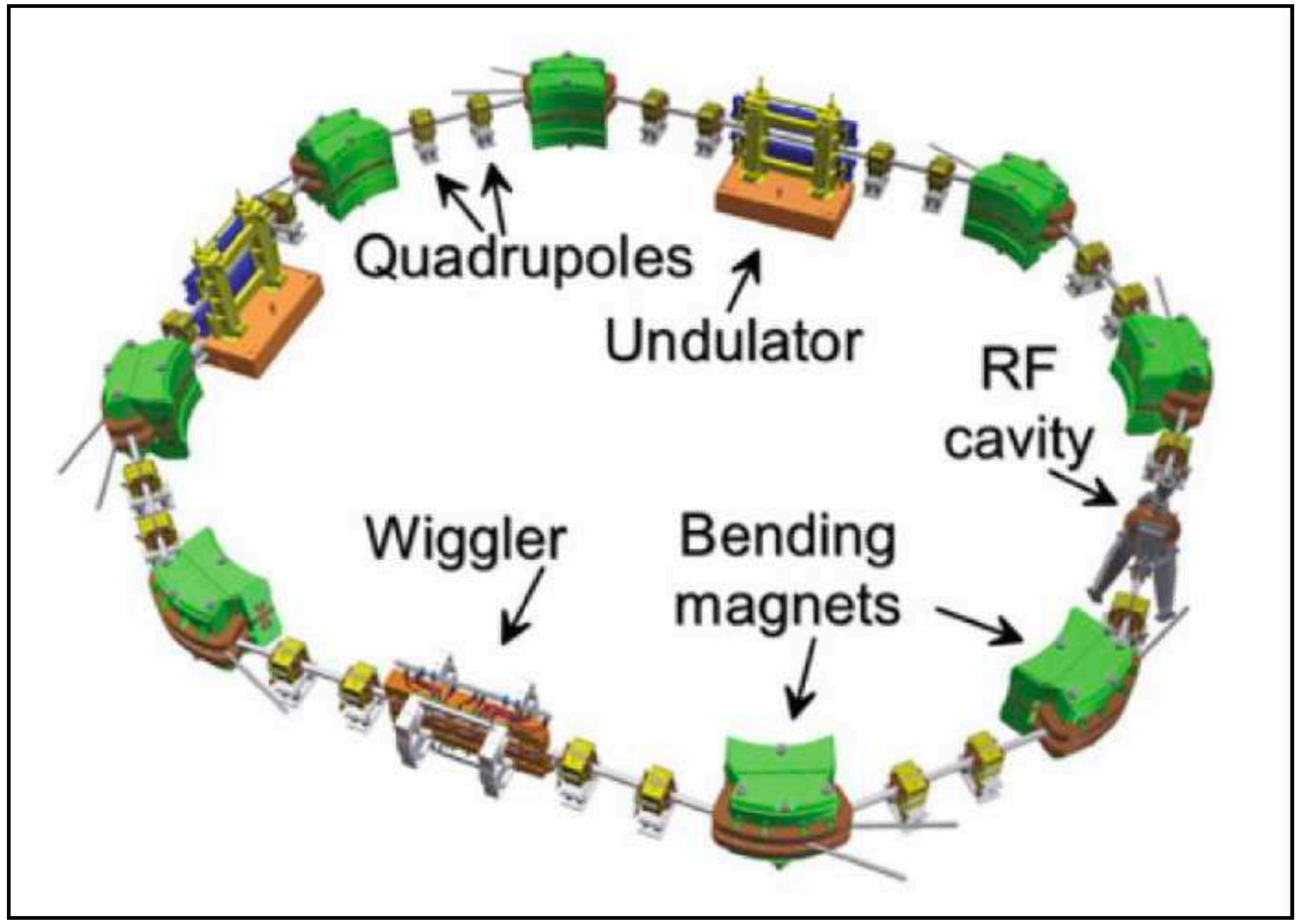
Quadrupoles
Undulator
RF
cavity
Wiggler
Bending
magnets

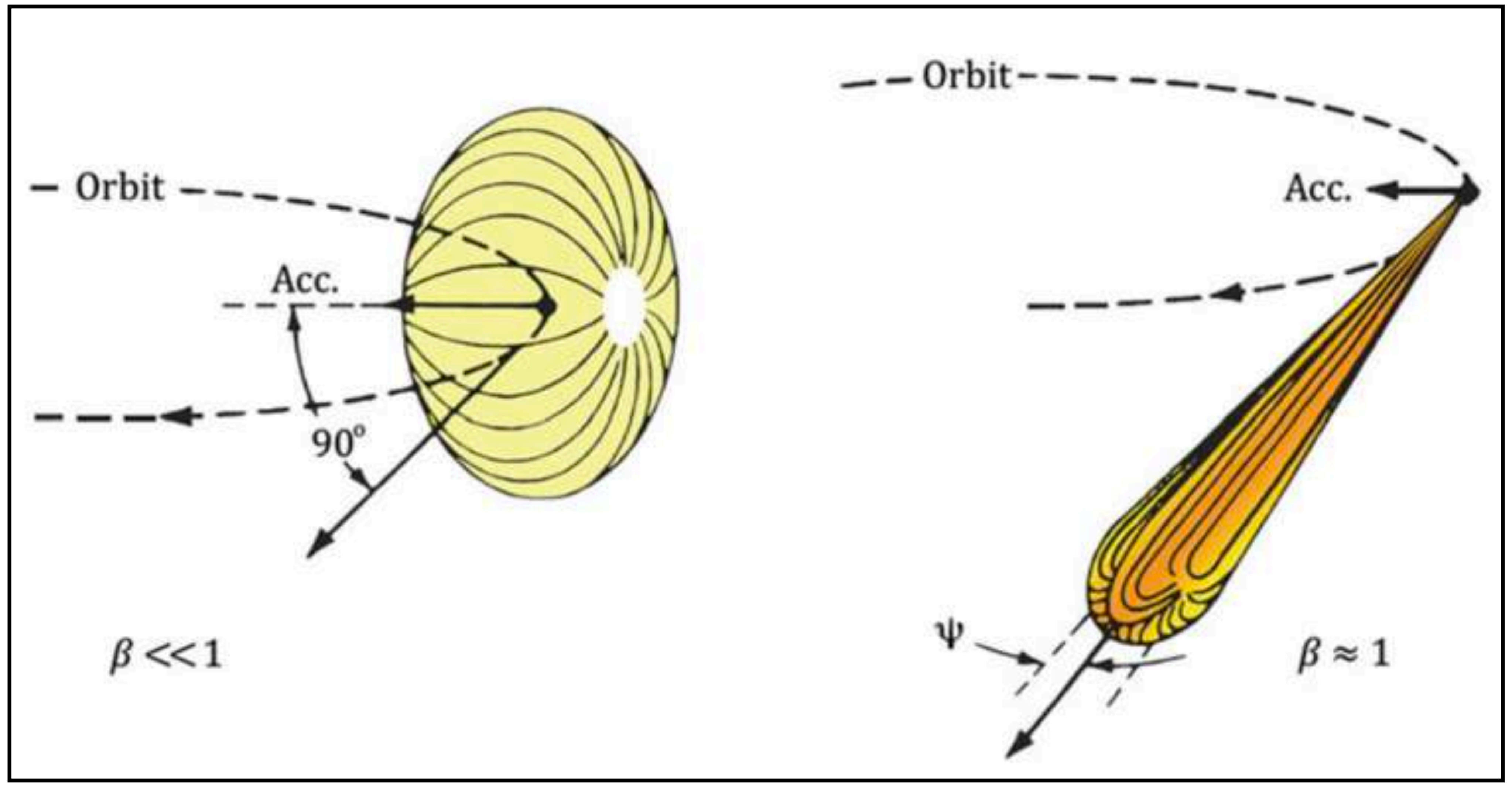
Orbit
Acc.
90°
β <<1
Orbit
Acc.
ψ
β ≈ 1

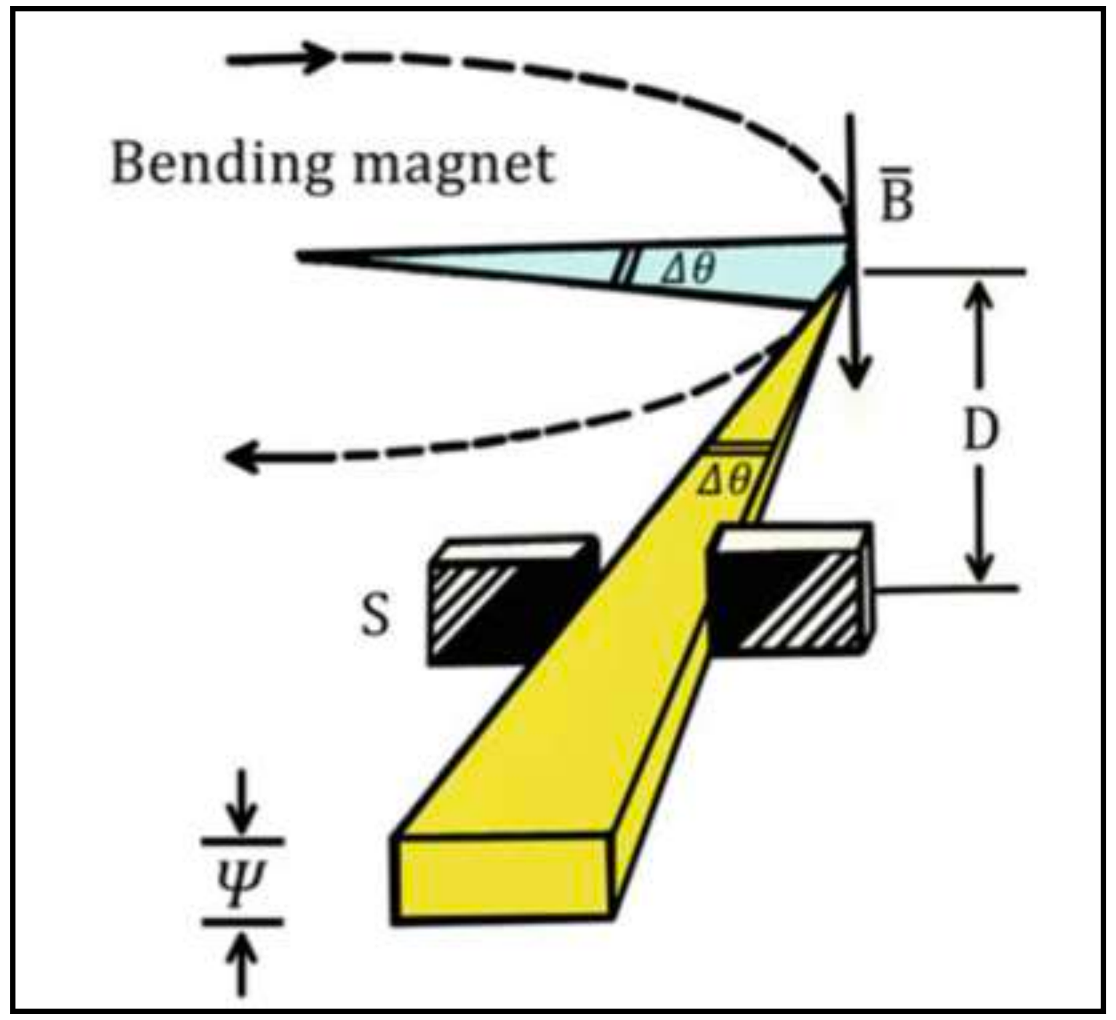
Bending magnet
B̄
Δθ
D
Δθ
S
Ψ


Settimio Mobilio · Federico Boscherini
Carlo Meneghini Editors
Synchrotron
Radiation
Basics, Methods and Applications

What are the key parameters of an undulator ?

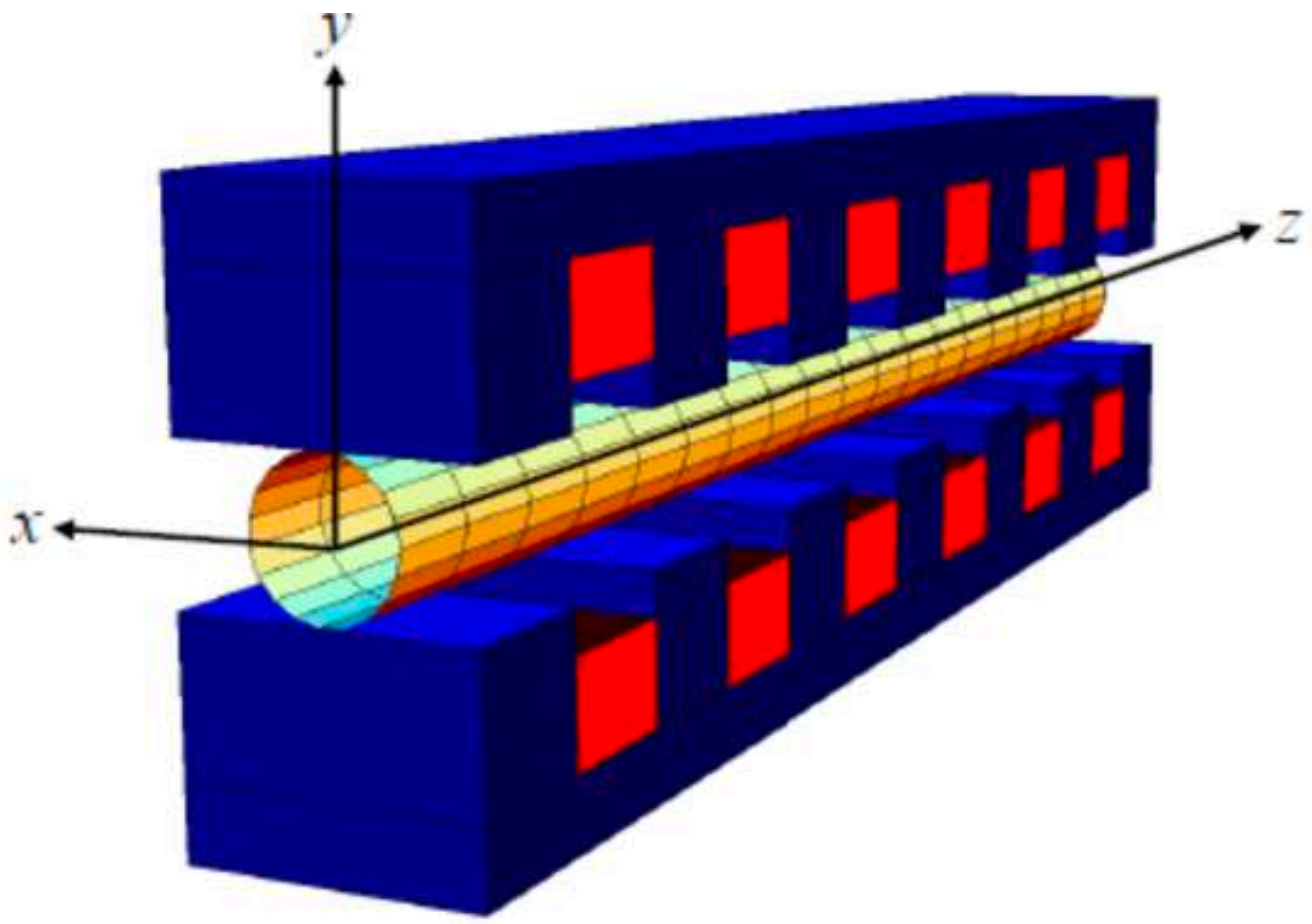

$$B_y = B_w \sin(k_z z)$$

Peak field = B_w

Period = $\lambda_w = \frac{2\pi}{k_z}$

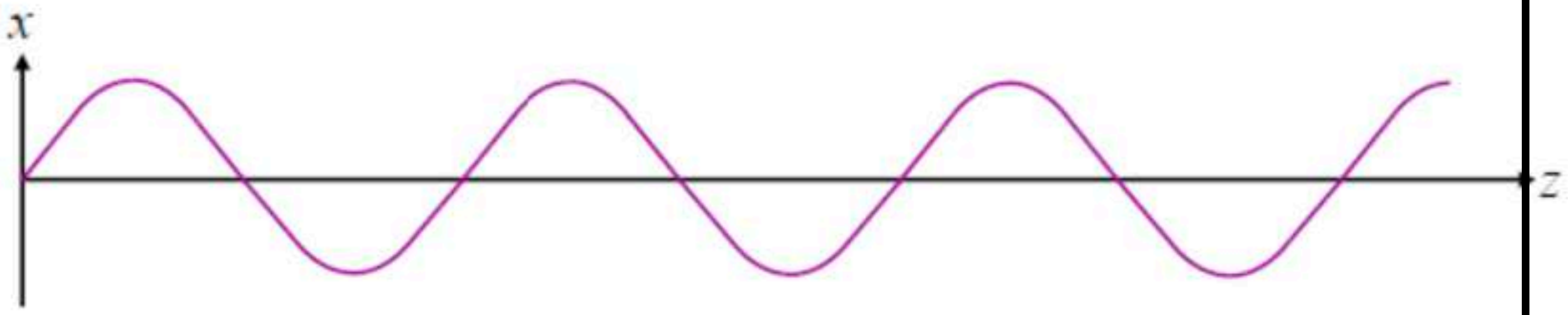

Deflection parameter K:

$$K = \frac{e}{2\pi m_o c} B_W \lambda_W = 0.934\, B_W[T]\, \lambda_W[cm]$$

What are the different types of undulators ?

Permanent magnet undulators, PMU
In-vacuum PMU
In vacuum cryogenically cooled undulators
Revolving undulators
Polarization manipulation undulators (APPLE_II)
Superconducting undulators

Wigglers
3-pole wigglers

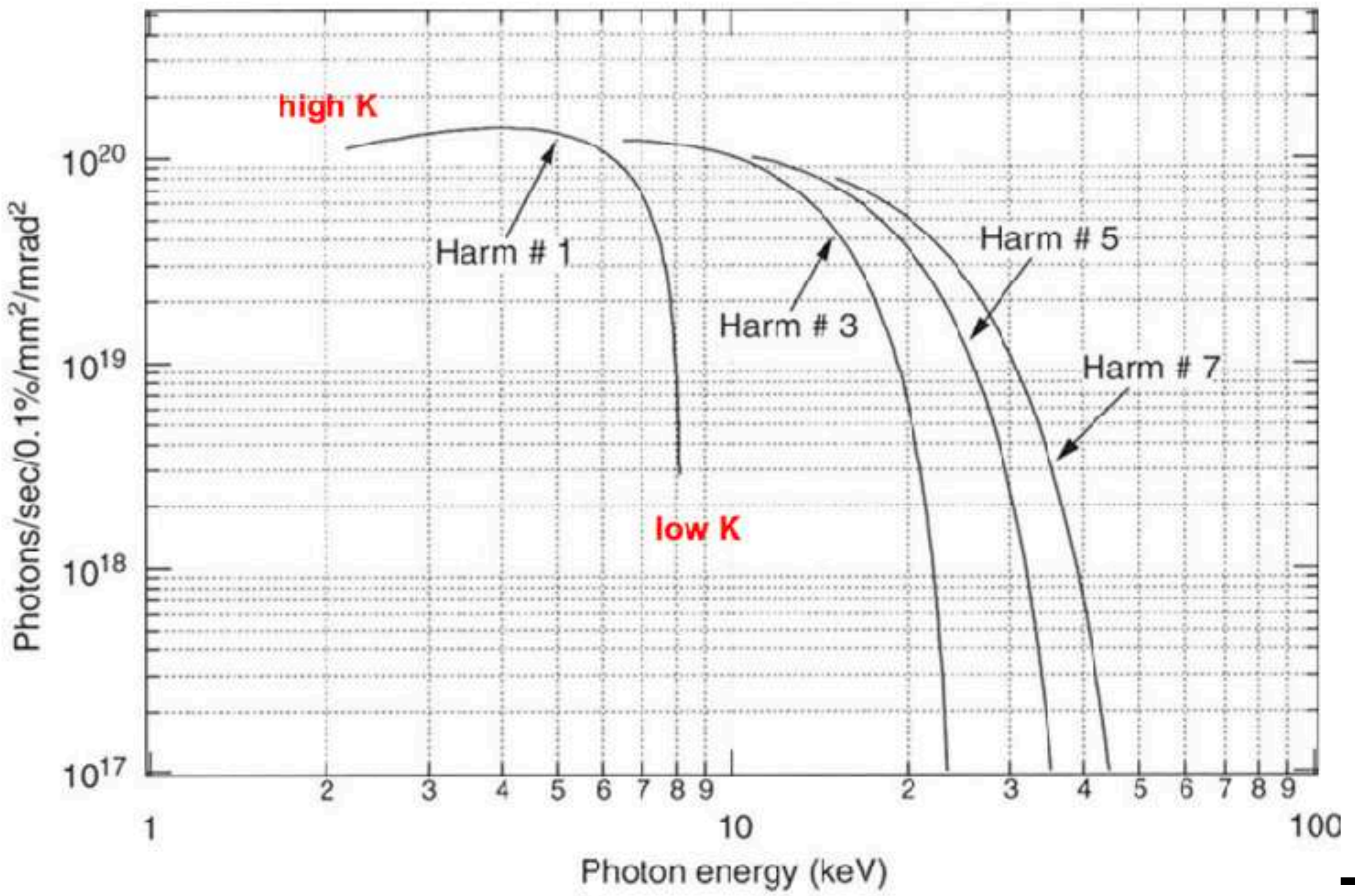

What are the key parameters of an undulator ?

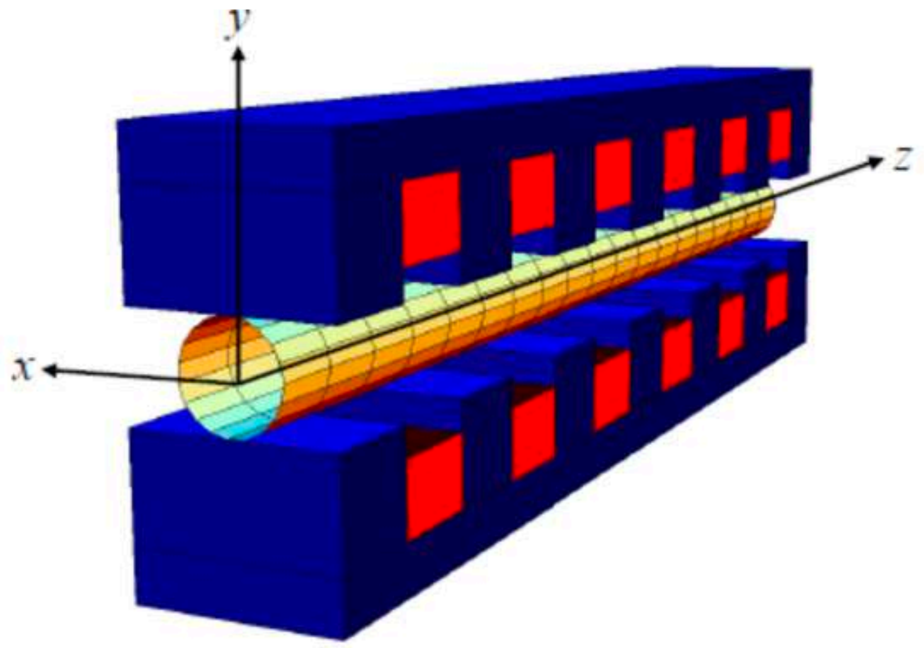

$$B_y = B_w \sin(k_z z)$$

Peak field $= B_w$

Period $= \lambda_w = \frac{2\pi}{k_z}$

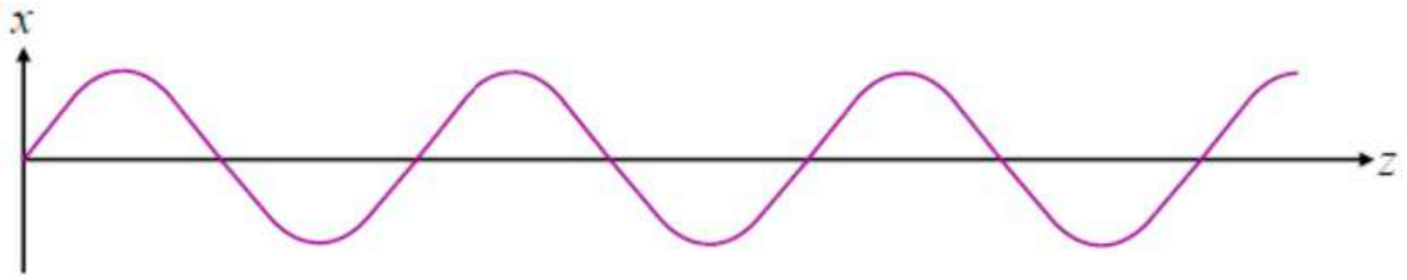

Deflection parameter K:

$$K = \frac{e}{2\pi m_o c} B_W \lambda_W = 0.934\ B_W[T]\ \lambda_W[cm]$$

In selecting an undulator for your application, you need to compromise between high heat load, energy tunability range, coverage of 1st, 3rd, and 5th harmonics, number of poles, and cost and reliability.

What are different types of undulators ?

Permanent magnet undulators, PMU
In-vacuum PMU
In vacuum cryogenically cooled undulators
Revolving undulators
Polarization manipulation undulators (APPLE_II)
Superconducting undulators

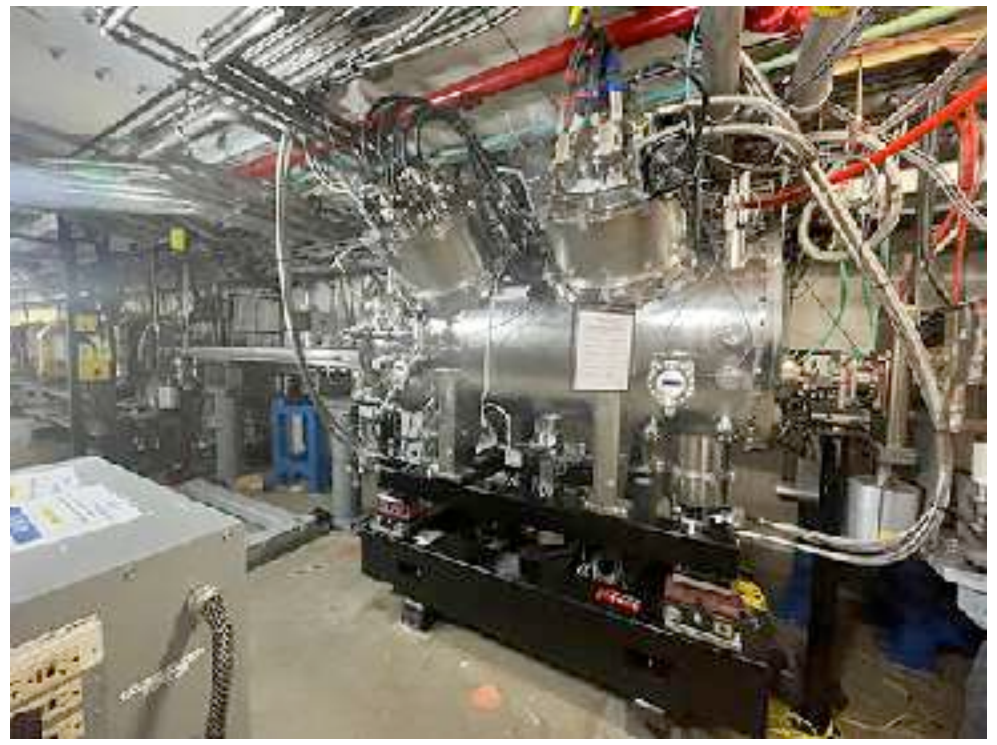

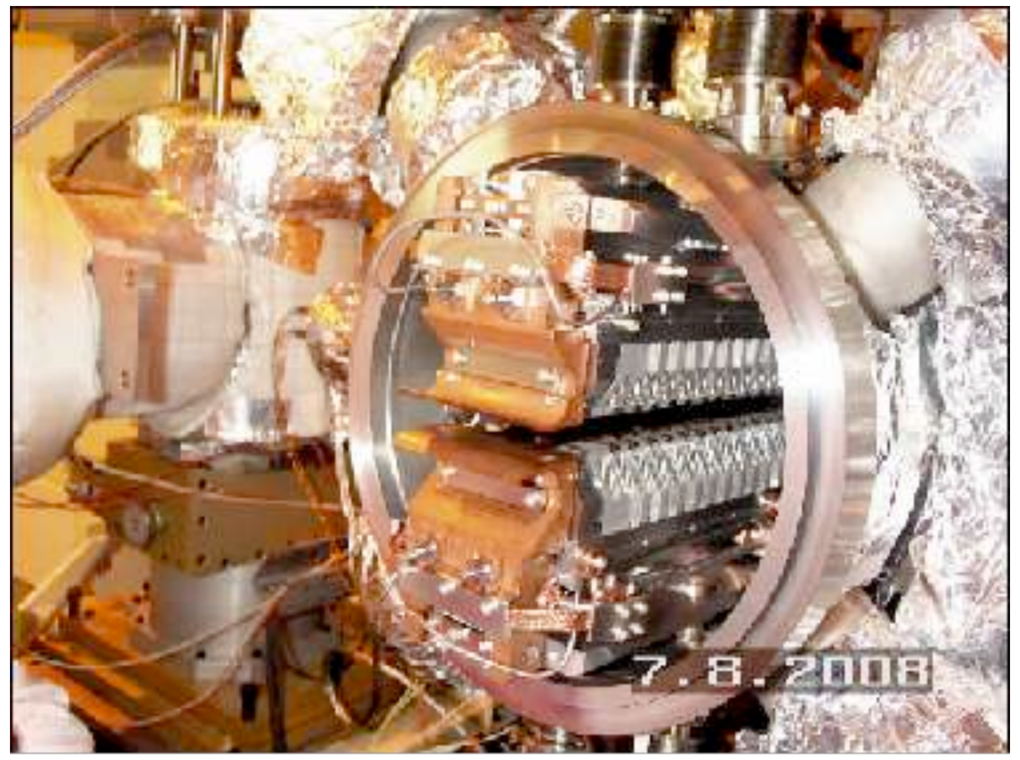

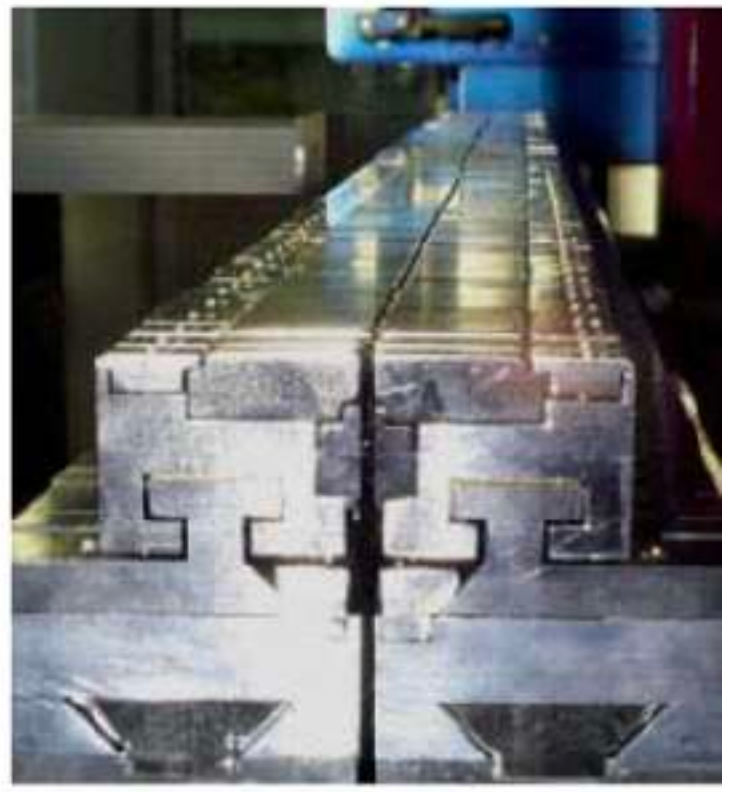

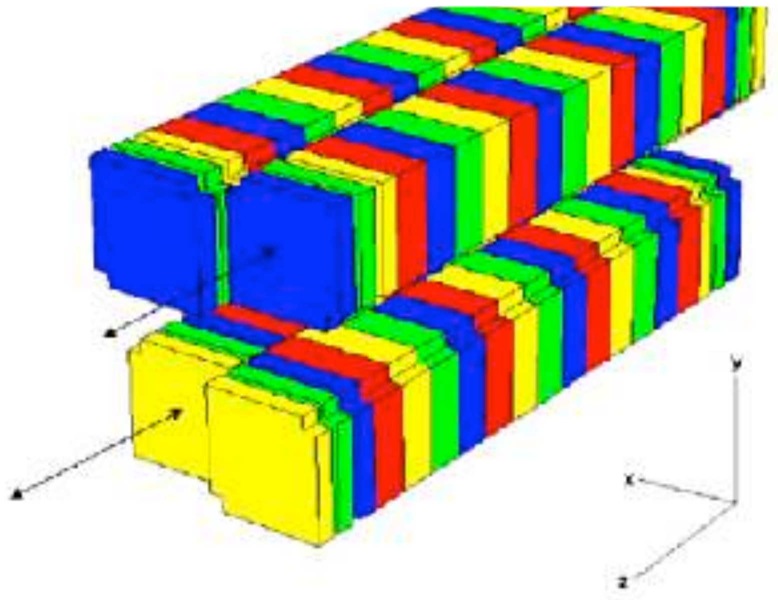

1. Bright
2. Collimated
3. Polarized
4. Pulsed
5. Tunable

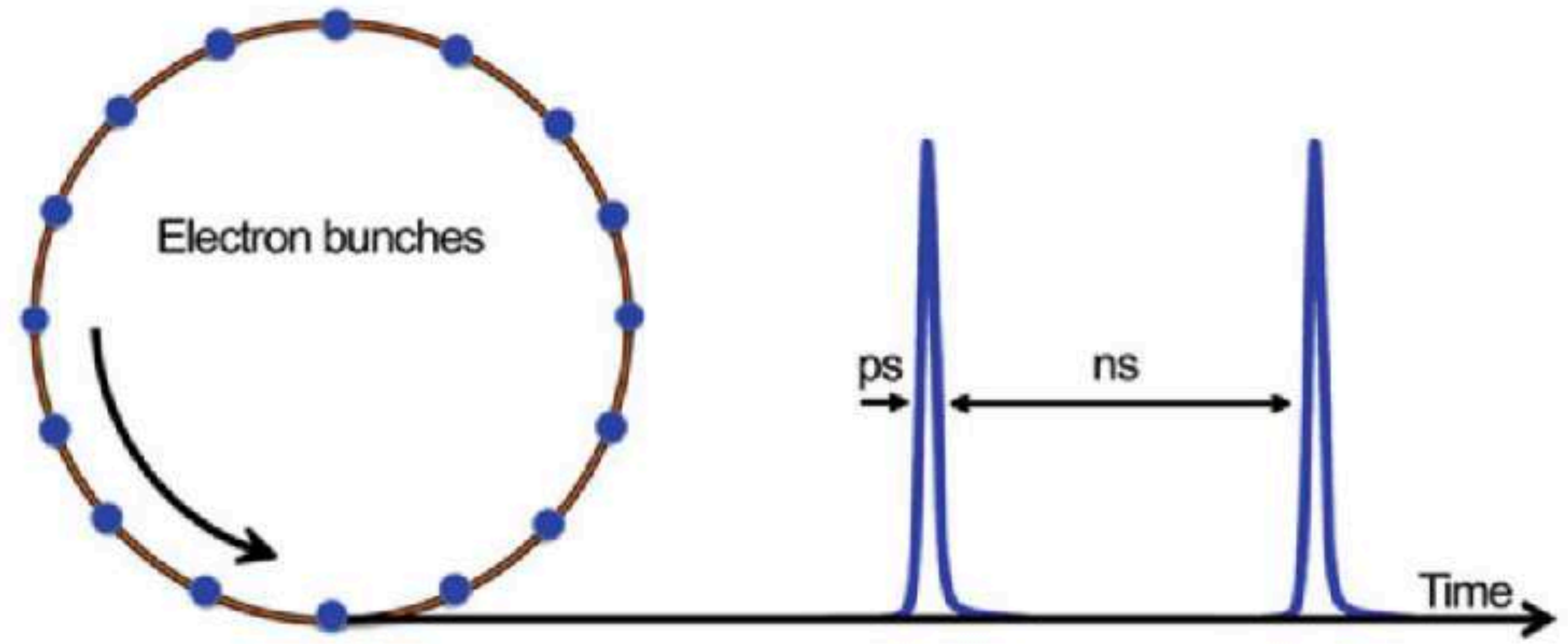

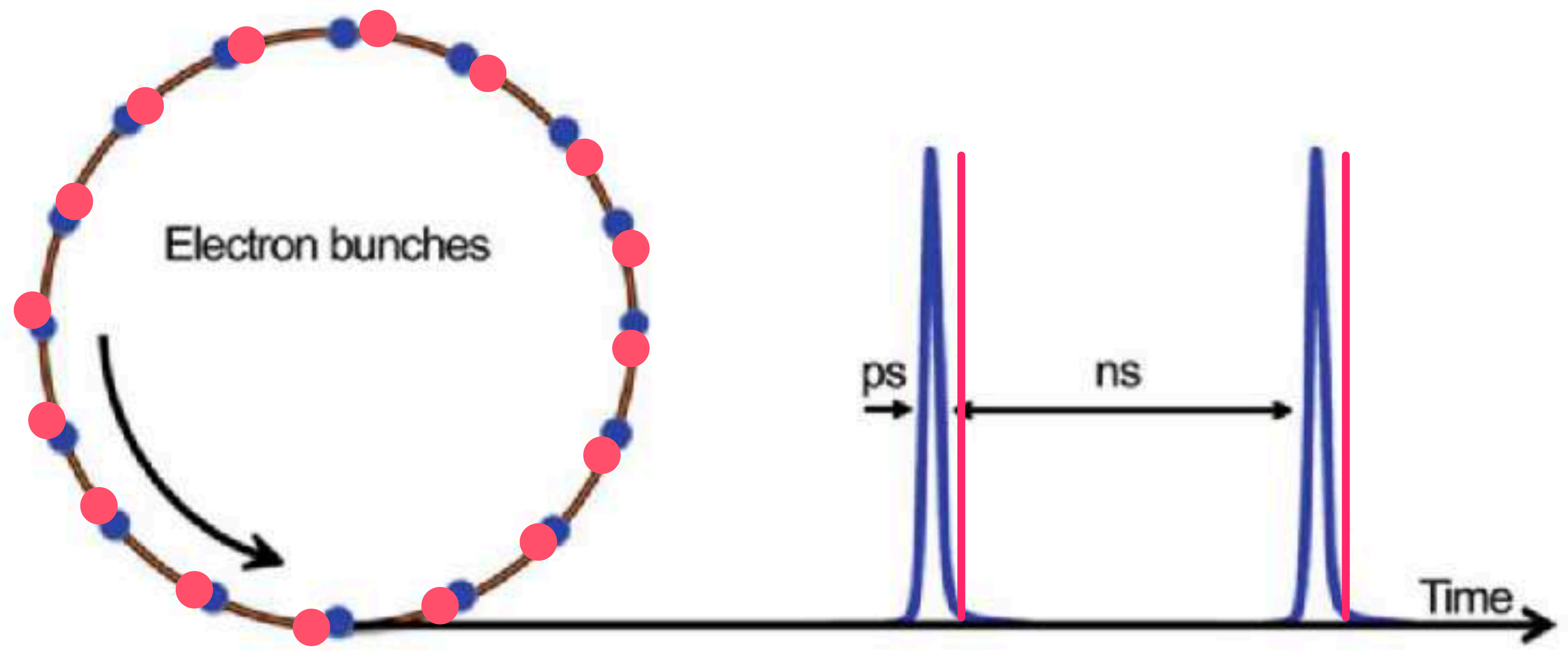

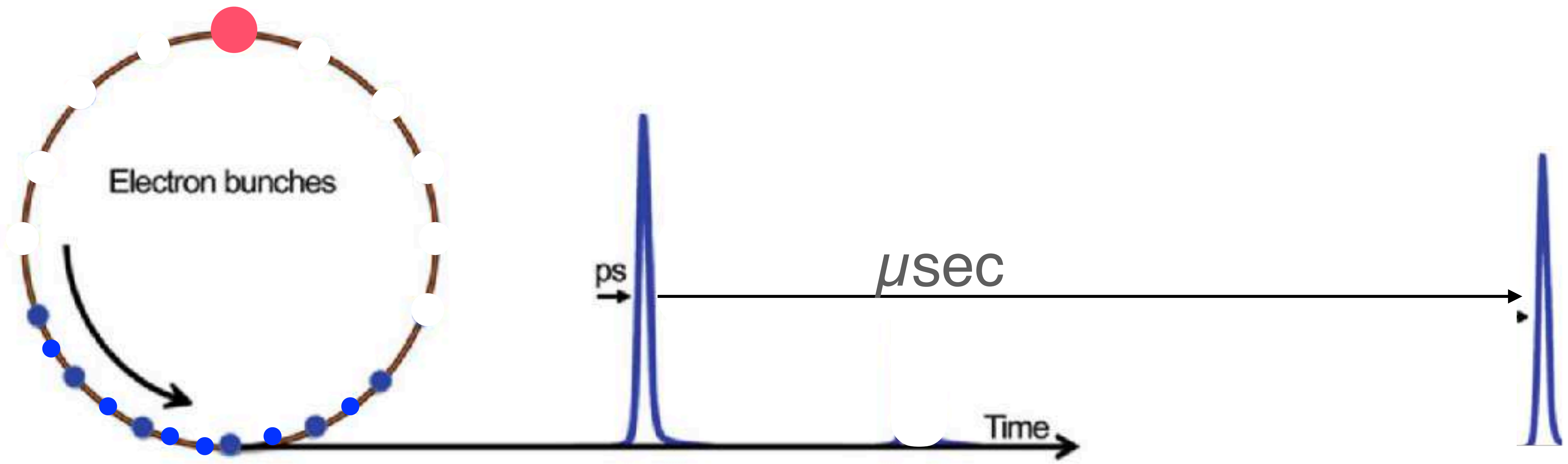

Advanced Photon Source
Argonne National Laboratory

Table 1.1. APS Upgrade Performance Parameters

	APS-U Timing Mode	APS-U Brightness Mode	APS Now	Units
Electron Beam Energy	6	6	7	GeV
Electron Beam Current	200	200	100	mA
Number of Bunches	48	324	24	
Effective Emittance	32	42	3113	pm
Emittance Ratio	1.0	0.1	0.013	
Horizontal Beam Size (rms)	12.9	14.7	280	μm
Horizontal Divergence (rms)	2.5	2.8	11.6	μrad
Vertical Beam Size (rms)	8.8	3.2	10.0	μm
Vertical Divergence (rms)	3.7	1.3	3.4	μrad
Stability of Beam Position/Angle	<10%	<10%	<10%	
Brightness - 20 keV(**)	154	325	0.6	10^{20} [a]
Pinhole Flux - 20 keV(**)	186	217	20.1	10^{13} [b]
Coherent Flux - 20 keV(**)	148	312	0.6	10^{11} ph/s
Single Bunch brightness – 20 keV	321	100	2.6	10^{18} [a]

[a] photons/sec/0.1%BW/mm^2 /mrad^2
[b] photons/sec/0.1%BW in 0.5mm *times* 0.5mm pinhole @ 30 m
** Nominal energy based on choice of insertion device. Maximum value for an ID optimized for 20keV

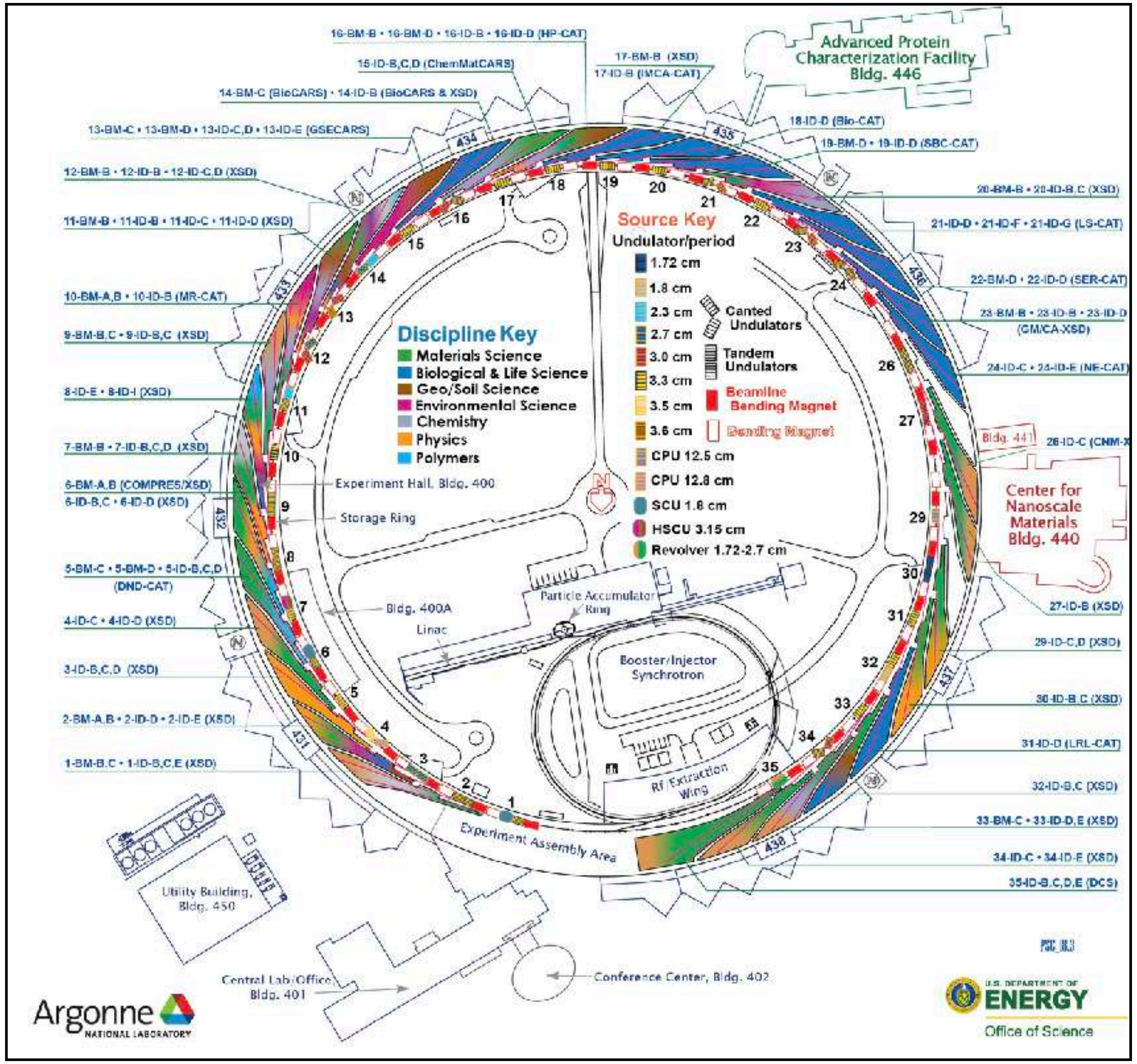

SESAME @ December, 2024

Five Operational Beamlines and one under construction:

1) IR- InfraRed Spectroscopy and Microscopy

2) XAFS/XRF- X-Ray Absorption/Fluorescence Spectroscopy

3) MS : Materials Science & X-Ray Diffraction

4) HESEB: Soft x-ray spectroscopy beamline:

+ TX-PES (funded, under construction)

5) BEATS: X-Ray Tomography

6) TX-PES: Turkish Photo Electron Spectroscopy

Mostly on the floor

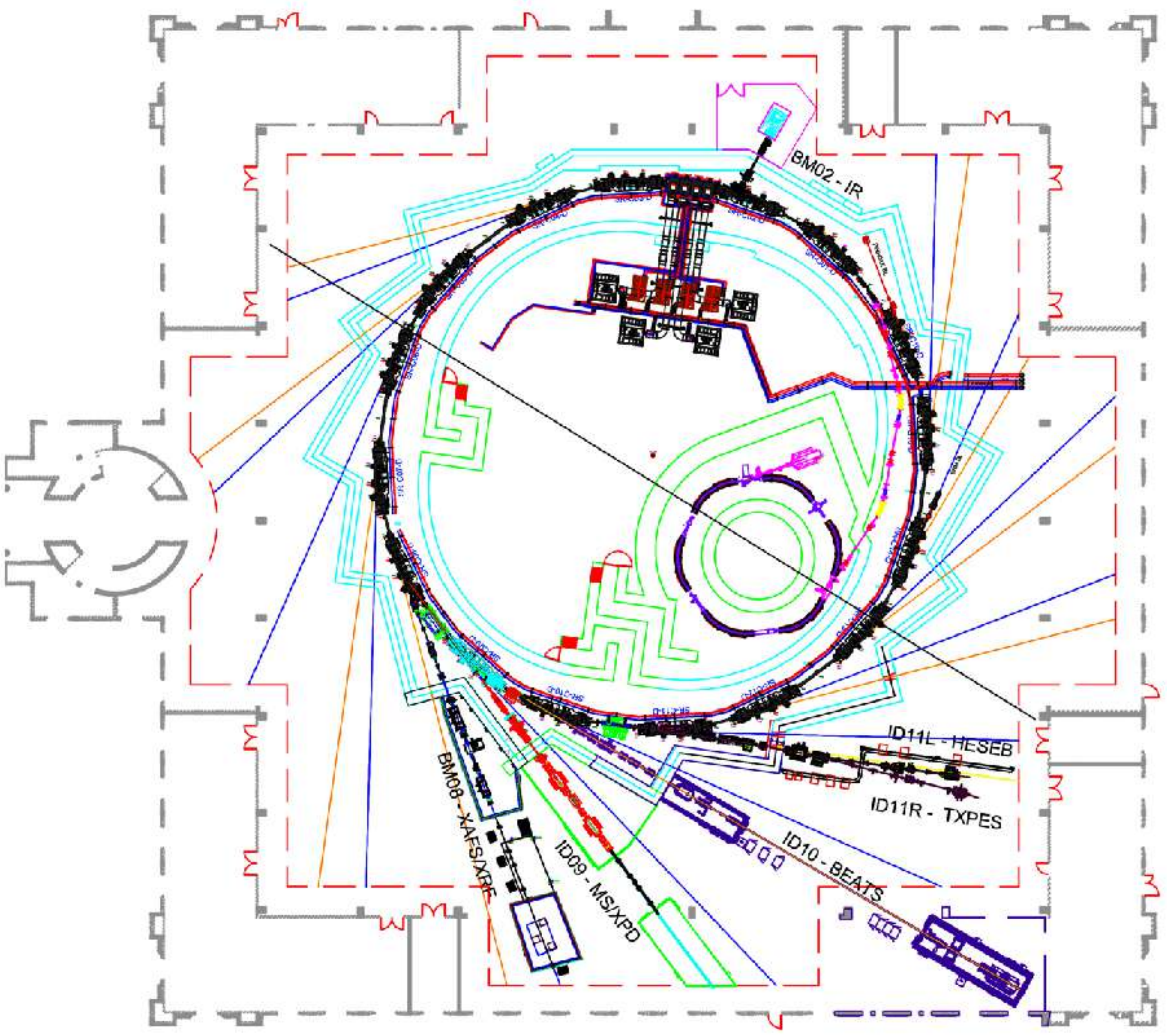

SESAME FACILITY

BESSY storage ring will not be used.

Main Ring Parameters:

Energy = 2.5 GeV

Circumference = 133.2 m

Emitt. = 26.0 nm.rad

16 Straights sections

{8 x 4.44 m + 8 x 2.38 m}

Up to 28 Beamlines:

12 Insertion Devices

16 Dipole ports.

Beamlines
length range from
21 m – 36.7 m

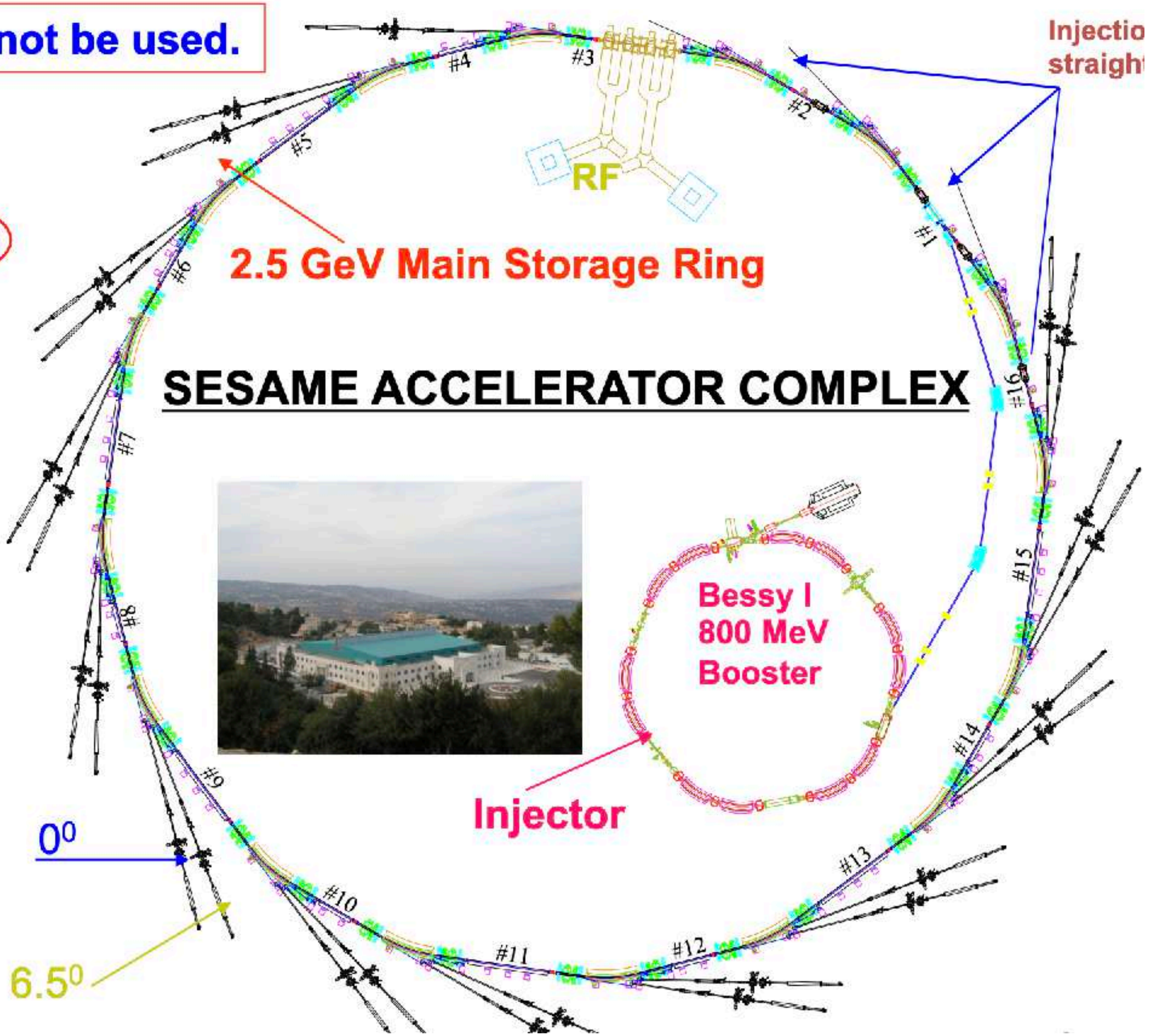

SESAME

Radiation from Bending Magnets, Wigglers and Undulators

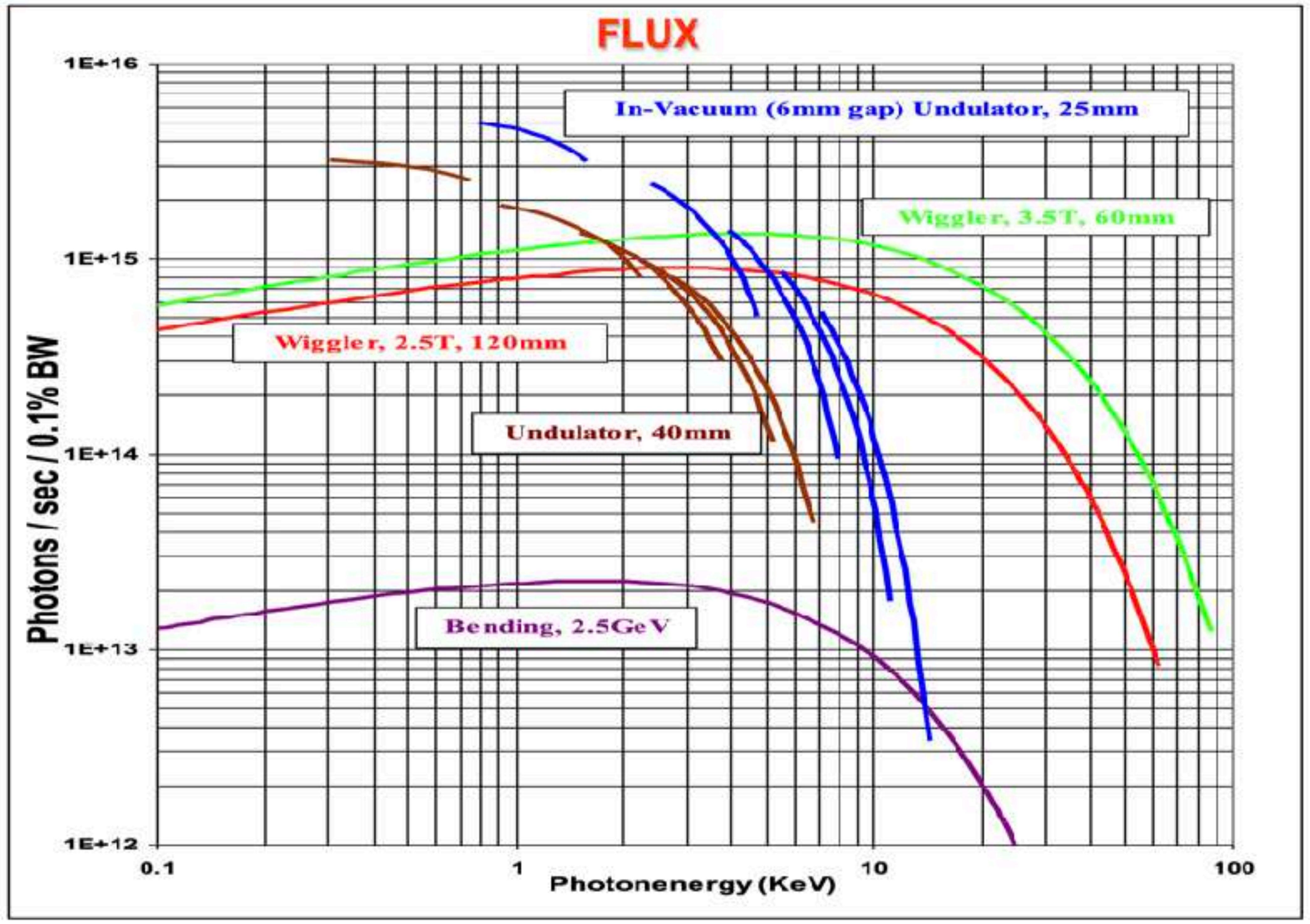

SESAME

Radiation from Bending Magnets, Wigglers and Undulators

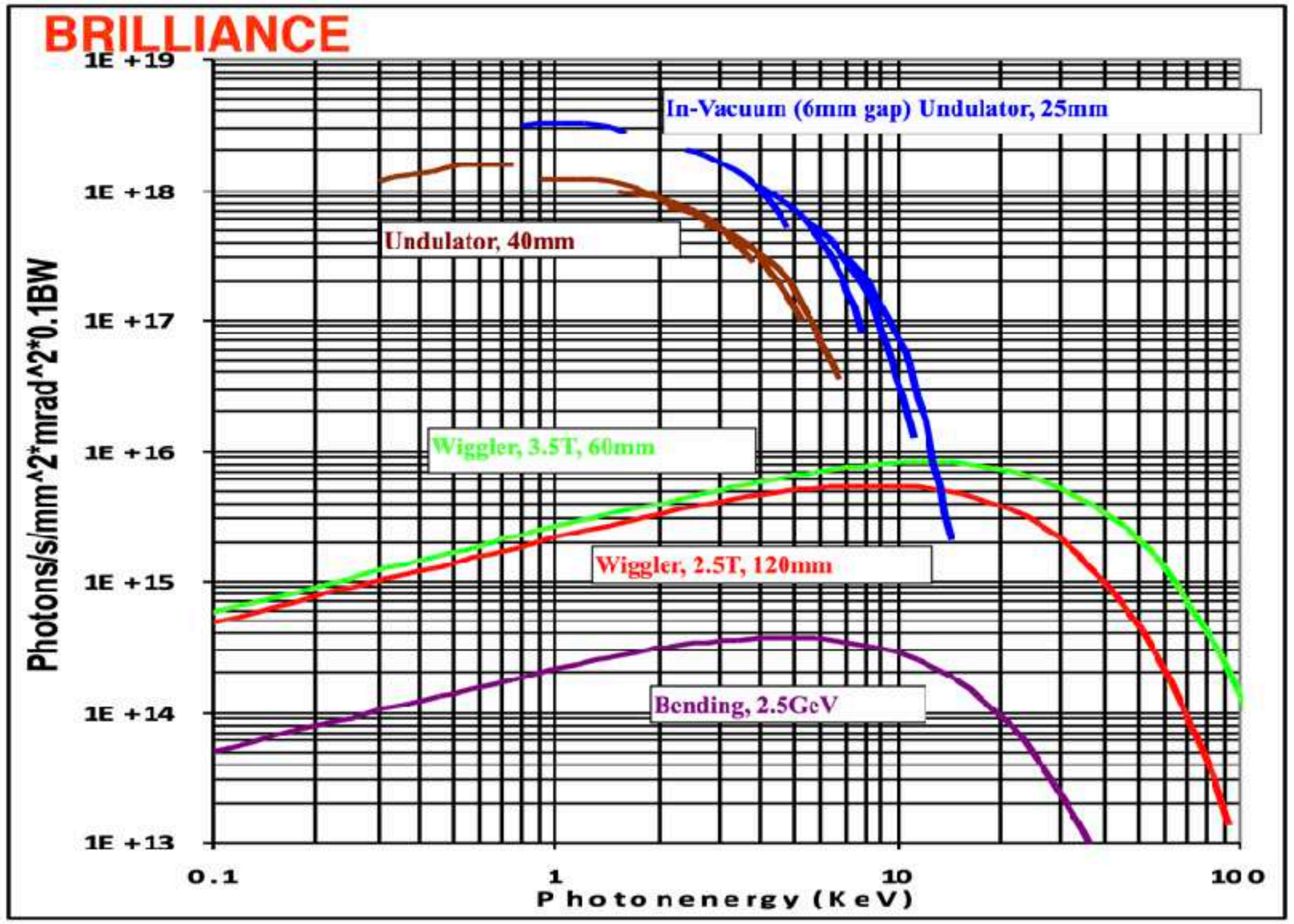

some methods used in material analysis

XRF

XRD

EXAFS

FTIR

IXS

AFM

XCD

NMR

PDF

NRS

MAD

NRIXS

Seeing the invisible

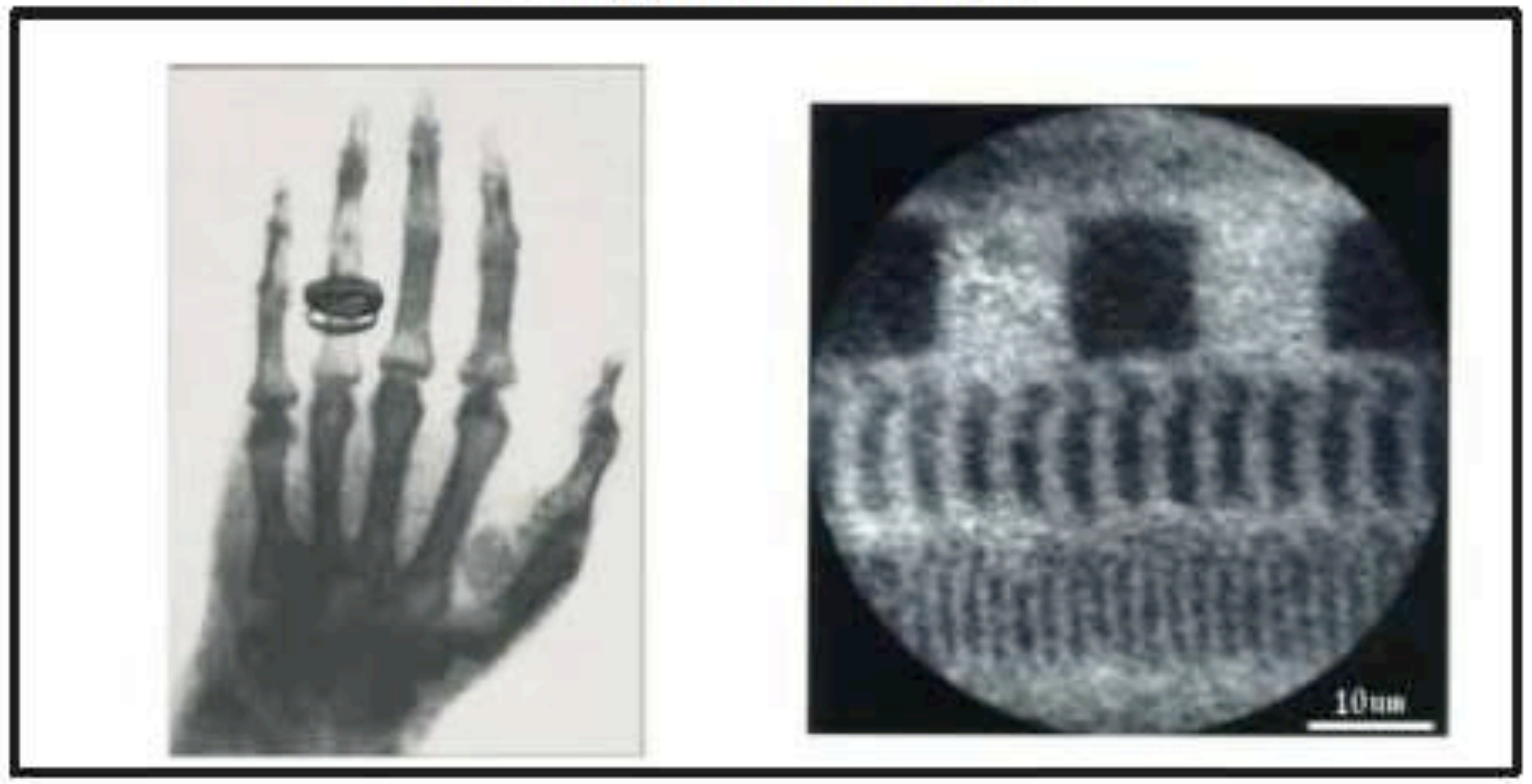

Where are the atoms?

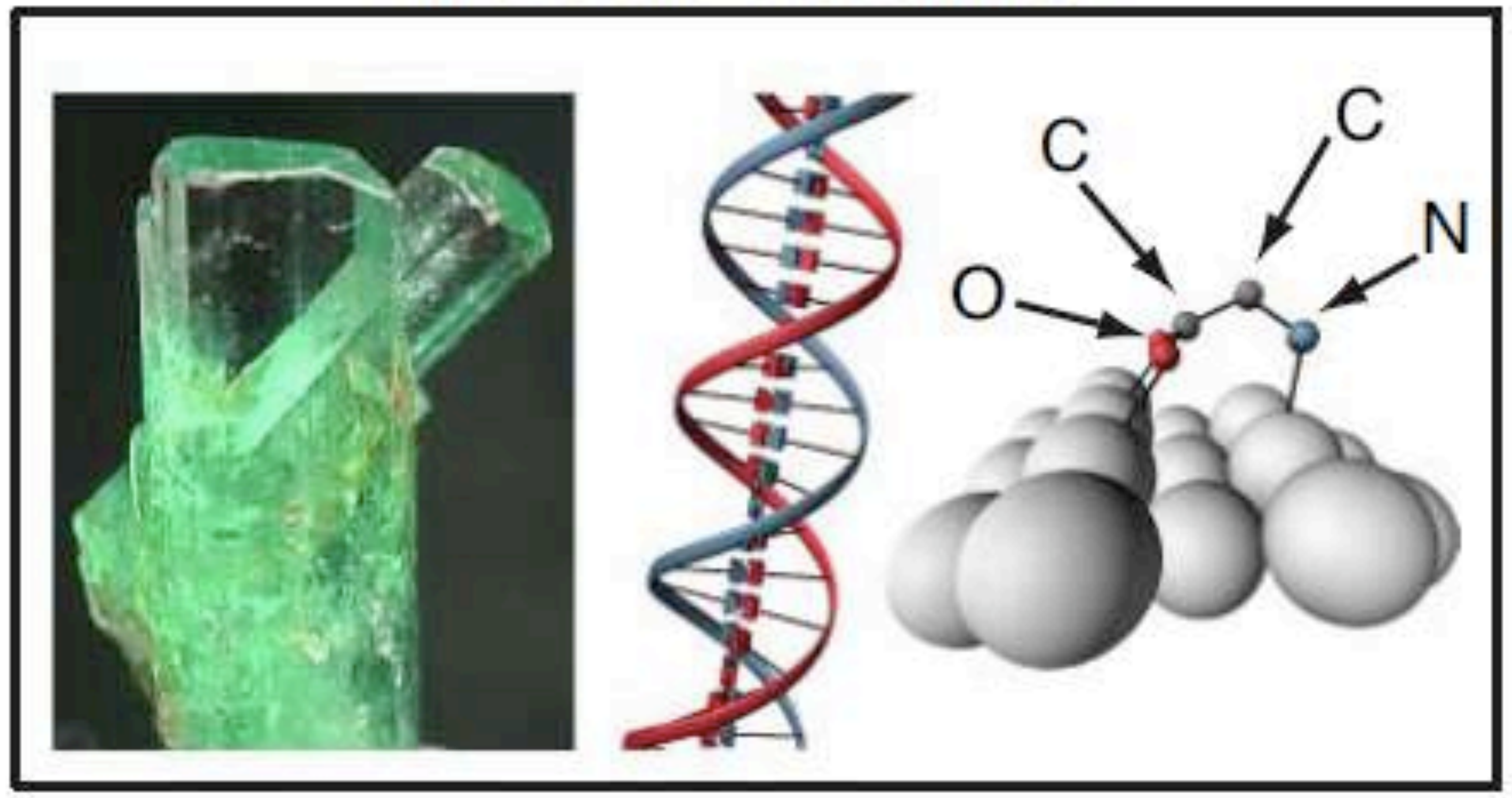

Where are the electrons?

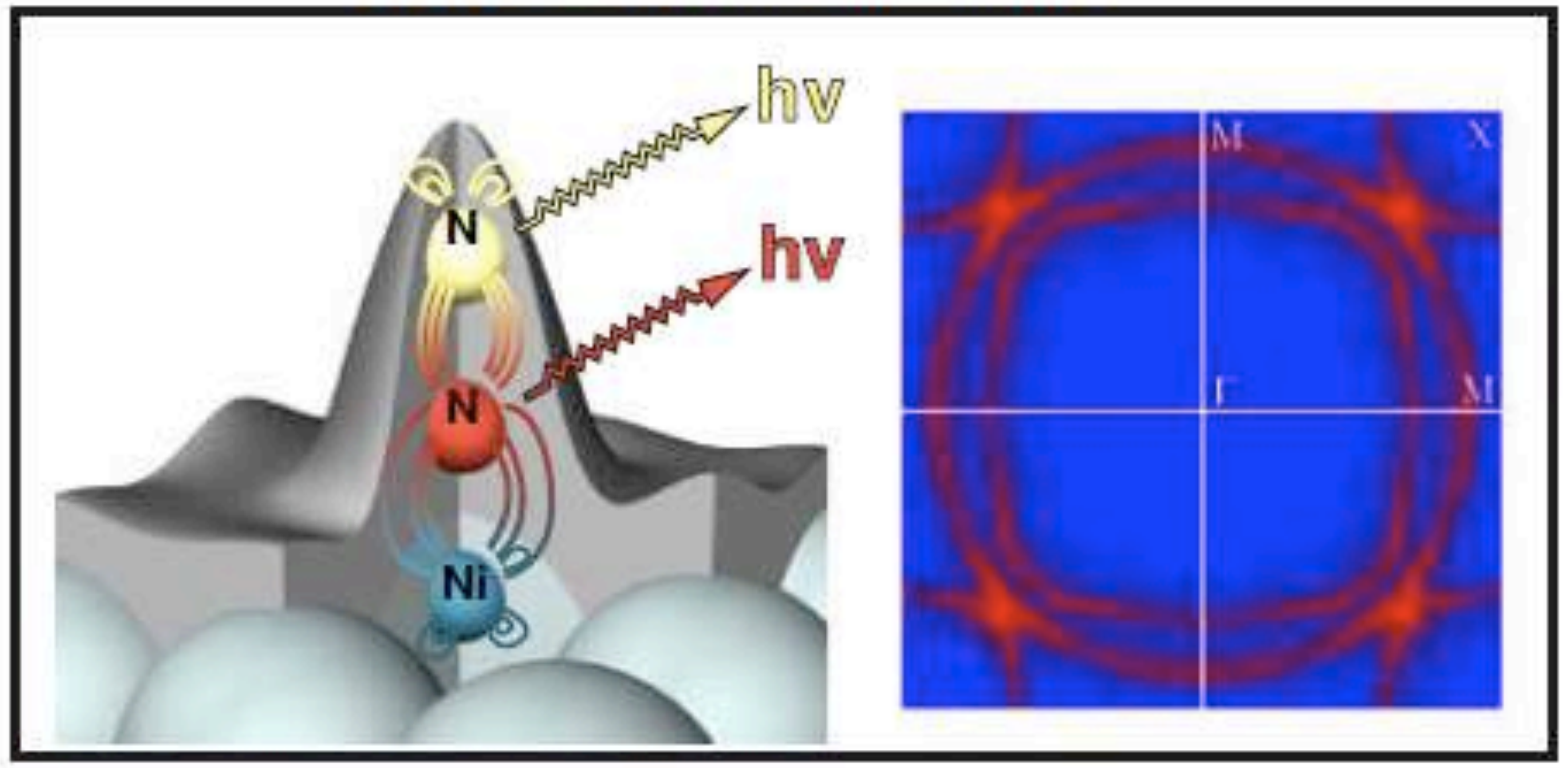

Where are the spins?

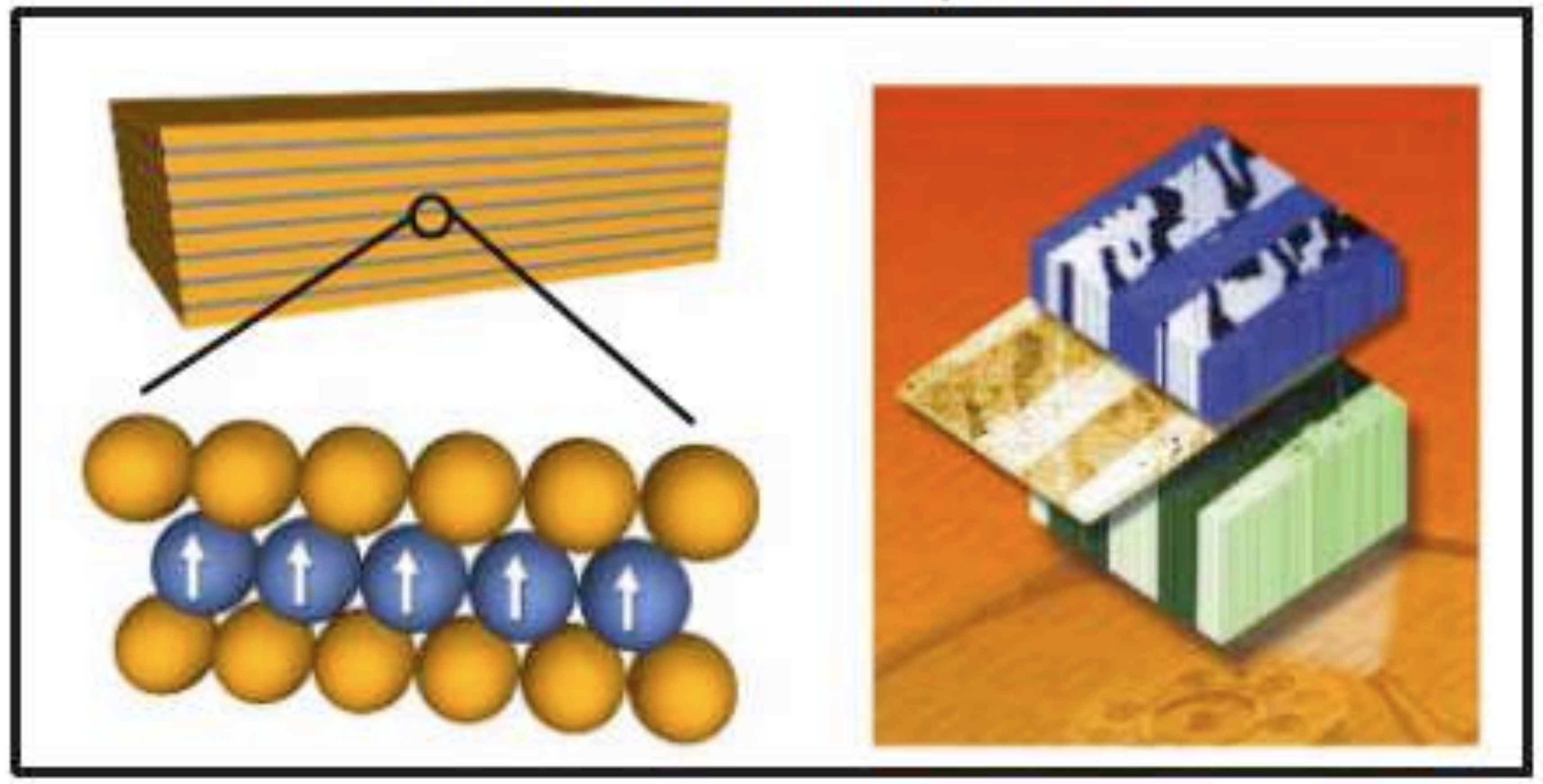

What are the basic techniques in synchrotron radiation ?

Scattering
Diffraction
Refraction
Absorption
Spectroscopy
Imaging
Ptychography

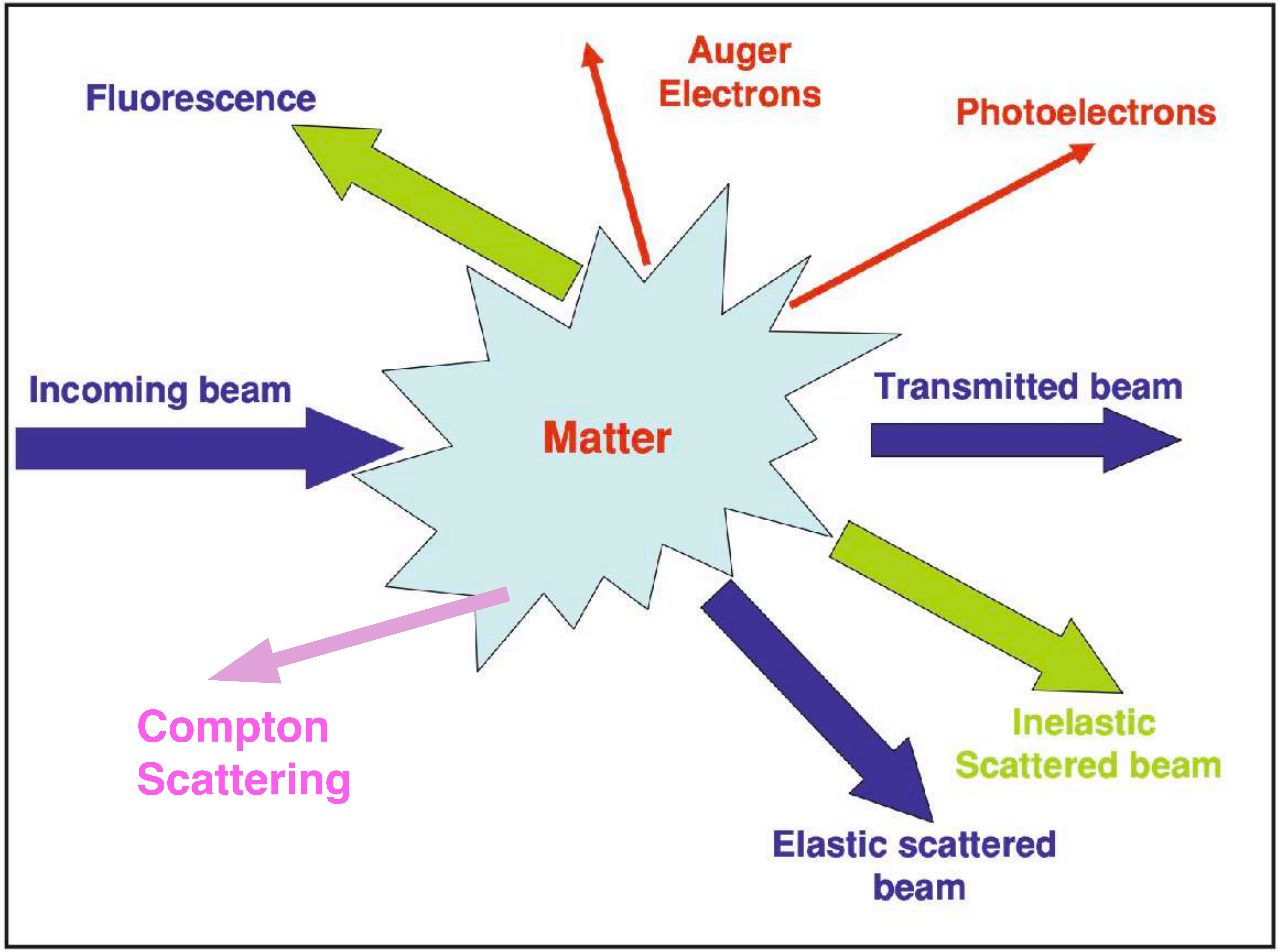

X-Ray techniques can be classified in many different ways. Here's one that I like

Real Space

Imaging,Tomography

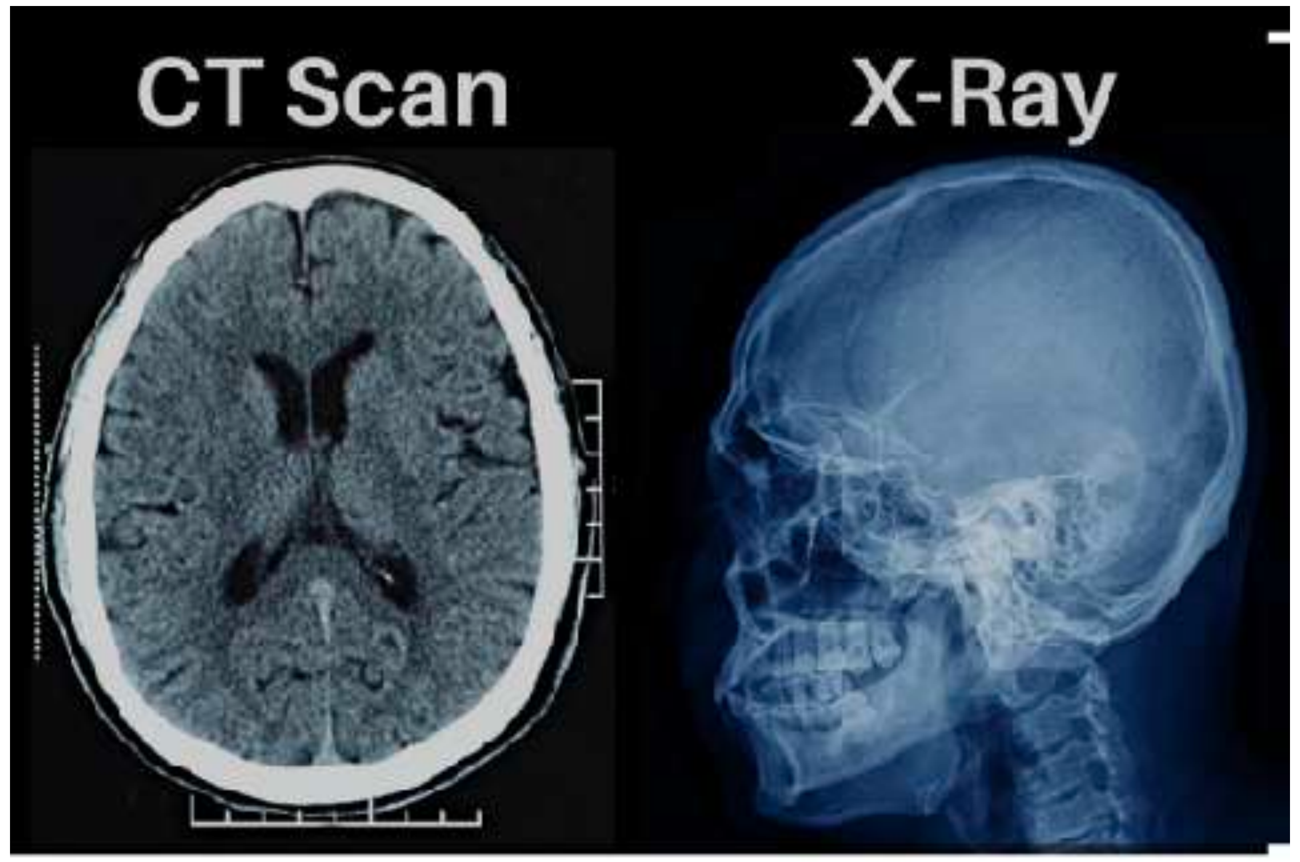

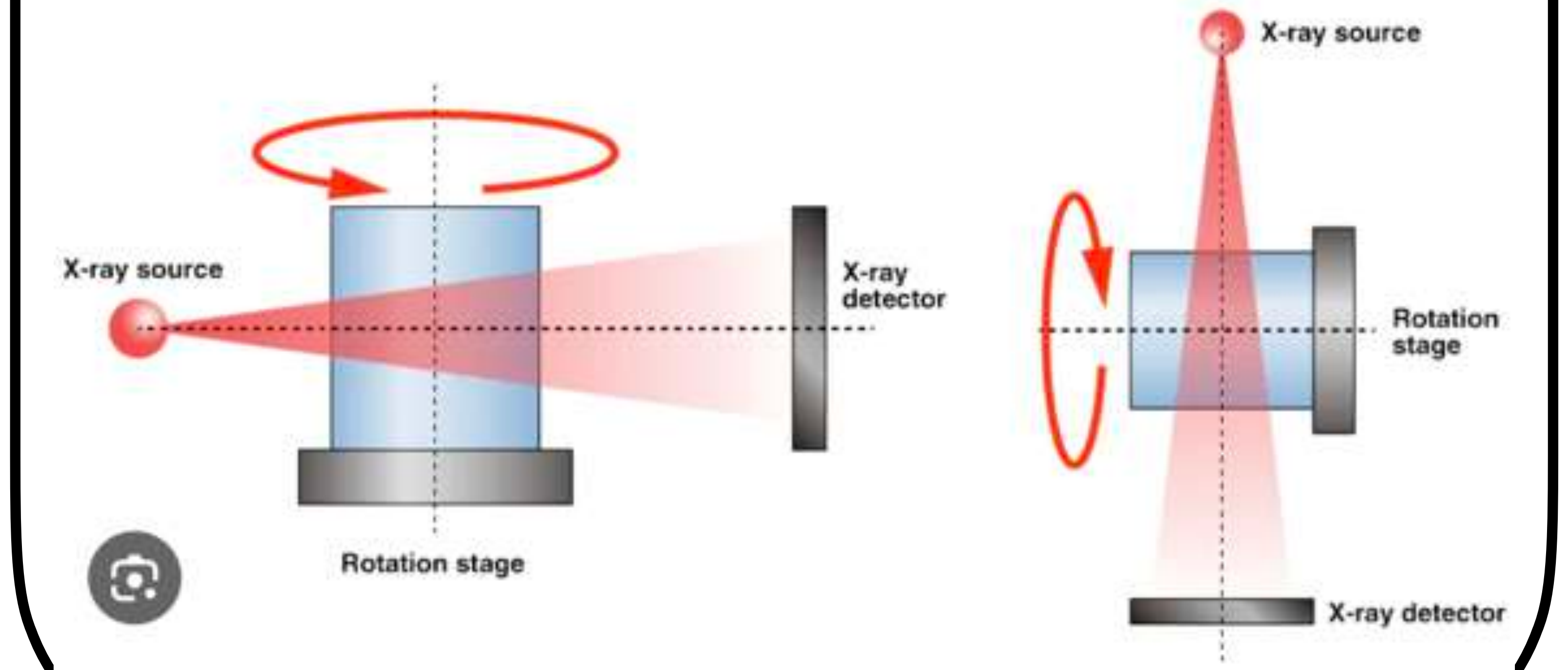

Reciprocal Space

X-Ray Diffraction, IXS

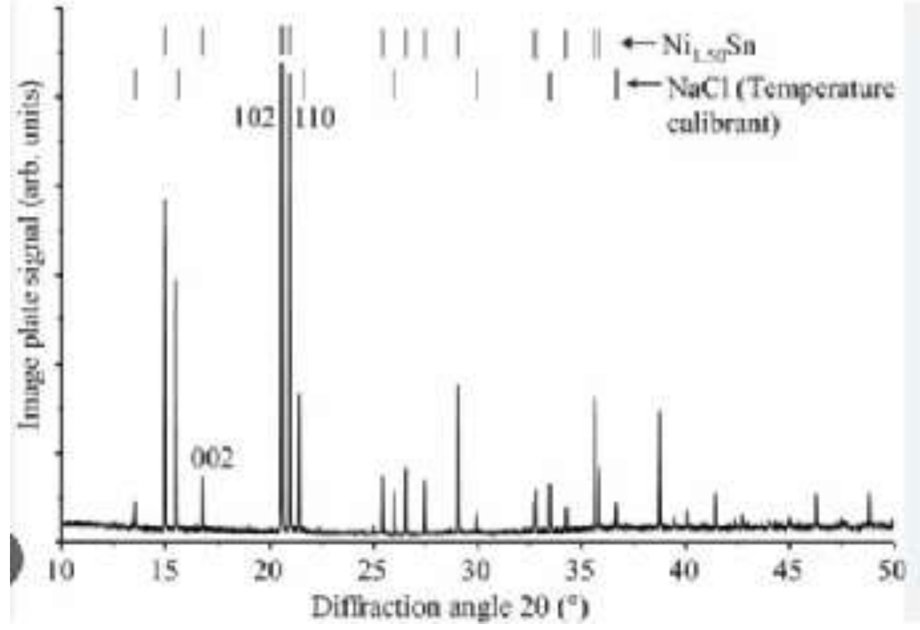

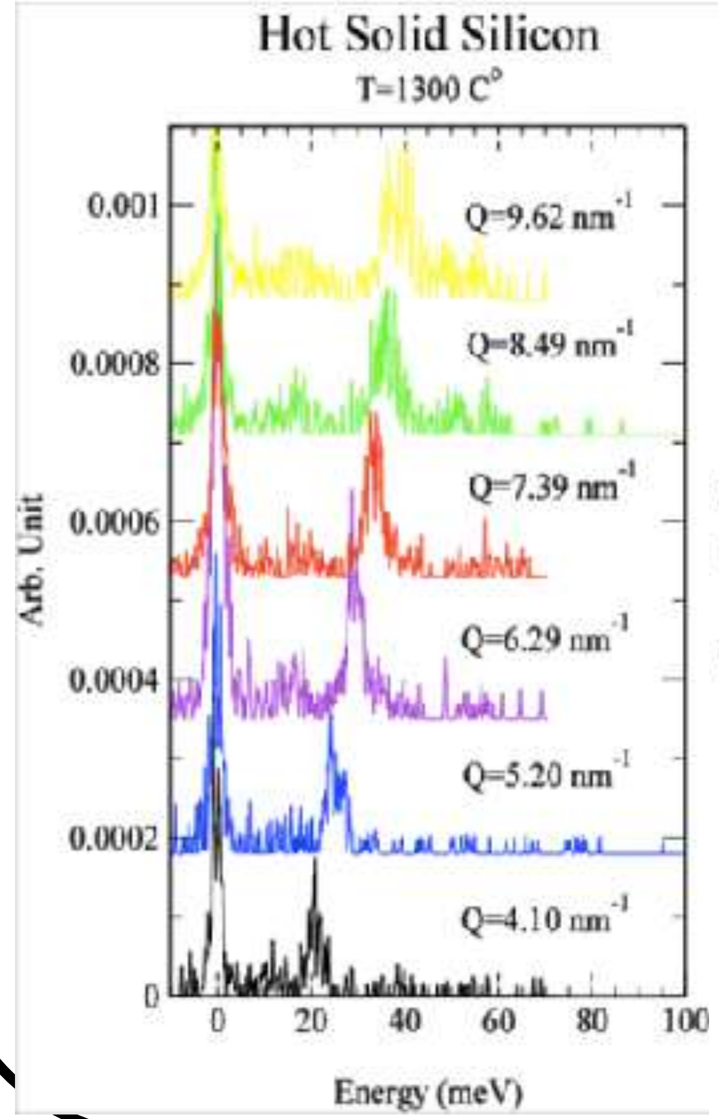

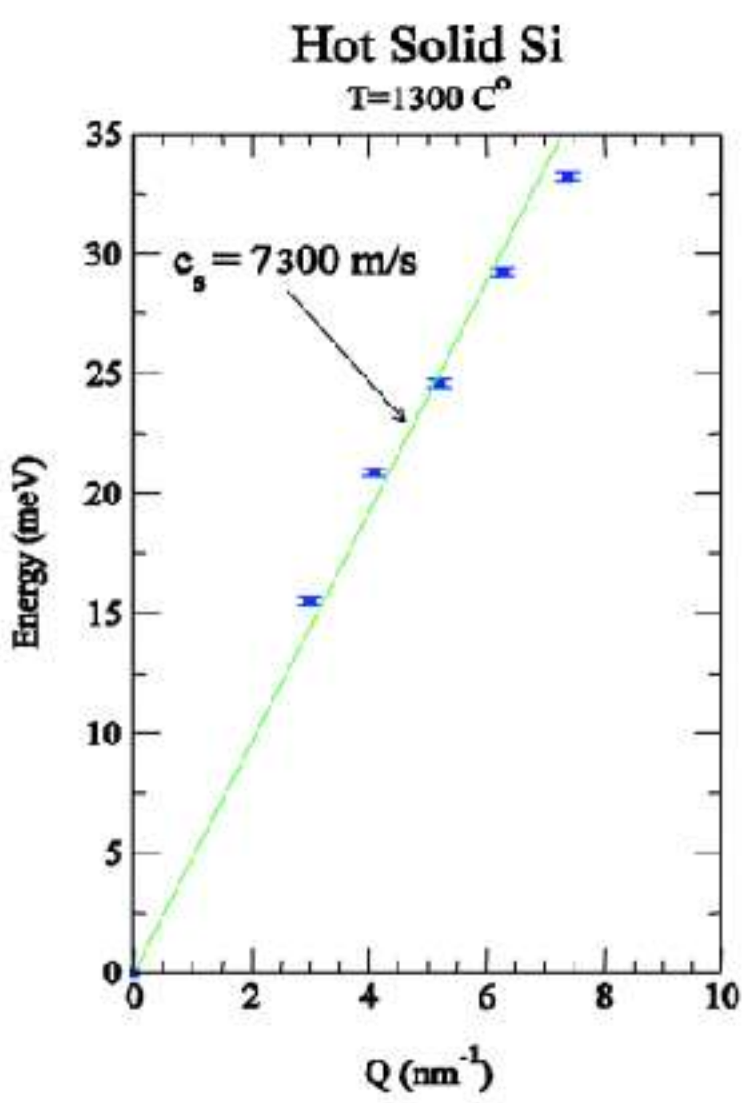

Time resolved

XRD, XAS, Mössbauer, imaging, catalysis…..

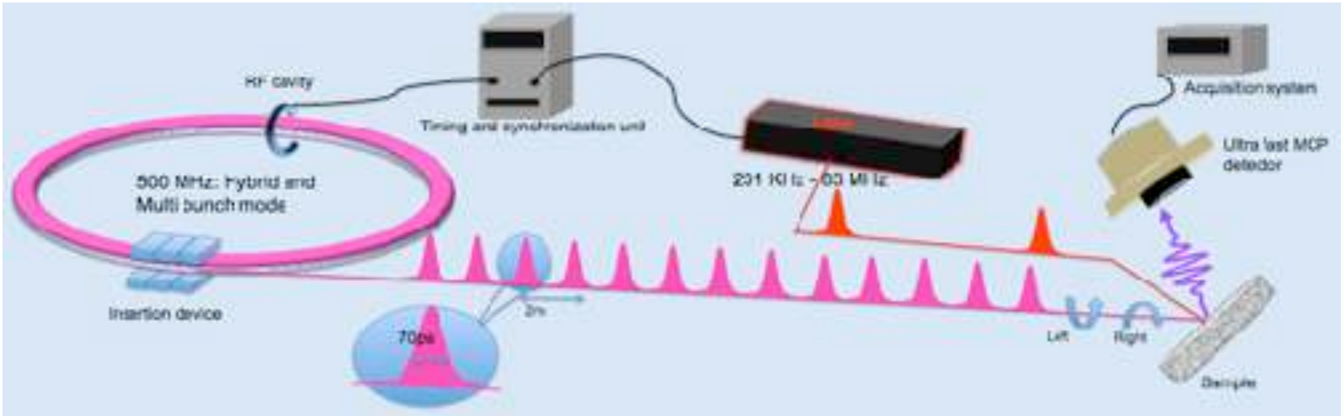

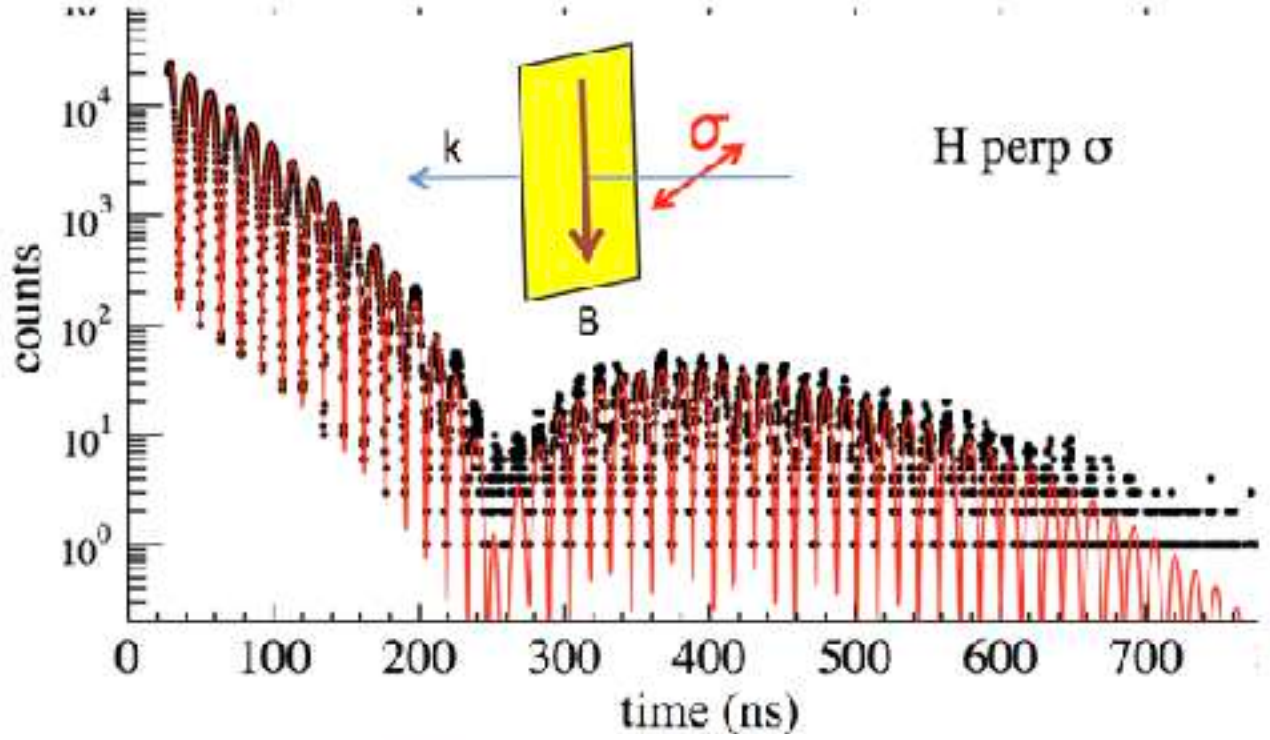

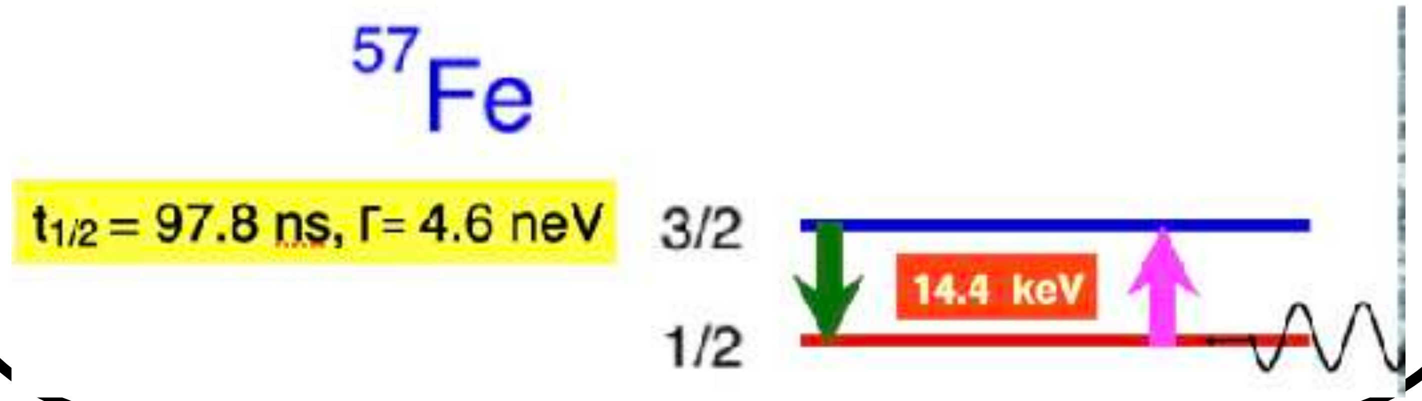

X-Ray techniques can be classified in many different ways. Here's one that I like

Energy domain

Spectroscopy

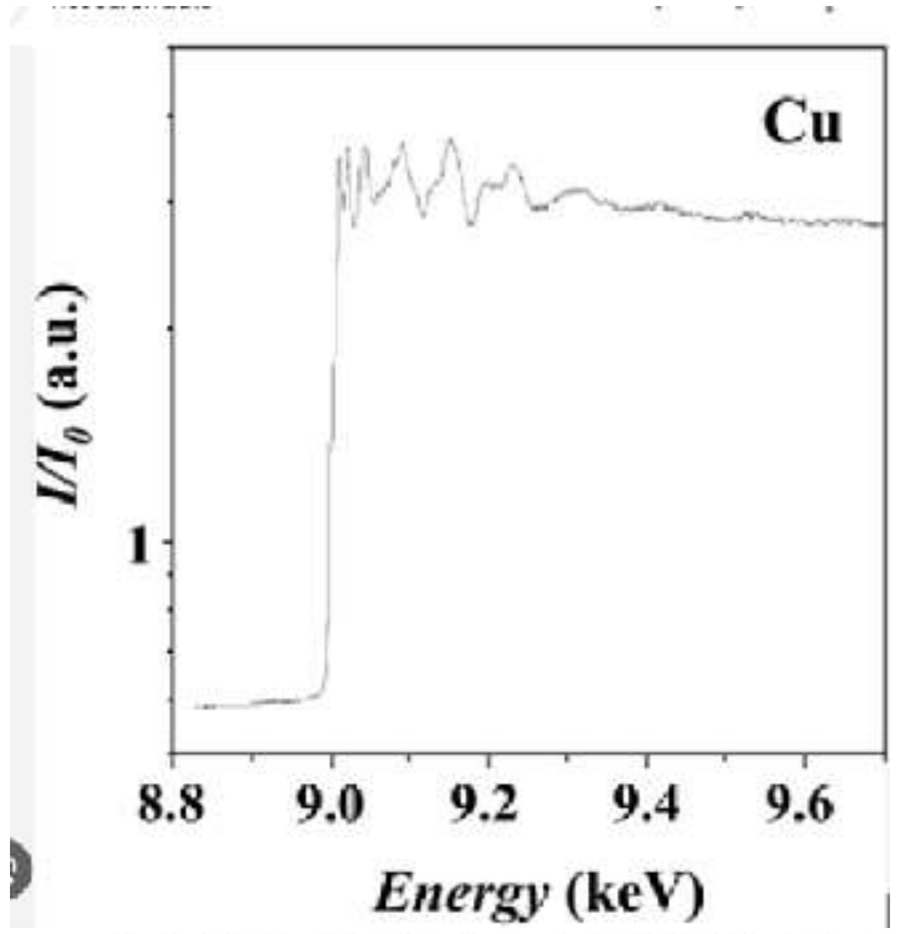

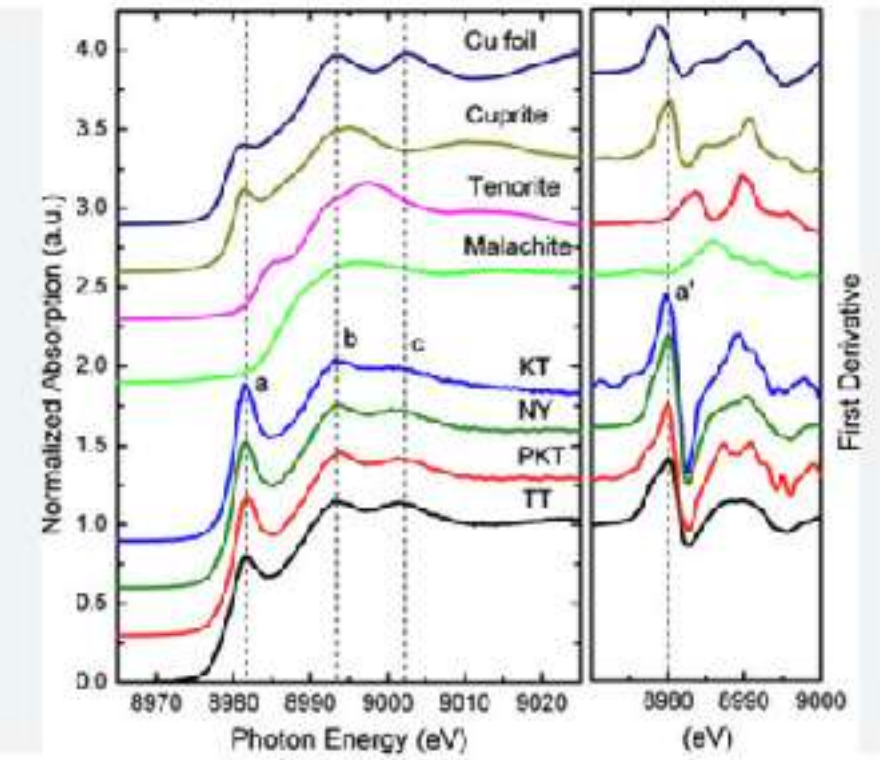

Polarization

Magnetic circular dichroism

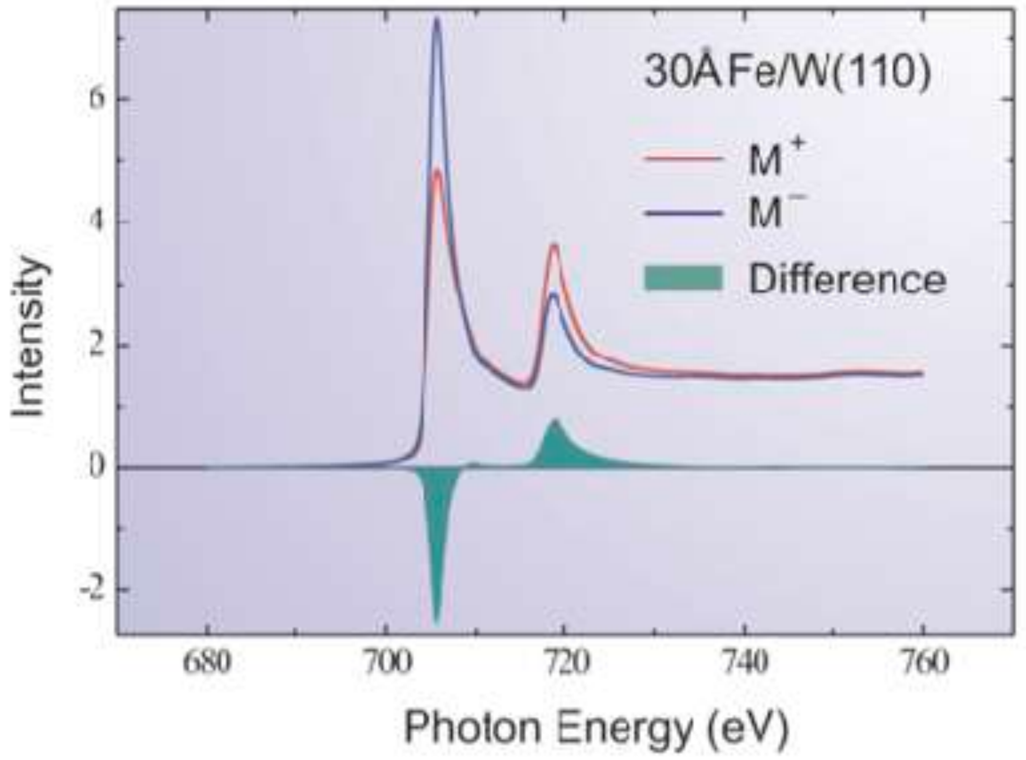

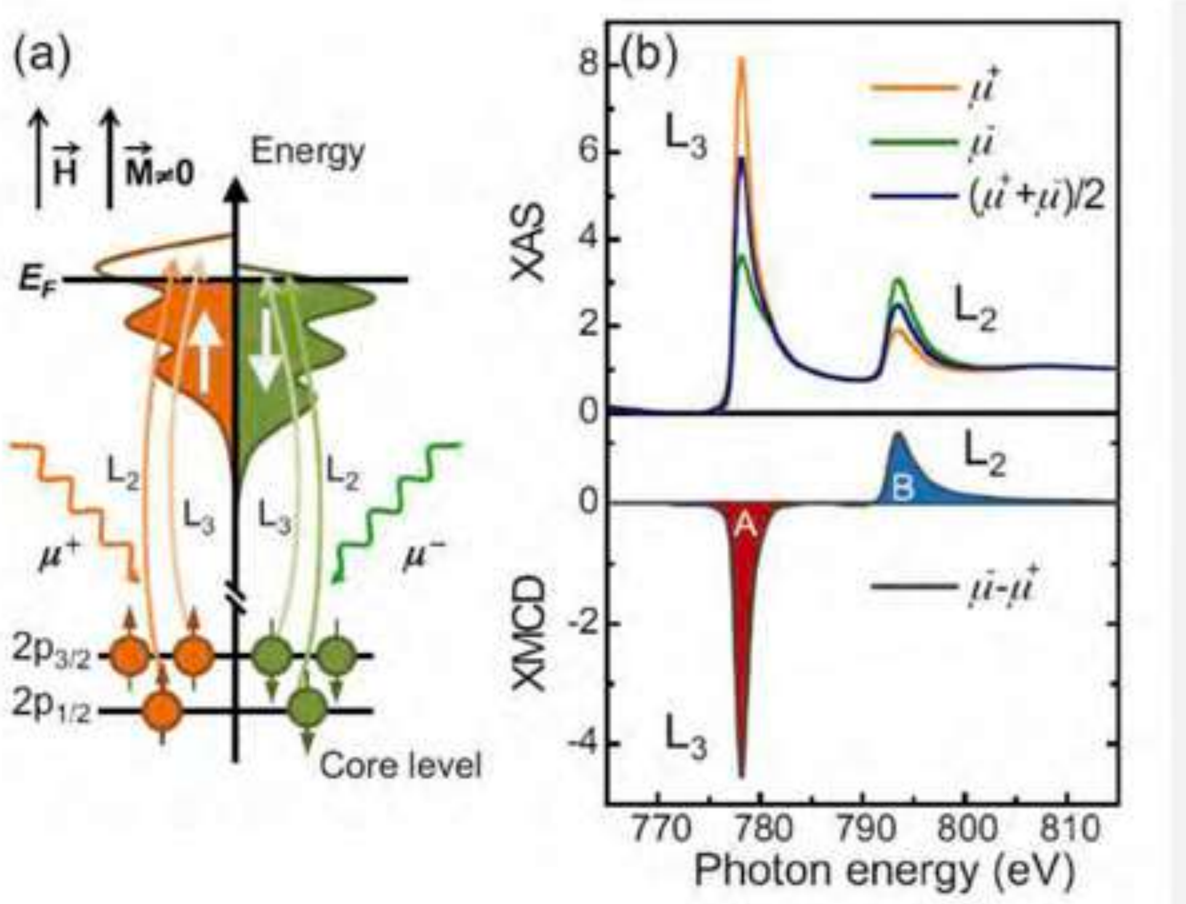

Coherence

Coherent Diffraction Imaging

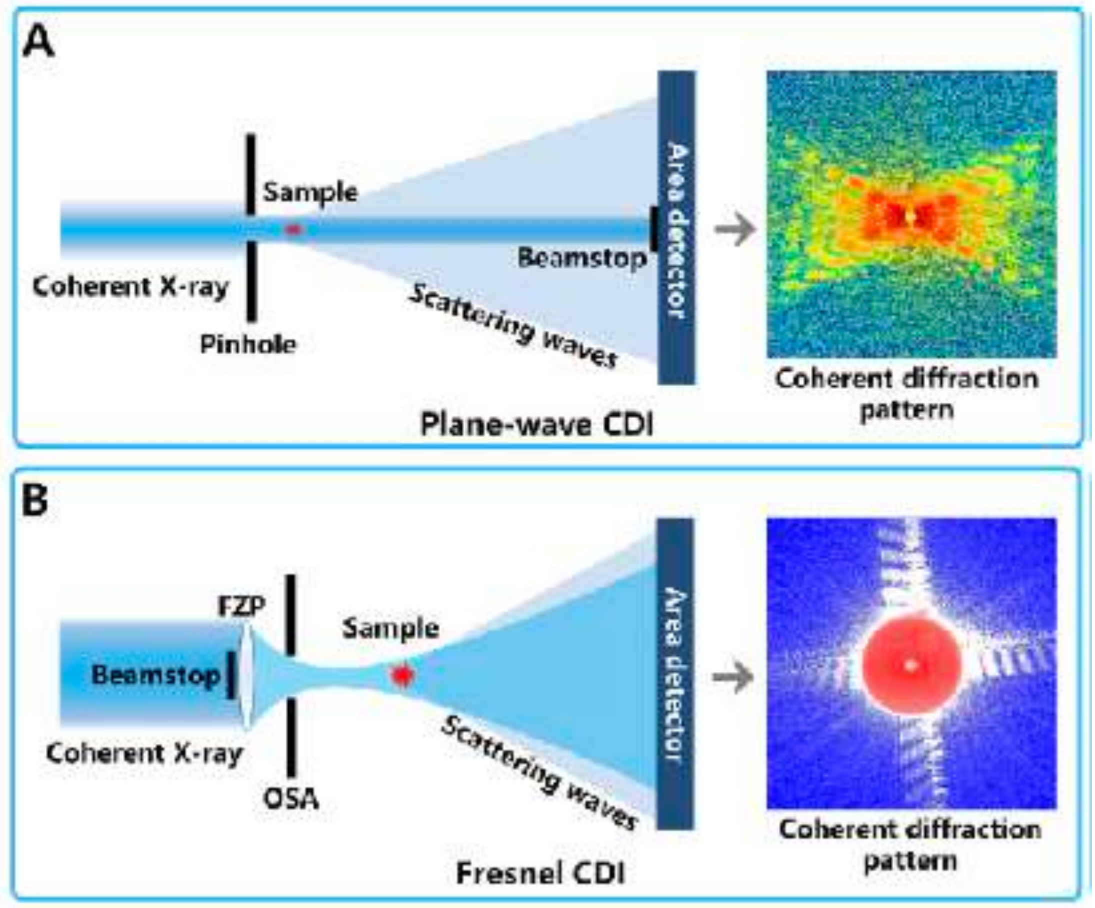

BM08 - XAFS/XRF (X-ray Absorption Fine Structure/X-ray Fluorescence) spectroscopy beamline

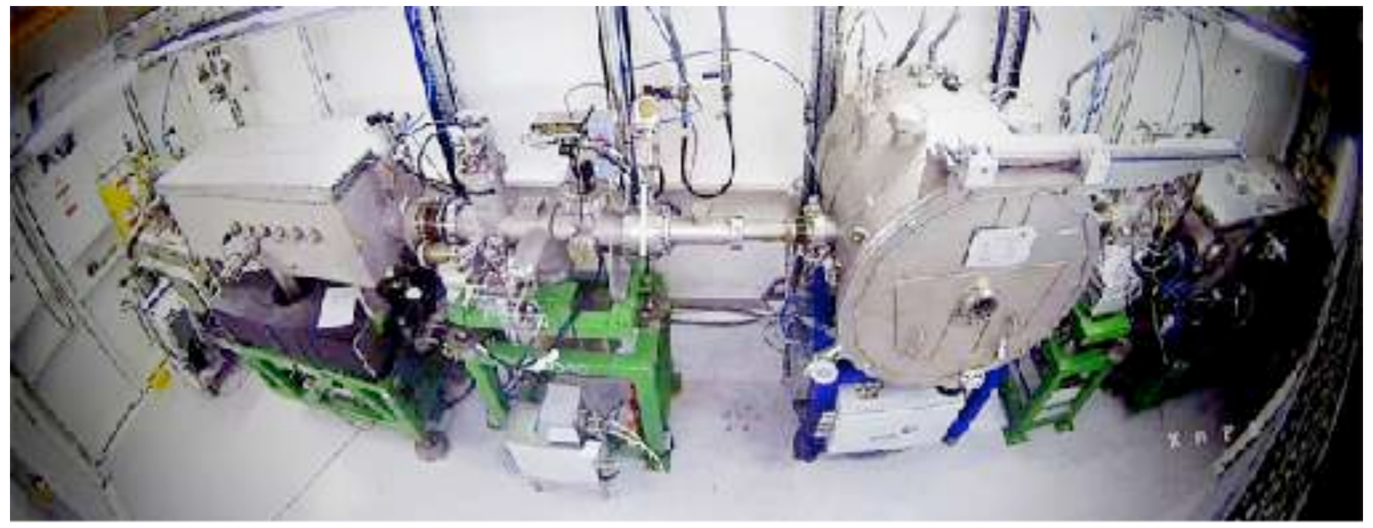

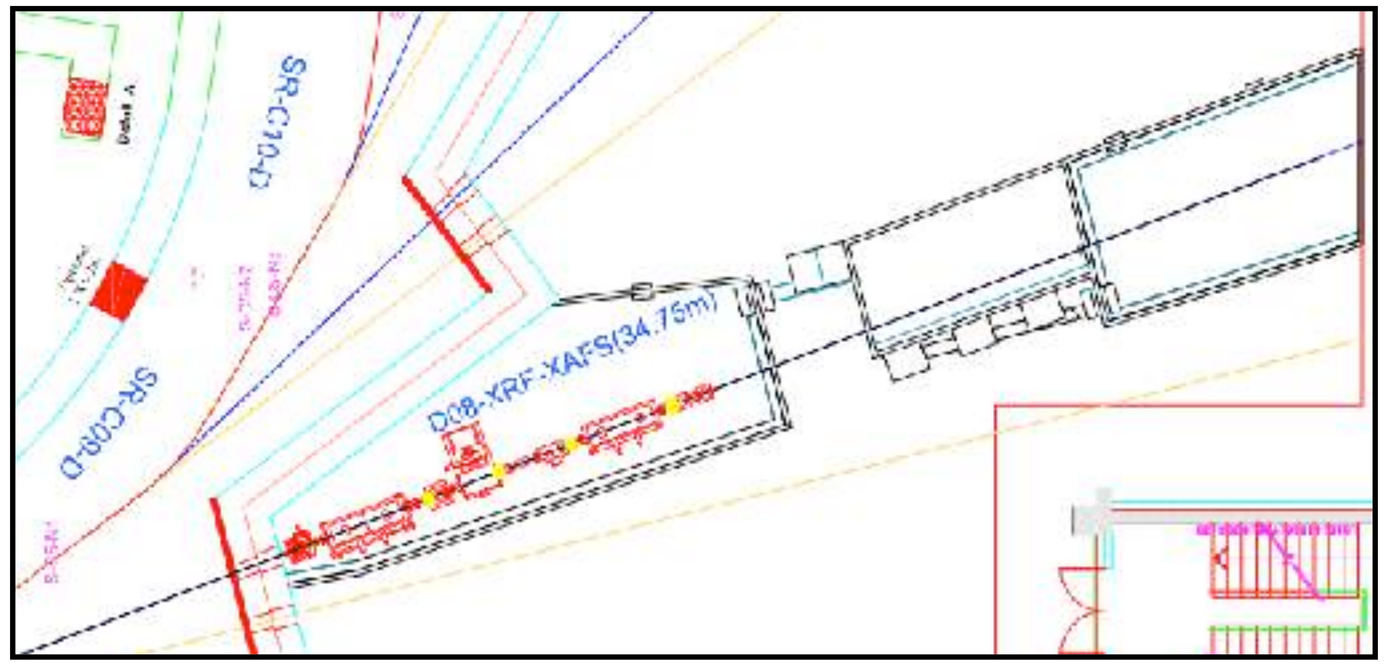

XAFS

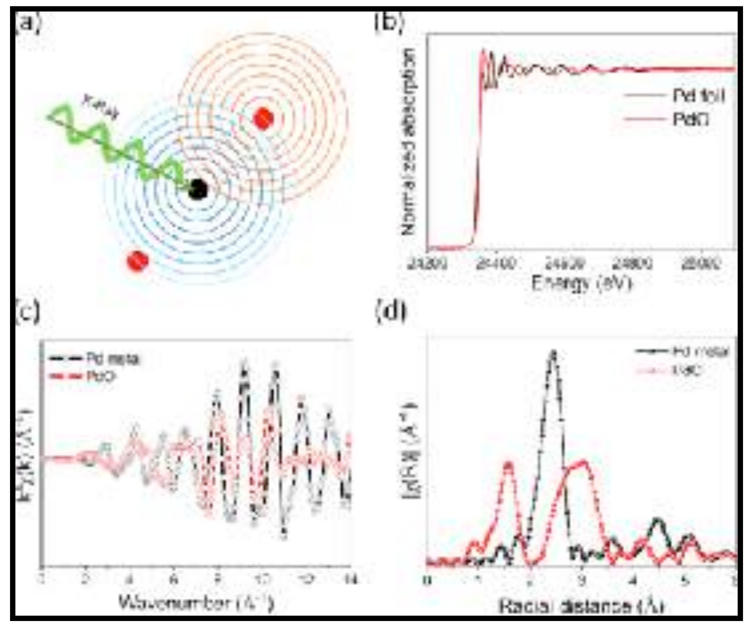

$$\chi(k) = \sum_i \frac{(N_i S_0^{\,2}) F_i(k)}{k R_i^{\,2}} \sin[2kR_i + \delta_i(k)] e^{-2\sigma_i^2 k^2} e^{-\frac{2R_i}{\lambda(k)}}$$

Saçınım genliği

Atomlar arası mesafe

Faz kayması

Debye Waller

Serbest elektron mesafesi

XANES: Near absorption edge gives information about valence state

EXAFS provides near neighbor distances and coordination number.

Applicable to crystalline and non-crystalline samples. Catalysis, amoprg=hous materials, surfaces and interfaces, dilute systems, environmental applications, soil science, meteorites, asteroids, time resolved phenomena (msec)

SESAME’s strength:
Fluorescence detector, experiments time, open for further development

XRF

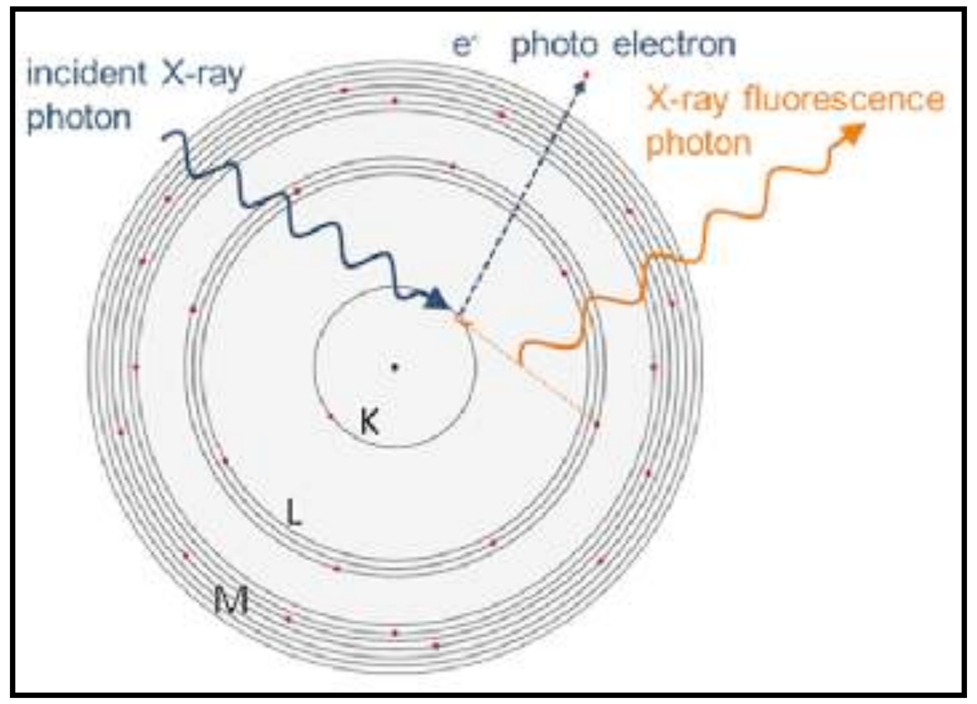

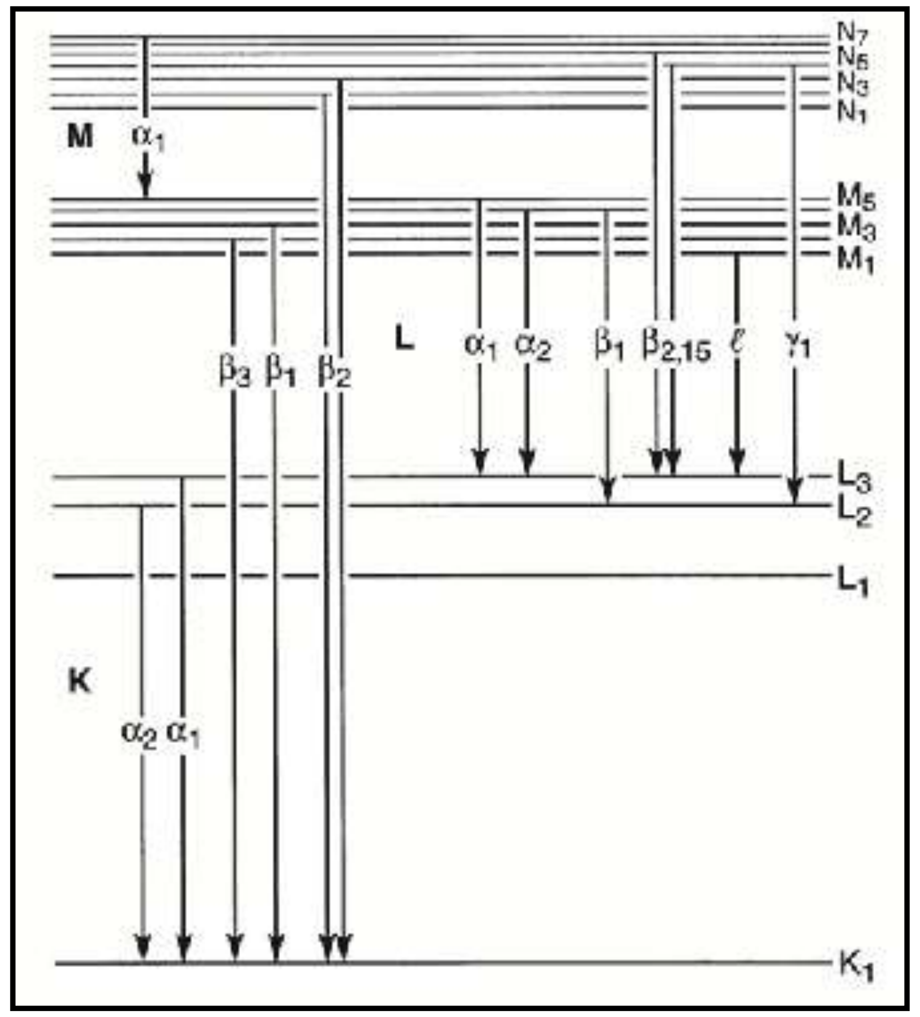

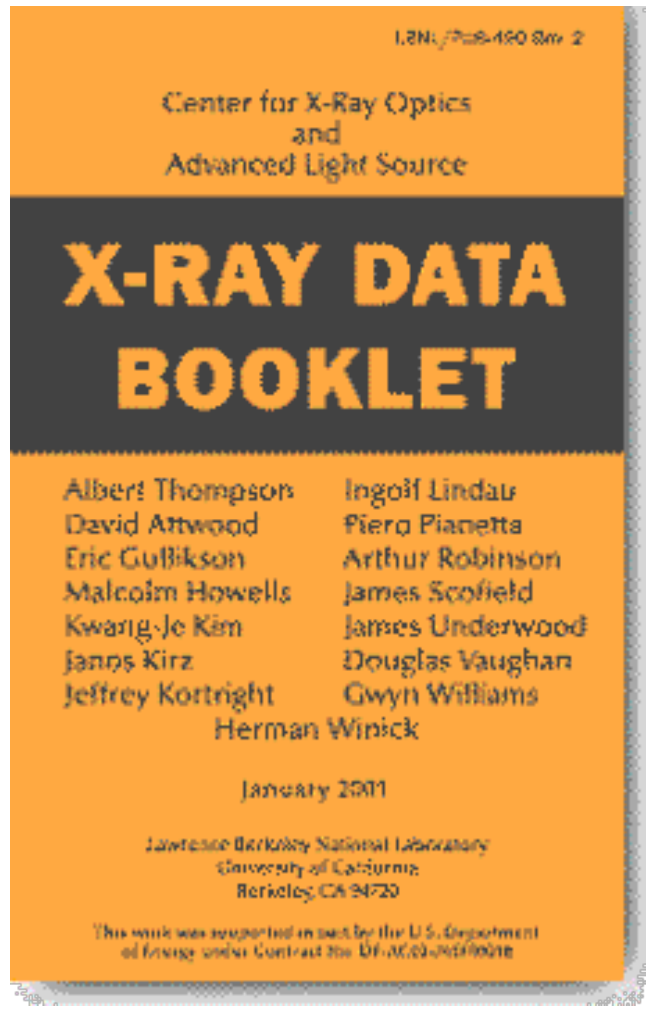

Table 1-2. Energies of x-ray emission lines (continue

Element	$K\alpha_1$	$K\alpha_2$	$K\beta_1$	$L\alpha_1$	$L\alpha_2$	$L\beta_1$
22 Ti	4,510.84	4,504.86	4,931.81	452.2	452.2	458.4
23 V	4,952.20	4,944.64	5,427.29	511.3	511.3	519.2
24 Cr	5,414.72	5,405.509	5,946.71	572.8	572.8	582.8
25 Mn	5,898.75	5,887.65	6,490.45	637.4	637.4	648.8
26 Fe	6,403.84	6,390.84	7,057.98	705.0	705.0	718.5
27 Co	6,930.32	6,915.30	7,649.43	776.2	776.2	791.4
28 Ni	7,478.15	7,460.89	8,264.66	851.5	851.5	868.8
29 Cu	8,047.78	8,027.83	8,905.29	929.7	929.7	949.8
30 Zn	8,638.86	8,615.78	9,572.0	1,011.7	1,011.7	1,034.7
31 Ga	9,251.74	9,224.82	10,264.2	1,097.92	1,097.92	1,124.8
32 Ge	9,886.42	9,855.32	10,982.1	1,188.00	1,188.00	1,218.5
33 As	10,543.72	10,507.99	11,726.2	1,282.0	1,282.0	1,317.0
34 Se	11,222.4	11,181.4	12,495.9	1,379.10	1,379.10	1,419.23
35 Br	11,924.2	11,877.6	13,291.4	1,480.43	1,480.43	1,525.90
36 Kr	12,649	12,598	14,112	1,586.0	1,586.0	1,636.6
37 Rb	13,395.3	13,335.8	14,961.3	1,694.13	1,692.56	1,752.17
38 Sr	14,165	14,097.9	15,835.7	1,806.56	1,804.74	1,871.72
39 Y	14,958.4	14,882.9	16,737.8	1,922.56	1,920.47	1,995.84
40 Zr	15,775.1	15,690.9	17,667.8	2,042.36	2,039.9	2,124.4

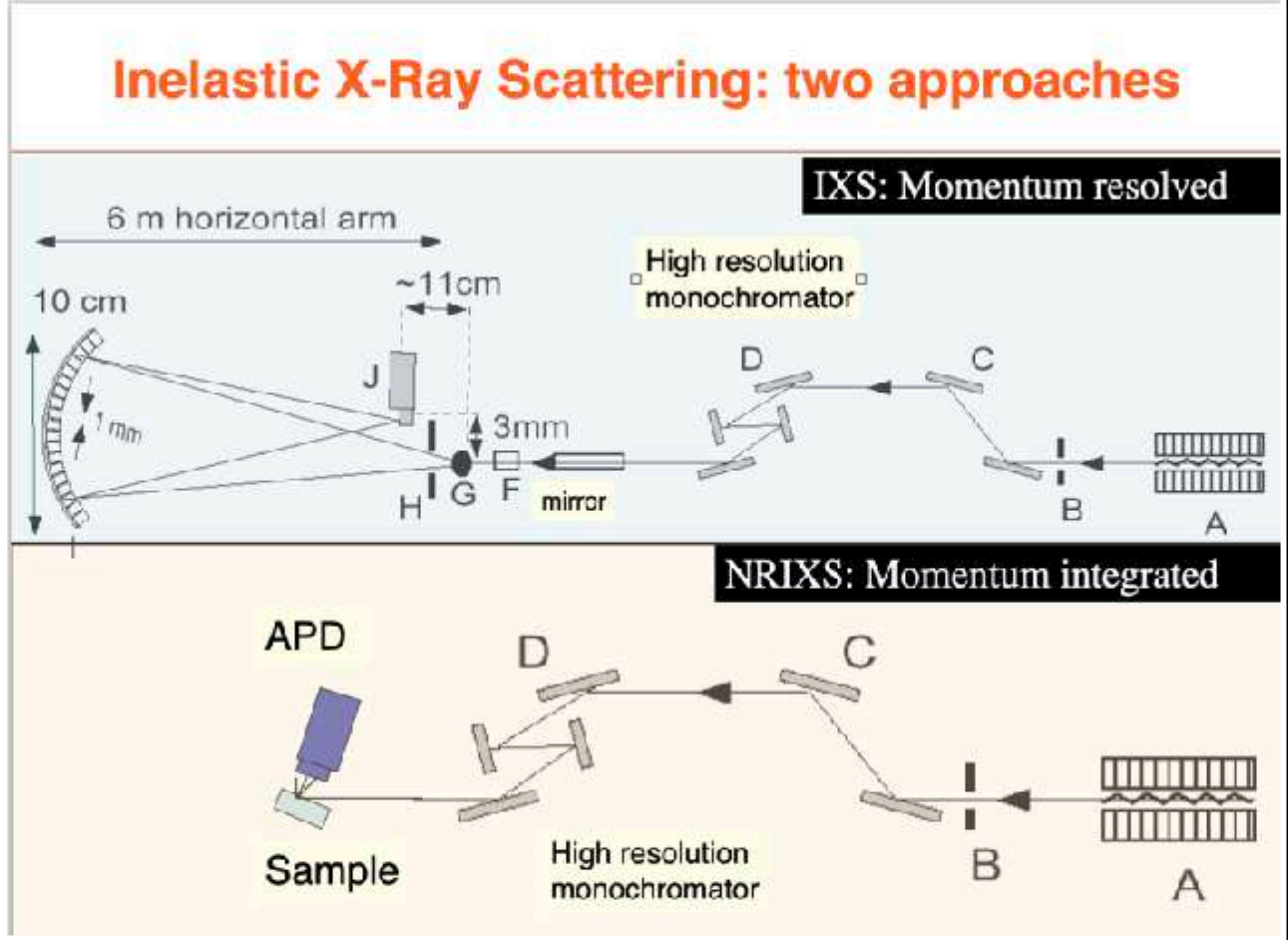
Inelastic X-Ray Scattering: two approaches
IXS: Momentum resolved
6 m horizontal arm
10 cm
~11cm
High resolution monochromator
1 mm
3mm
mirror
J
H
G
F
D
C
B
A
NRIXS: Momentum integrated
APD
Sample
D
C
High resolution monochromator
B
A

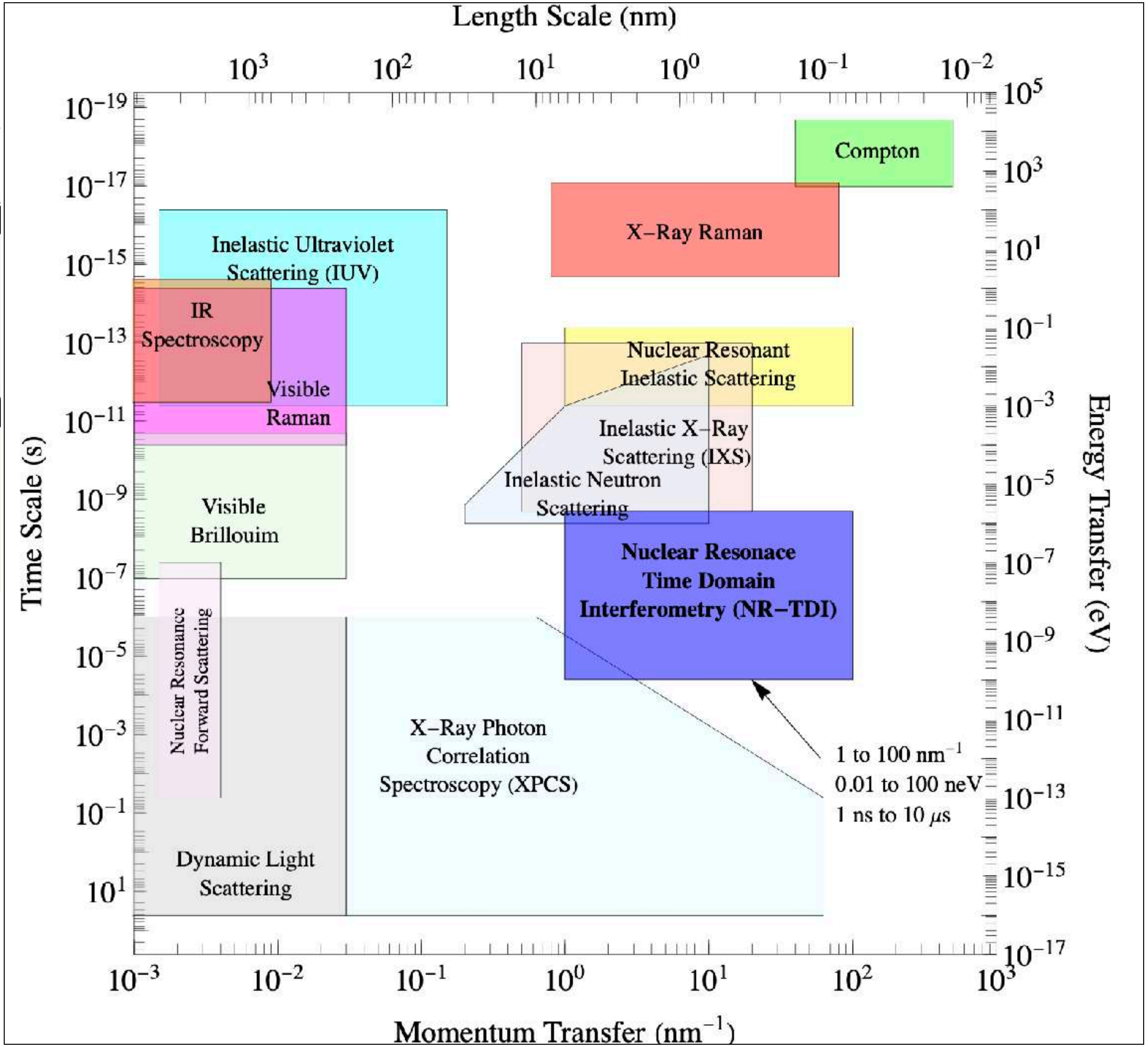
Length Scale (nm)
Time Scale (s)
Energy Transfer (eV)
Momentum Transfer (nm^{-1})
Compton
X−Ray Raman
Inelastic Ultraviolet Scattering (IUV)
IR Spectroscopy
Visible Raman
Nuclear Resonant Inelastic Scattering
Inelastic X−Ray Scattering (IXS)
Inelastic Neutron Scattering
Visible Brillouim
Nuclear Resonance Time Domain Interferometry (NR−TDI)
Nuclear Resonance Forward Scattering
X−Ray Photon Correlation Spectroscopy (XPCS)
Dynamic Light Scattering
1 to 100 nm^{-1}
0.01 to 100 neV
1 ns to 10 μs

Inelastic X-Ray Scattering: A plethora of different techniques

IXS

Non-Resonant

Resonant

ΔE ~ meV
IXS

ΔE ~ 1 meV
Nuclear resonant

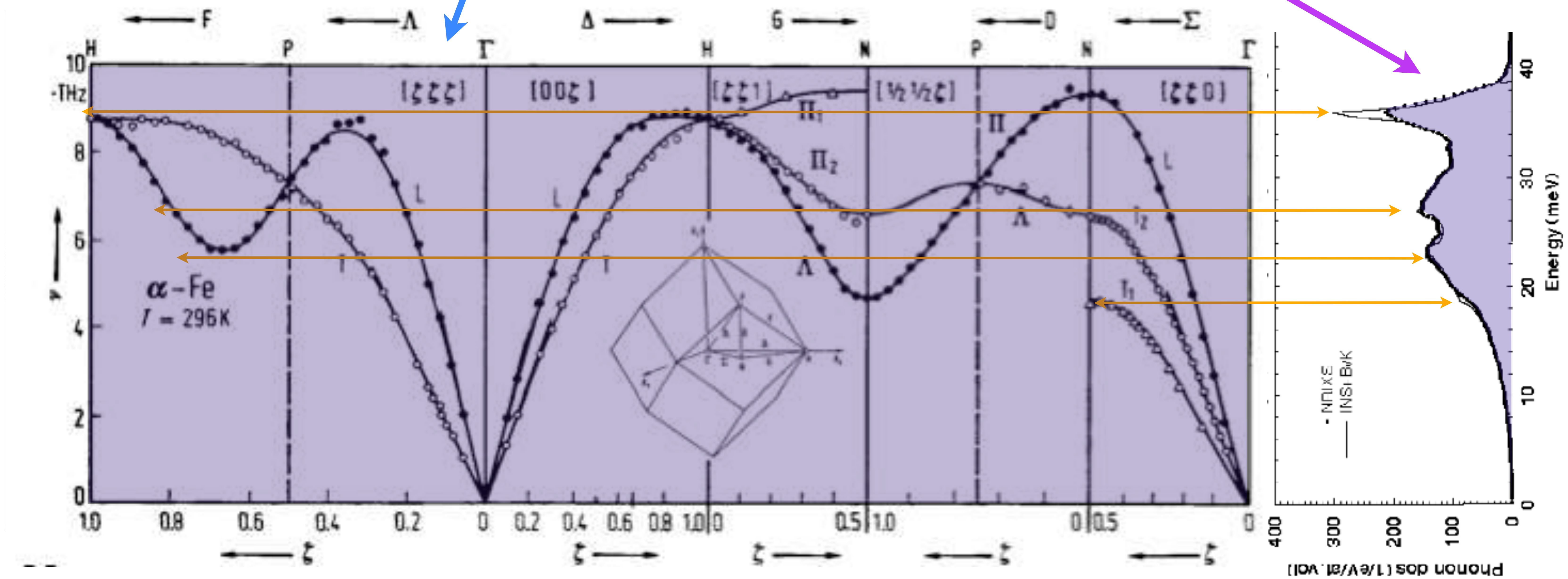

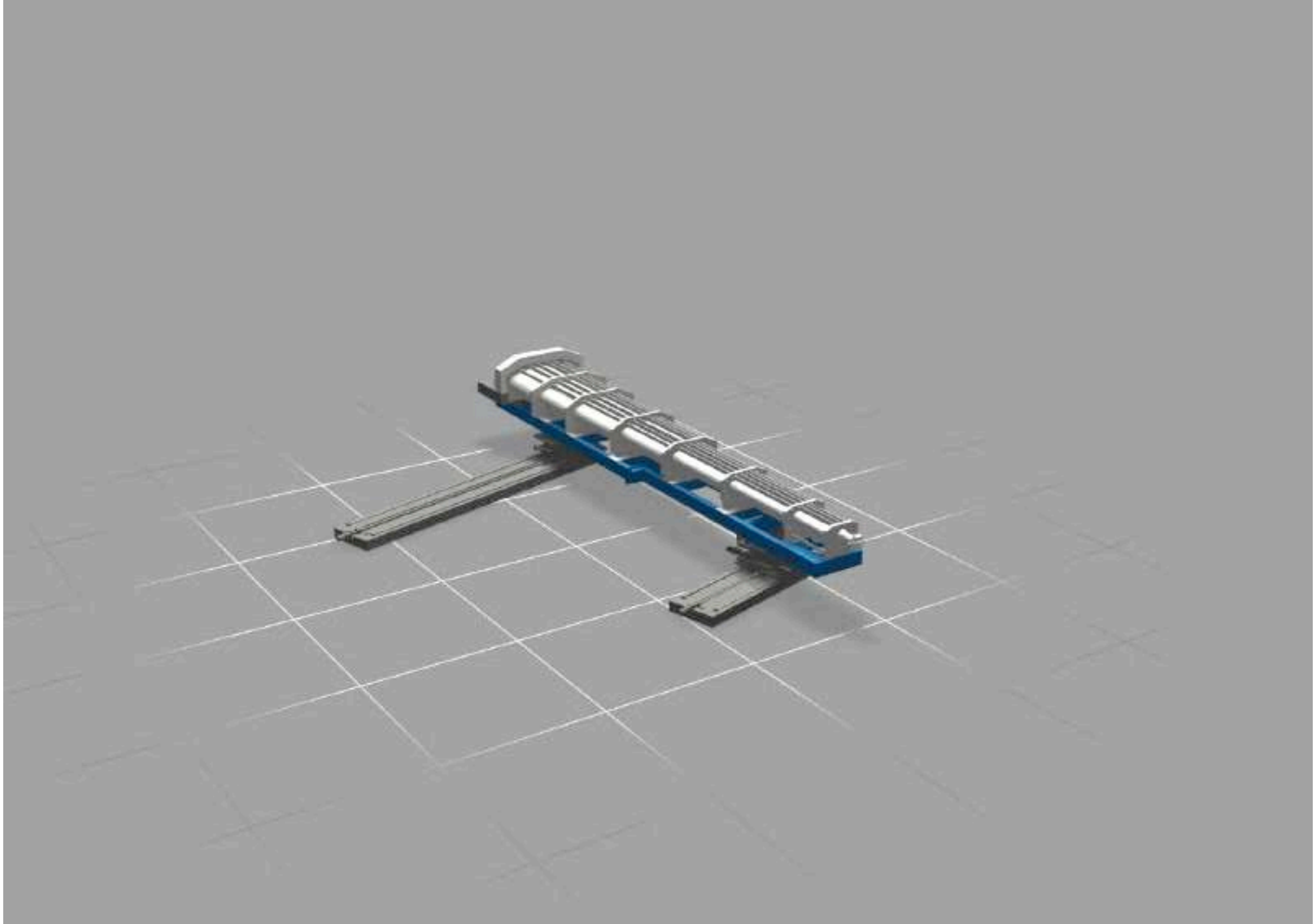

PHONON's: $\phi\omega\nu\acute{\eta}$ (phonē), *sound*

- Phonons are periodic oscillations in condensed systems.

- They are inherently involved in thermal and electrical conductivity.

- They can show anomalous (non-linear) behavior near a phase transition.

- They can carry sound (acoustic modes) or couple to electromagnetic radiation or neutrons (acoustical and optical).

- Have energy of $\hbar\omega$ as quanta of excitation of the lattice vibration mode of angular frequency ω. Since momentum, $\hbar k$, is exact, they are delocalized, collective excitations.

- Phonons are bosons, and they are not conserved. They can be created or annihilated during interactions with neutrons or photons.

- They can be detected by Brillouin scattering (acoustic), Raman scattering, FTIR (optical).

- Their dispersion throughout the BZ can ONLY be monitored with x-rays (IXS), or neutrons (INS).

- Accurate prediction of phonon dispersion require correct knowledge about the force constants: COMPUTATIONAL TECHNIQUES ARE ESSENTIAL.

What is being measured ?

$$\frac{d^2\sigma}{d\Omega\, d\omega} = r_0^2 \frac{\omega_f}{\omega_i} \left|\mathbf{e}_i \cdot \mathbf{e}_f\right| N \sum_{i,f} \left| \langle i | \sum e^{i\mathbf{Q}\mathbf{r_j}} | f \rangle \right|^2 \delta(E_f - E_i - \hbar\omega)$$

Thomson cross section — **Dynamical structure factor S(Q,w)**

$$S(\mathbf{Q},\omega) = \frac{1}{2\pi} \int dt\, e^{-i\omega t} \langle \phi_i | \sum_{ll'} f_l(\mathbf{Q}) e^{-i\mathbf{Q}\cdot\mathbf{r}_l(t)} f_{l'}(\mathbf{Q}) e^{i\mathbf{Q}\cdot\mathbf{r}_{l'}(0)} | \phi_i \rangle$$

Density-density correlations

$$f(Q) = f_{ion}(Q) + f_{valence}(Q)$$

Atomic form factor

Dynamic structure factor

Sum over phonon branch j at reduced momentum transfer, q

Sum over different atoms in the unit cell

Atomic form factor for each atom

scaling with square root of mass

Debye-Waller factor to account for bond strength

phonon occupation probability

$$S(Q,\omega) = \sum_{q,j} \left| \sum_{s} f_s(Q) \frac{\hbar}{\sqrt{2m_s}} e^{-W_s} e^{i\vec{Q}\bullet\vec{R}_s} \left[\vec{Q}\cdot\vec{e}(q,s,j))\right] \right|^2 \frac{\left(\frac{1}{e^{\hbar\omega/kT}-1} + \frac{1}{2} \pm \frac{1}{2}\right)}{\omega_{q,j}} \delta(\omega \pm \omega_{q,j})$$

Phase of the scattering amplitude

Polarization factor between momentum transfer and phonon’s polarization vector

phonon frequency

delta-function in ω

External probe-photon

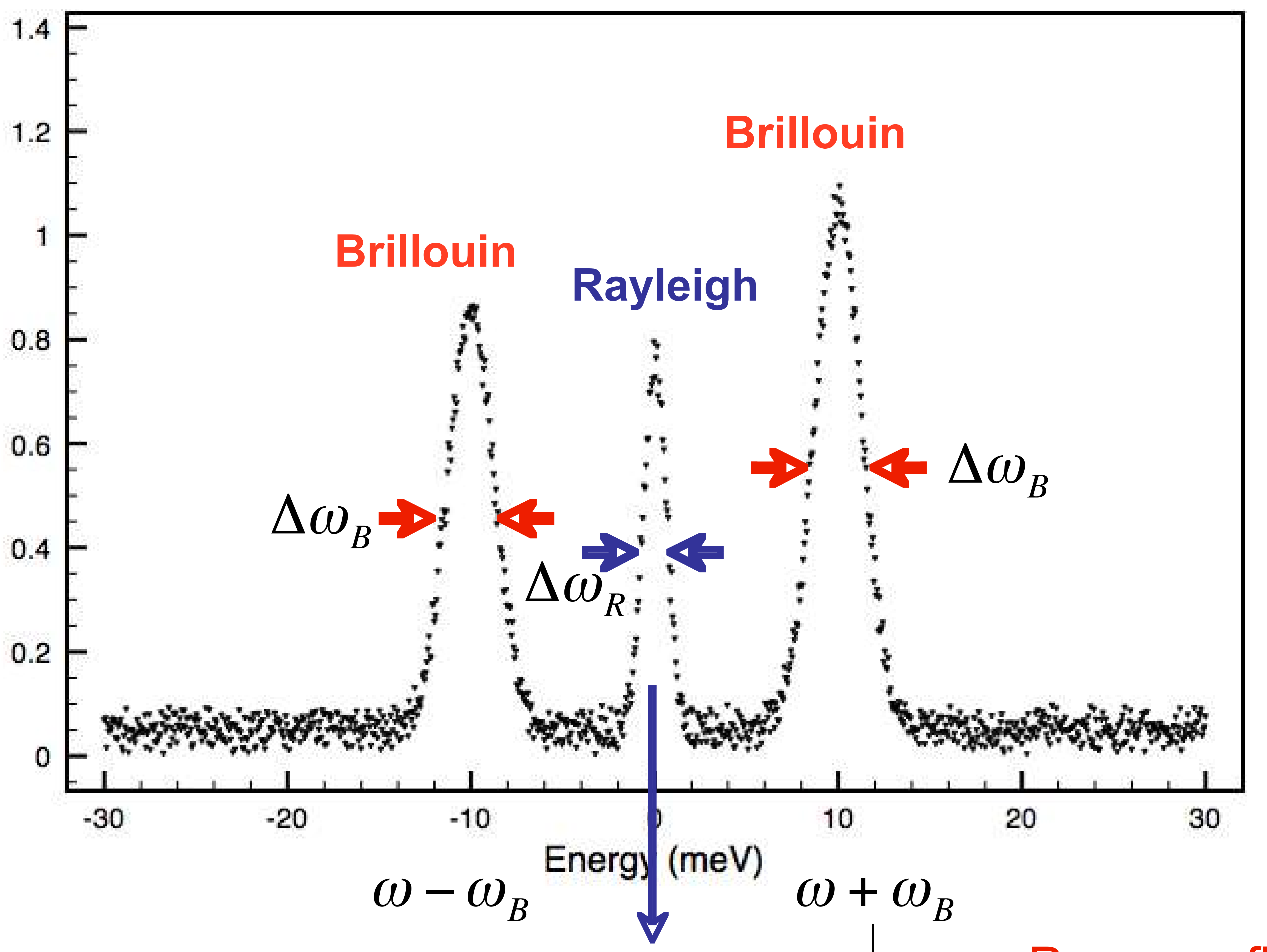

Entropy fluctuations, $\Delta\omega_R \sim \alpha q^2$

Concentration fluctuations $\Delta\omega_R \sim D q^2$

Pressure fluctuations

$$\omega_B(q) = V \cdot q$$

$$\Delta\omega_B \sim V q^2$$

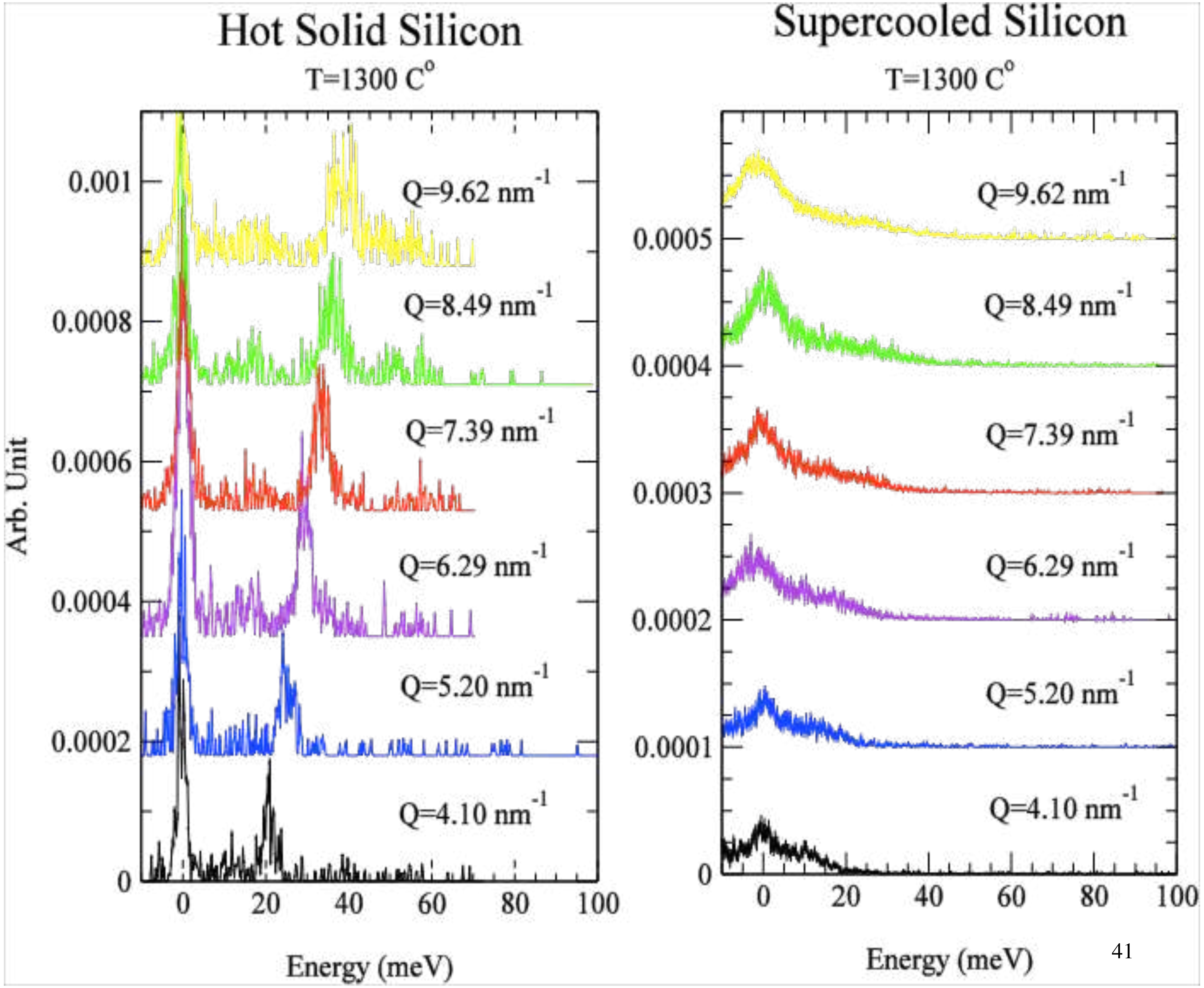

Hot Solid Silicon
T=1300 C°
Supercooled Silicon
T=1300 C°
Arb. Unit
Q=9.62 nm^-1
Q=8.49 nm^-1
Q=7.39 nm^-1
Q=6.29 nm^-1
Q=5.20 nm^-1
Q=4.10 nm^-1
0.001
0.0008
0.0006
0.0004
0.0002
0
0.0005
0.0004
0.0003
0.0002
0.0001
0 20 40 60 80 100
Energy (meV)
Energy (meV)

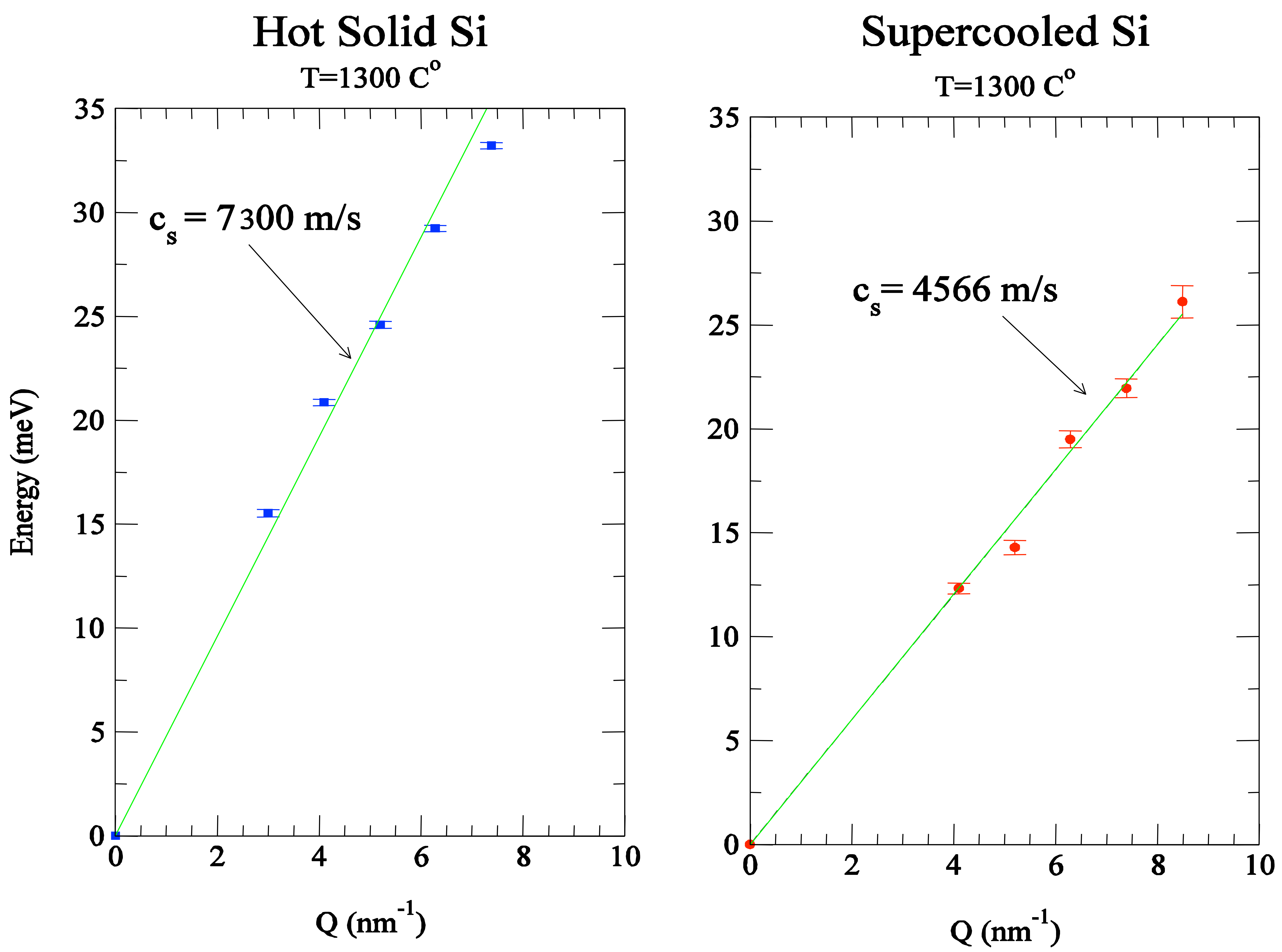

Hot Solid Si
T=1300 C°
cs = 7300 m/s
Energy (meV)
Q (nm-1)
Supercooled Si
T=1300 C°
cs = 4566 m/s
Q (nm-1)

Nuclear Resonant Inelastic X-Ray Scattering

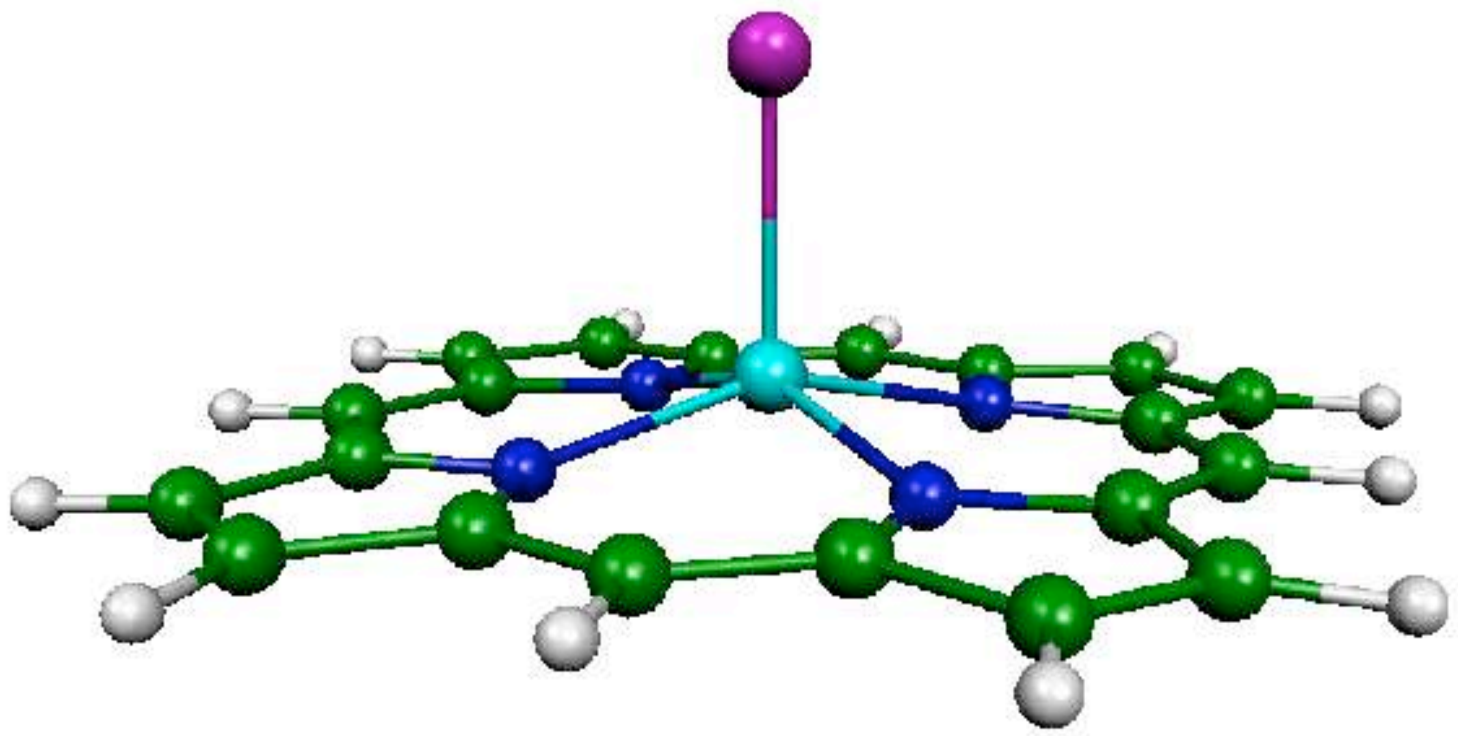

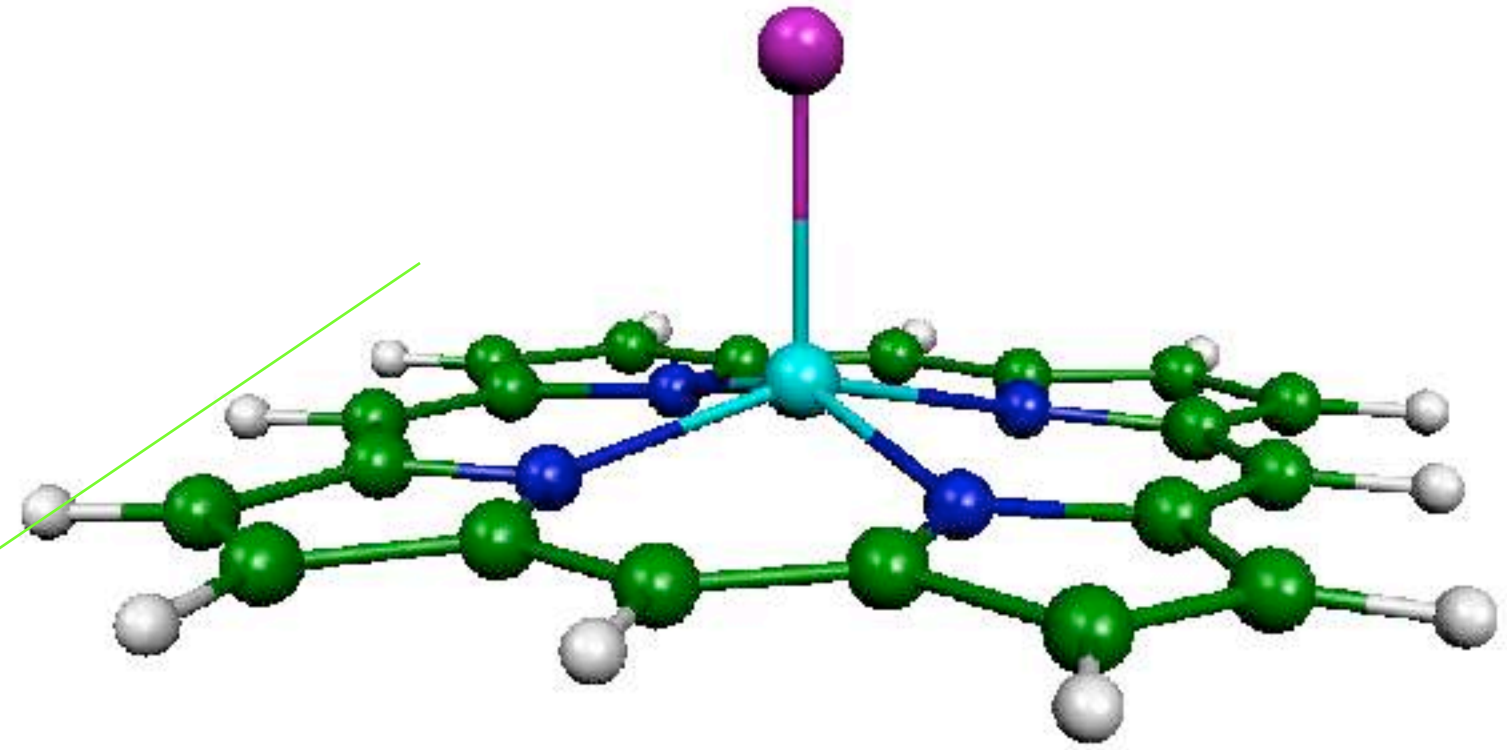

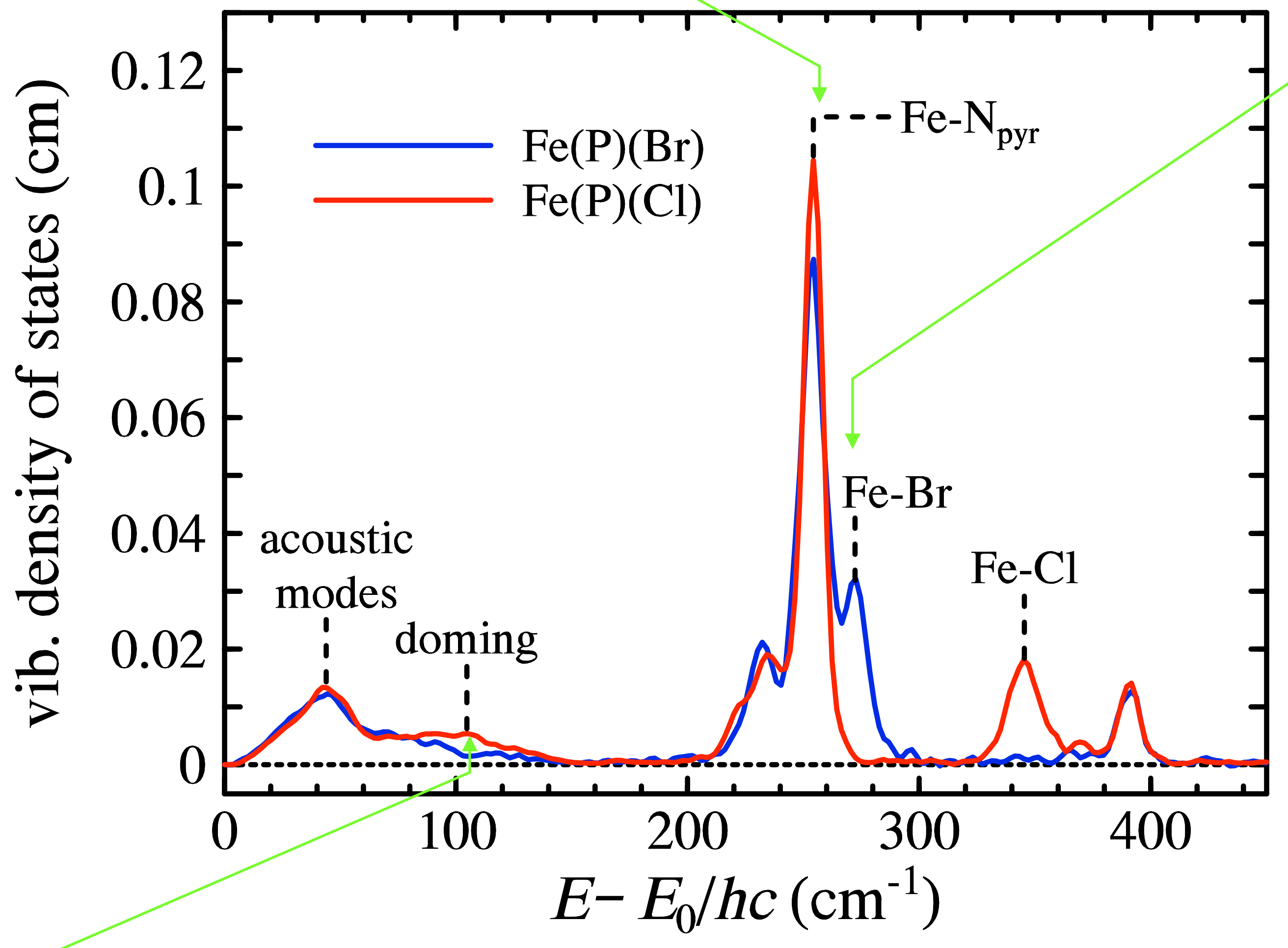

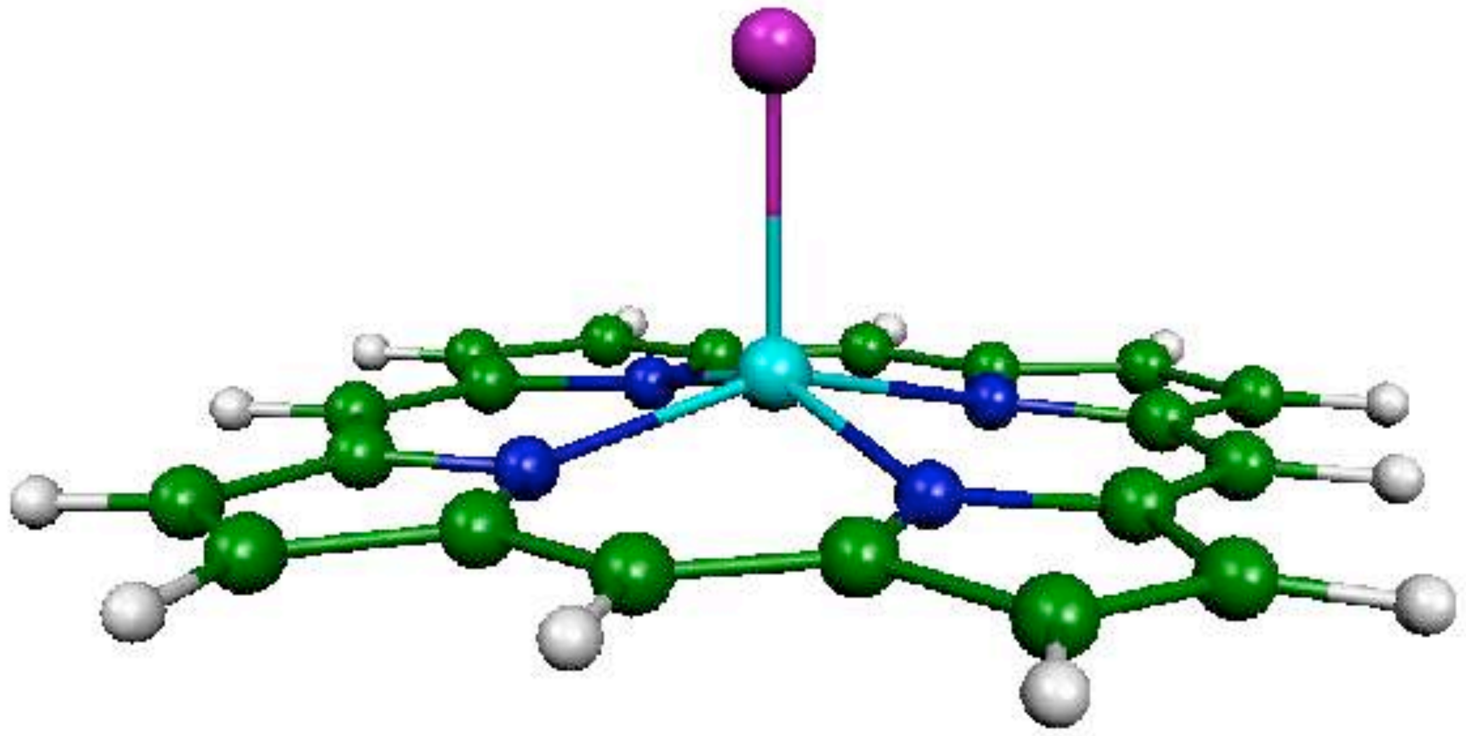

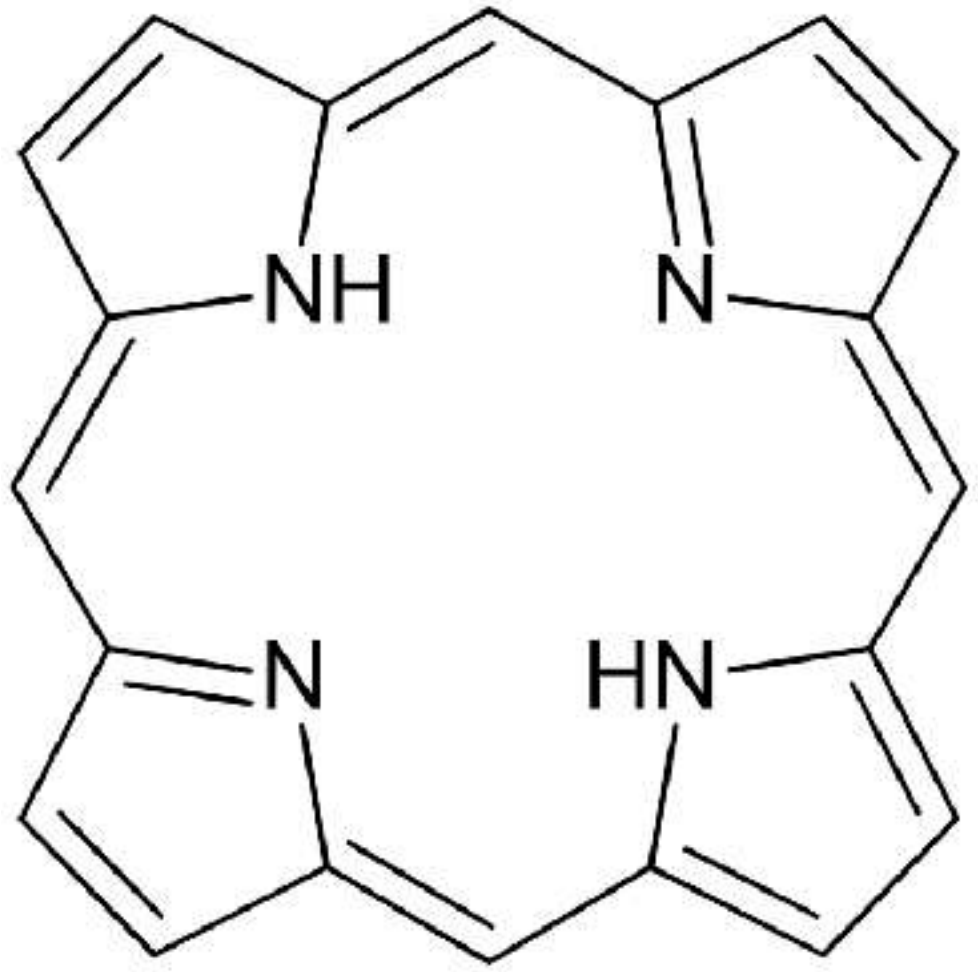

Phonon excitation probability

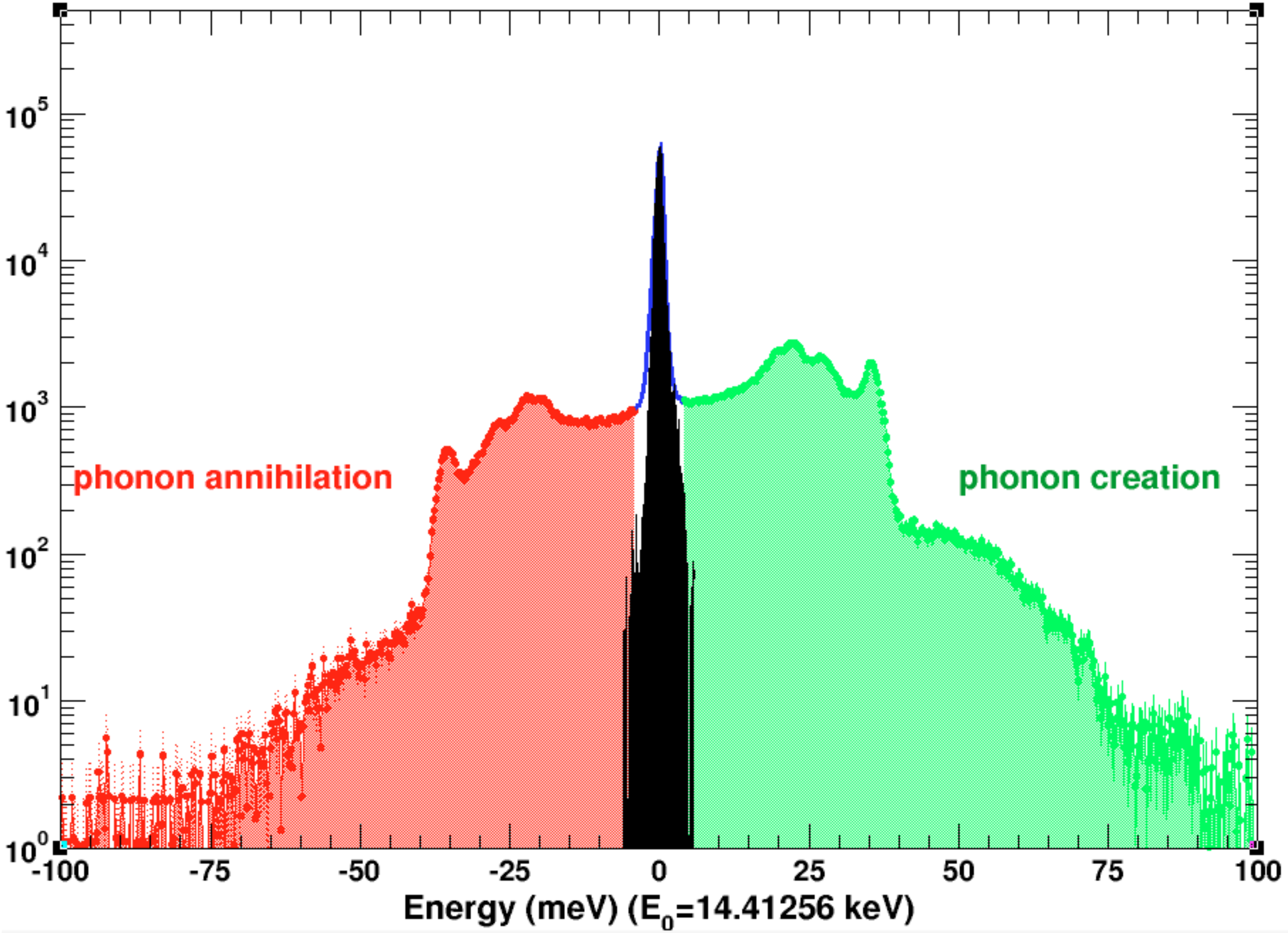

Information from NRIXS spectra:

- directly from the data, S(E)
  - temperature
    $$T = -\frac{E}{k_B} \ln\left[\frac{S(-E)}{S(E)}\right]$$
  - mean square displacement
    $$\langle u^2 \rangle = -\frac{1}{k^2} \ln\left[1 - \int \{S(E) - S(0)\}\, dE\right]$$
  - kinetic energy
    $$E_{kin} = \frac{1}{4E_R} \int (E - E_R)^2 S(E) dE$$
  - average force constant
    $$D = \frac{k^2}{2E_R^2} \int (E - E_R)^3 S(E) dE$$

- quasi-harmonic lattice model
  - partial phonon density of states
    $$\mathcal{D}(E)$$
  - Debye sound velocity
    $$v_D = \left(\frac{M}{2\rho\pi^2\hbar^3} \frac{E^2}{\mathcal{D}(E \to 0)}\right)^{1/3}$$
  - Grüneisen parameter
    $$\gamma_D = \frac{1}{3} + \frac{\rho}{v_D}\left(\frac{\partial v_D}{\partial \rho}\right)_T$$
  - isotope fractionation
    $$\ln \beta = -\frac{\Delta m}{M} \frac{1}{8(k_B T)^2} \int E^2 \mathcal{D}(E)\, dE$$

k ~ wave number of nuclear transition
E_R ~ recoil energy
ρ ~ mass density

M ~ mass of resonant isotope
Δm ~ isotope mass difference
k_B ~ Boltzmann's constant
T ~ temperature

Courtesy: W. Sturhahn

Phonon density of states is a key ingredient for many thermodynamic properties

If we choose to write in terms of energy, $E = \hbar\omega, \quad \beta = 1/k_B T$

$$c_v(T) = 3k_B \int (\beta E/2)^2 \operatorname{csc}h(\beta E) \cdot g(E) \cdot dE$$

Vibrational specific heat

$$S_v(T) = 3k_B \int_0^\infty \{\beta E/2 \bullet \cot h(\beta E) - \ln[2 \sin h(\beta E)]\} \cdot g(E) \cdot dE$$

Vibrational entropy

$$f_{LM} = e^{-E_R \int \{g(E)/2\}.\coth(\beta E/2)} dE$$

Lamb-Mössbauer factor

$$g(E) = \frac{3m}{2\pi^2 \hbar^3 \rho v_D^3} E^2$$

Debye Sound velocity

$$\langle F \rangle = \frac{M}{\hbar^2} \int_0^\infty E^2 g(E)\, dE$$

Average restoring force constant

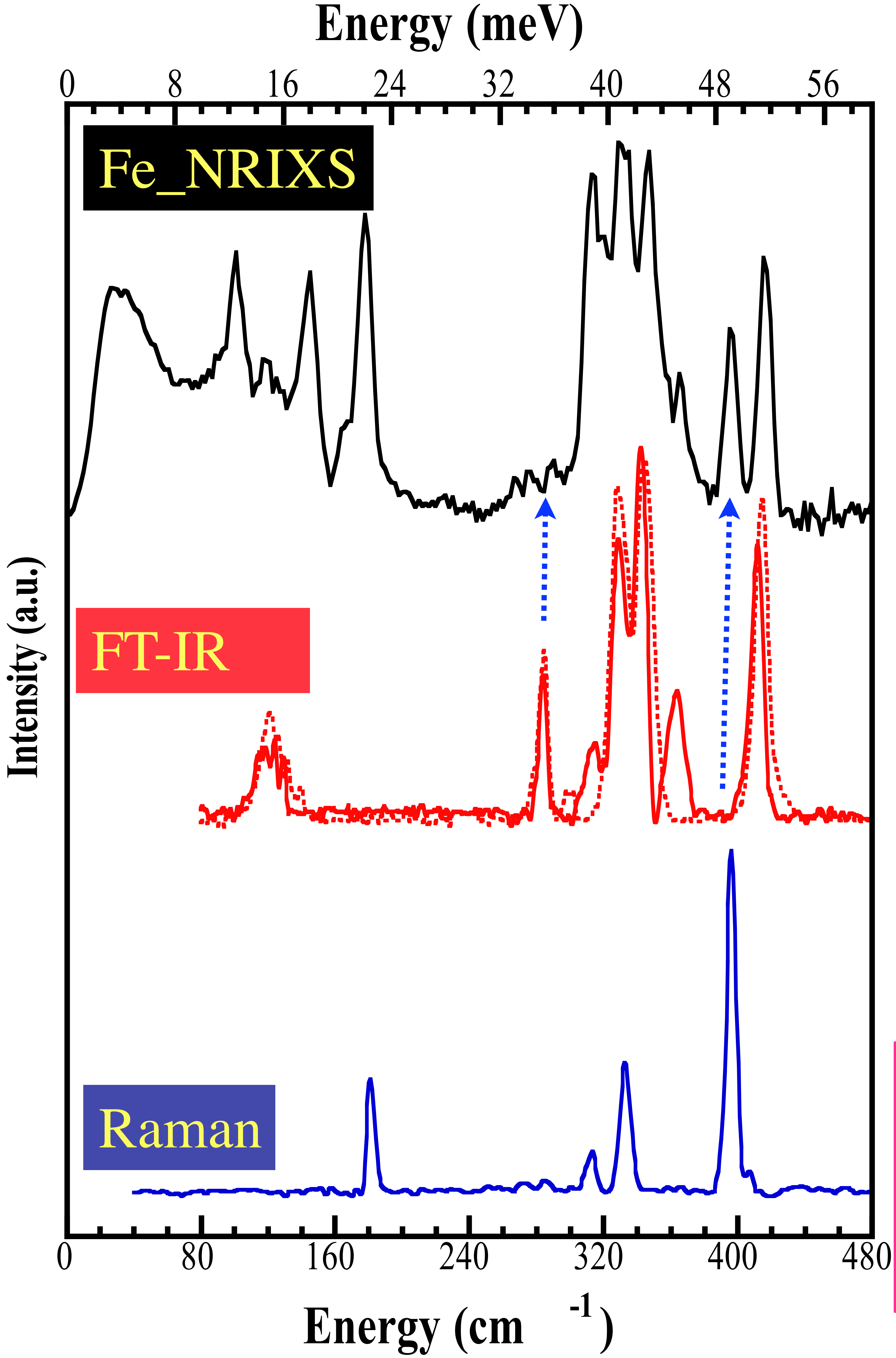

$[NEt_4]_2[Fe_2S_2Cl_4]$.

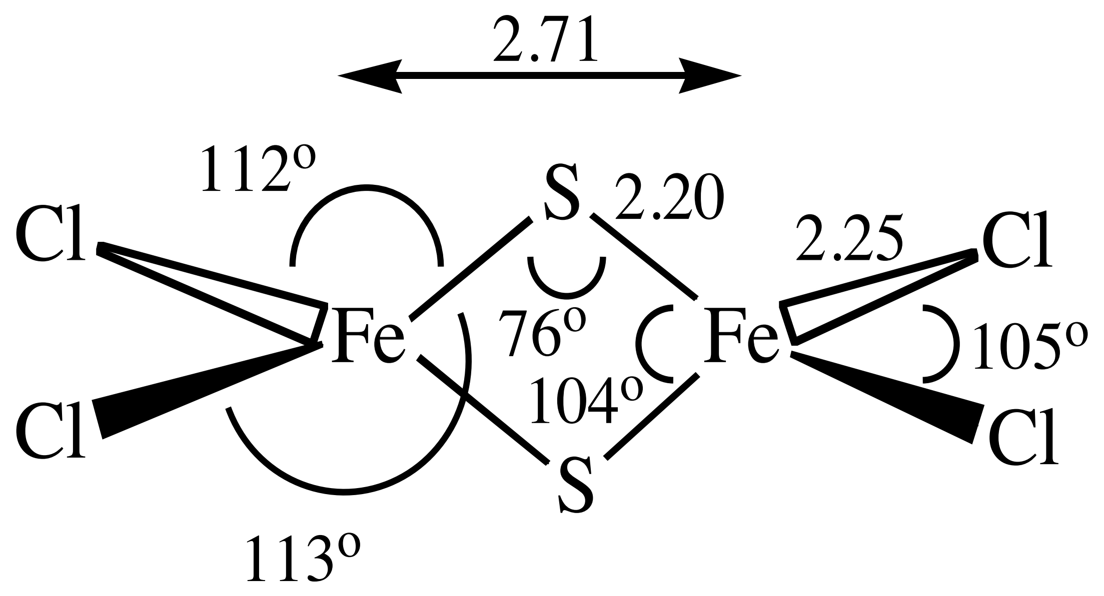

Some unique advantages of NRIXS

1. Low frequency motions: ~ total mass
2. No selection rule except motion of atoms along x-ray propagation
3. Peak intensity ~ mode participation ~ actual displacement
4. No matrix effects or limitations
5. Element and isotope selective
6. No unpredictable cancellations in scattering terms

$$\phi_\alpha = \frac{1}{3}\frac{\overline{v}_R}{\overline{v}_\alpha} e_{j\alpha}^2 (\overline{n}_\alpha + 1) f$$

Matt Smith, et al, Inorganic Chemistry, 2005, 44,5562

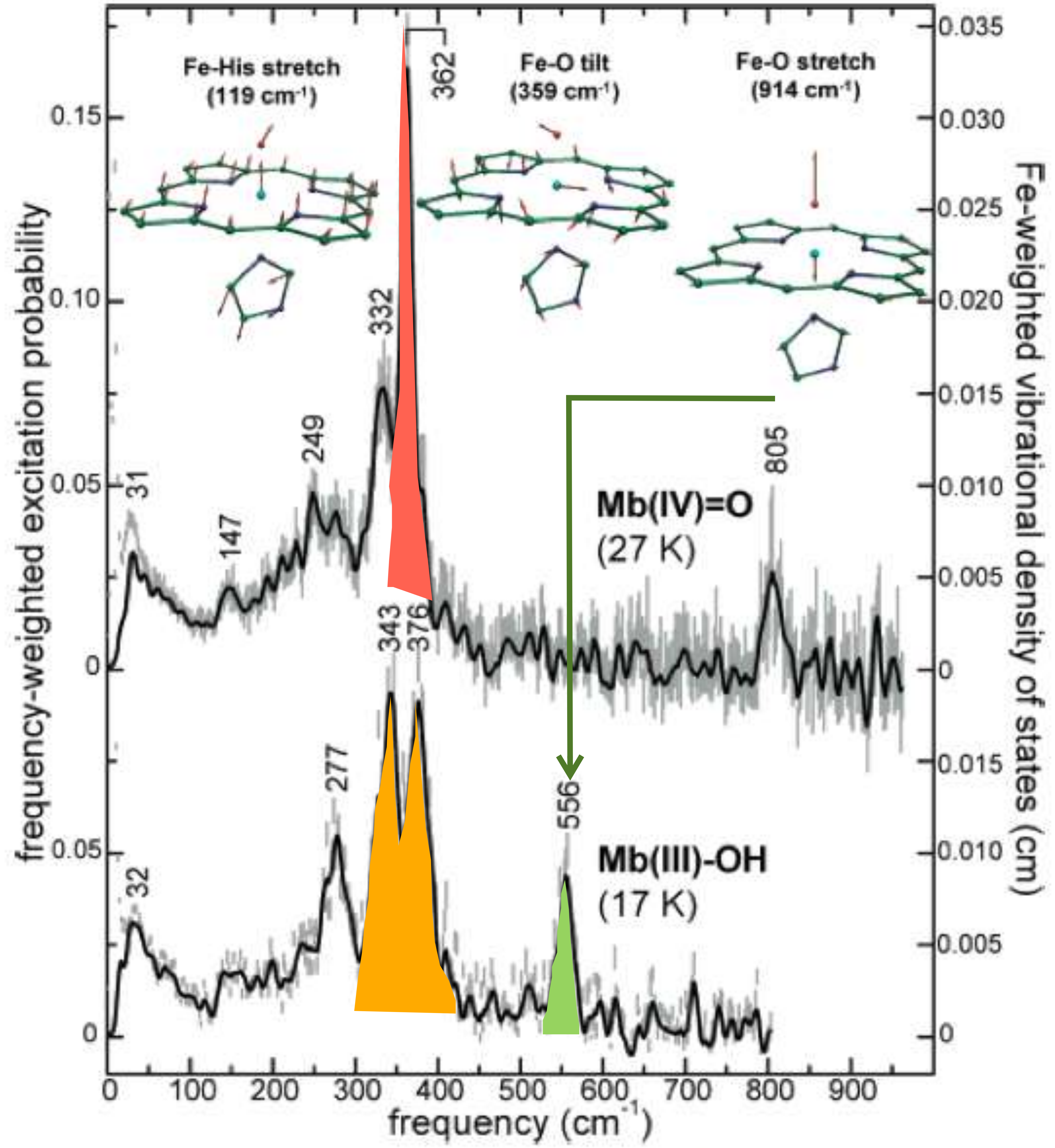

Fe-O tilting

Fe-O tilting

Figure 1. Vibrational dynamics of the heme Fe reveal an unprotonated oxo ligand in Mb(IV)═O, in contrast with the bound hydroxyl group in Mb(III)−OH. Protonation of the oxo ligand results in a downshift of the Fe−O stretching frequency from 805 cm^{-1} to 556 cm^{-1}, and splits the Fe−O tilting vibrations, which are degenerate near 362 cm^{-1} in Mb(IV)═O, but are separated by 33 cm^{-1} in the asymmetrically protonated heme Mb(III)−OH complex. Error bars represent the normalized experimental signal,

Science areas where SMS and NRIXS has become effective:

- Magnetism superconductivity and nematicity in iron chalcogenides, e.g. FeSe
- Magnetism of rare earth elements and compounds under high-pressure, e.g. Eu, Dy
- Single molecule magnets, Dy
- Search for Kagome lattice, e.g. Jarosite: KFe3(OH)6(SO4)2
- Magnetocaloric effect and the role of phonons in multiferroics, e.g. $LaFe_{13-x}Si_x$
- Mechanisms of pressure induced polymorphism and amorphization, e.g. SnI_4, Fe-metal
- Phonon glass materials, e.g. clathrates, skuterrudites
- Alloy thermodynamics and vibrational entropy
- Phonon confinement in multilayered nanomaterials
- New phases of iron oxides: Fe_4O_5, and more
- Isotope geochemistry

Imaging:

+

=

Mössbauer
Microscope

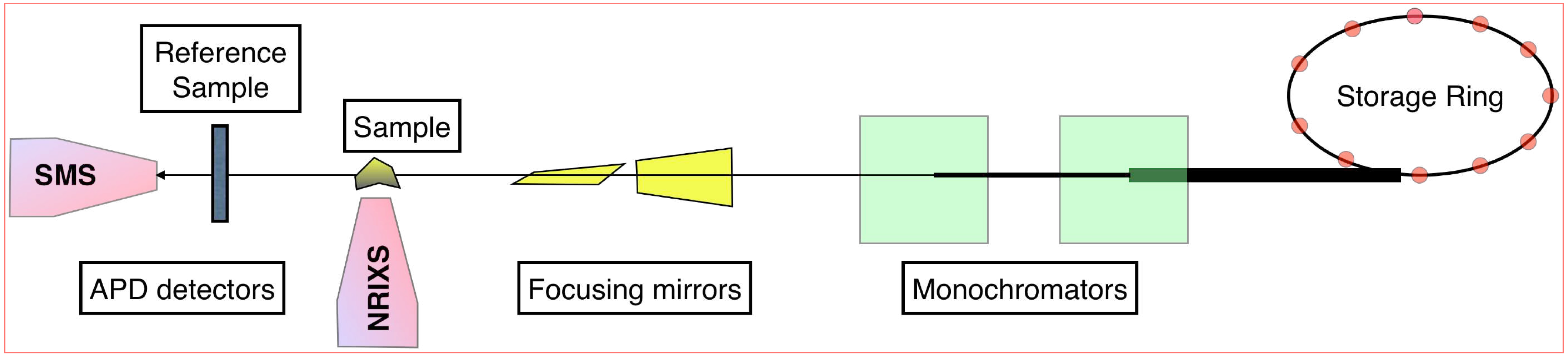

Estacado meteorite (H8): chondritic , Texas, 1883

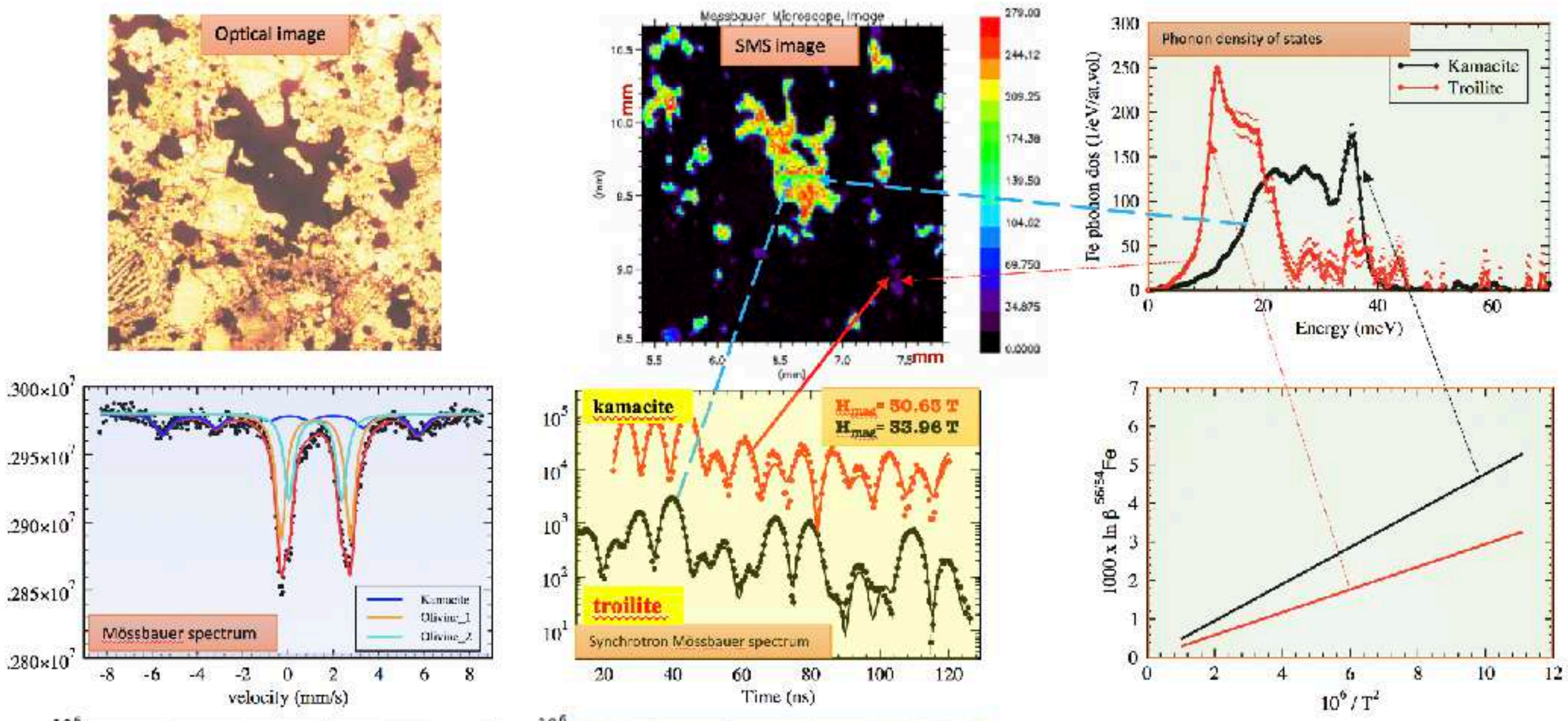

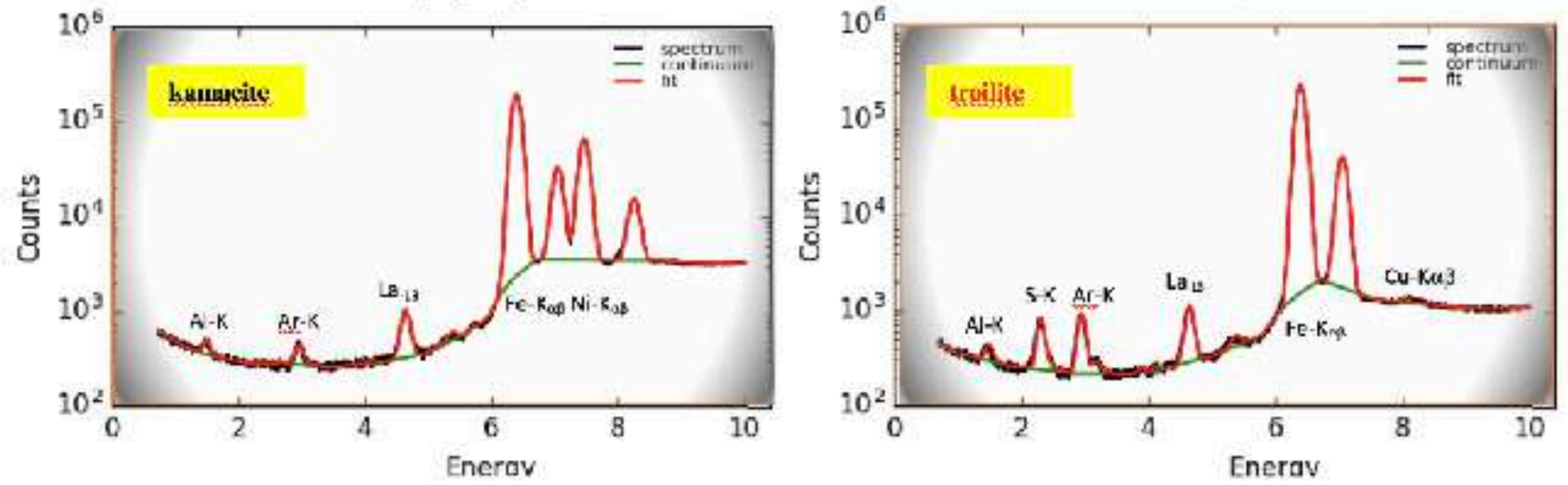

Phase	H1 (Tesla)	H2 (Tesla)	eQV_{zz} (mm/s)	<F> (N/m)
Kamacite	33.96	-	0	164
Troilite	30.63	27.2	1.14	101.6

Estacado is a stony meteorite older than earth itself. In the energy domain spectrum only two phases identified; kamacite and olivine (left, middle). However, a minority troilite phase is identified in the SMS spectrum (Middle, middle). The phonon density of states derived from the NRIXS spectrum clearly identifies the troilite phase separate from Olivine (top, right). NRIXS data or phonon density of states are used to extract isotope fractionation factors as described earlier (*V. Polyakov, Science* ***323*** *(2009) 912*, and *N. Dauphas et al, GCA,* ***94*** *(2012) 254*).

On the bottom left and the middle, x-ray induced fluorescence spectra are shown. Kamacite is identifiable from the nickel K_{α} and K_{β} peaks, while troilite can be idntified by the Sulphur K_{α} peak.

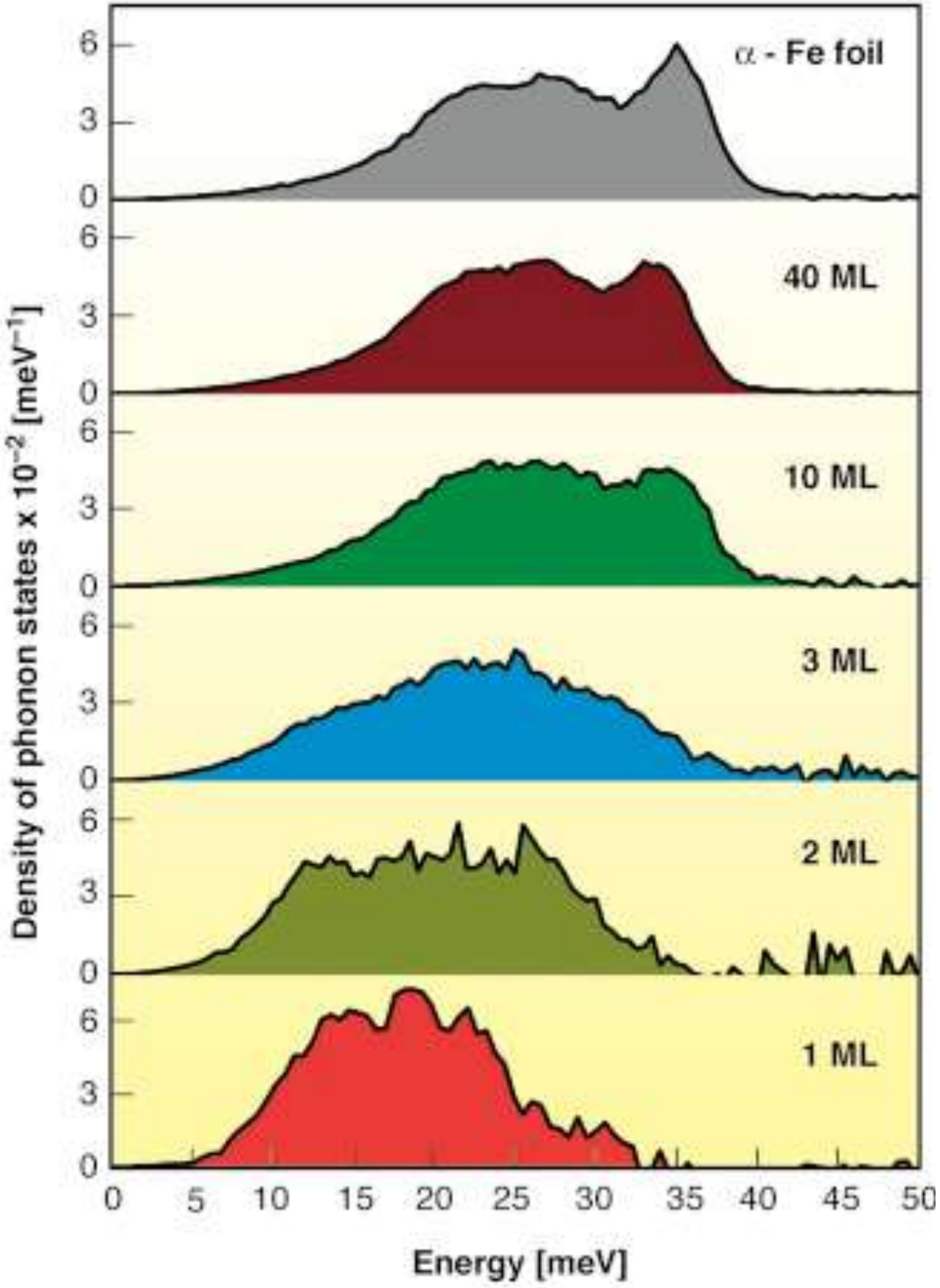

Fe films deposited on W(110)

Transition from the bulk to a single iron monolayer

S. Stankov, R. Röhlsberger, T. Slezak, M. Sladecek, B. Sepiol, G. Vogl, A. I. Chumakov, R. Rüffer, N. Spiridis, J. Lazewski, K. Parlinski, and J. Korecki,

ESRF Highlights 2006

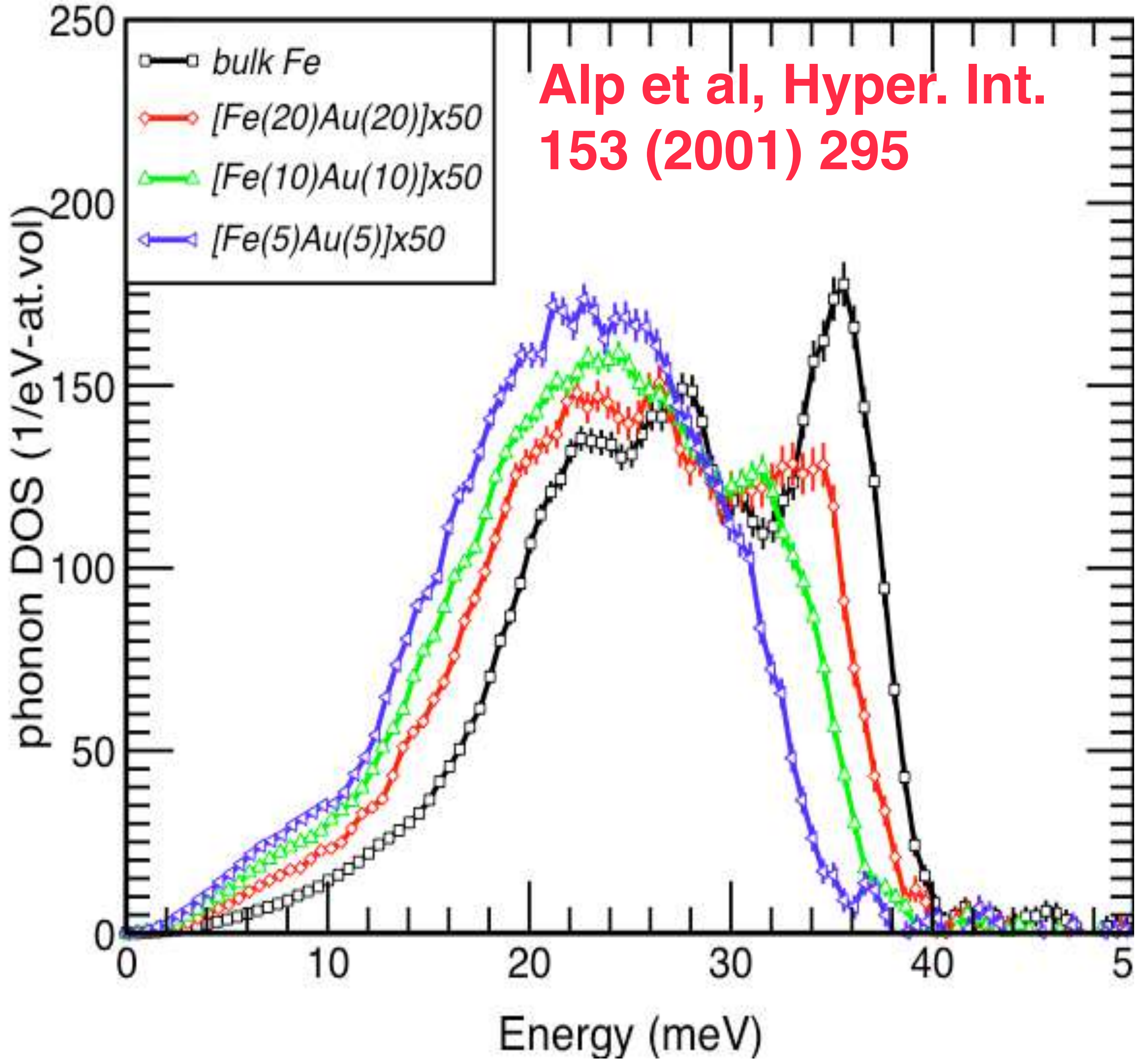

Alp et al, Hyper. Int. 153 (2001) 295

Thank You...